


Summer 8-14-2020

## Exosomes Secreted under Hypoxia Enhance Stemness in Ewing's Sarcoma and Transform Microenvironment Cells

Matthew J. Kling  
*University of Nebraska Medical Center*

Tell us how you used this information in this [short survey](#).

Follow this and additional works at: <https://digitalcommons.unmc.edu/etd>

 Part of the [Biological Phenomena, Cell Phenomena, and Immunity Commons](#), and the [Nanomedicine Commons](#)

---

### Recommended Citation

Kling, Matthew J., "Exosomes Secreted under Hypoxia Enhance Stemness in Ewing's Sarcoma and Transform Microenvironment Cells" (2020). *Theses & Dissertations*. 482.  
<https://digitalcommons.unmc.edu/etd/482>

This Dissertation is brought to you for free and open access by the Graduate Studies at DigitalCommons@UNMC. It has been accepted for inclusion in Theses & Dissertations by an authorized administrator of DigitalCommons@UNMC. For more information, please contact [digitalcommons@unmc.edu](mailto:digitalcommons@unmc.edu).

**Exosomes Secreted under Hypoxia Enhance Stemness in  
Ewing's Sarcoma and Transform Microenvironment Cells**

by

**Matthew J. Kling**

A DISSERTATION

Presented to the Faculty of  
The Graduate College in the University of Nebraska  
in Partial Fulfillment of the Requirements  
for the Degree of Doctor of Philosophy

Genetics, Cell Biology and Anatomy  
Graduate Program

Under the Supervision of Professor Shantaram S. Joshi

University of Nebraska Medical Center  
Omaha Nebraska

August, 2020

Supervisory Committee:

Hamid Band M.D., Ph.D.	Don Coulter M.D.
Graham J. Sharp, Ph.D.	Timothy McGuire, Pharm D.
Samuel Pirruccello, M.D.	

## Acknowledgements

First and foremost, I want to thank my wife, Jess, for her patience and loving support throughout my graduate studies at UNMC. Without you, I would have never made it this far. Thank you for lending a thoughtful ear and putting up with my insanity. Your constant optimism helped me find the joy in every day. I love you very much.

I want to thank Dr. Joshi for his guidance and constant support. I am very grateful for him giving me the opportunity to work in his lab and explore interesting ideas. I am especially thankful for his encouragement and fatherly mentorship throughout my research and teaching experiences. Thank you for fighting to give me as many teaching opportunities as possible. You taught me how to balance and strive for excellence in scholarship, teaching and service.

I want to thank Dr. Nagendra Chaturvedi and Dr. Ashima Shukla for their mentorship and all the help they gave me with my experiments. Special thanks to Nagendra for your friendship and your ability to assuage my concerns when attempting new experiments. Thank you for always being there to listen and engaging in discussions on science and life.

I want to thank my graduate supervisory committee members, Drs. Graham Sharp, Timothy McGuire, Hamid Band, Sam Pirruccello and Donald Coulter for their mentorship and guidance in my research. I especially would like to thank Dr. Sharp and Dr McGuire for the numerous “water cooler talks” that we had throughout my graduate education. These discussions helped shape my scientific mind and inspired me to pursue challenging scientific questions. I want to thank Dr. Coulter for his unwavering support in my research contributions to the Pediatric Research Group. His charisma and dedication to translational medicine in pediatric cancer serves as a constant inspiration.

I want to thank Dr. Andrew Dudley and Dr. Kishor Bhakat for running a truly transformative journal club. I especially want to thank Dr. Dudley for fostering an environment that values creativity and promotes curiosity. These weekly experiences significantly developed my scientific mind and critical thinking skills.

I want to thank the anatomy teaching faculty. They are the reason that I decided to come to UNMC and further my education in the anatomical sciences. Special thanks to Drs. Carol Lomneth, Robert Binhammer, Sarah Keim, Kim Latacha, Gib Willett, Rob Norgren, Ryan Splittgerber, Carrie Elzie, Keely Cassidy, Samantha Simet, Travis McCumber and Alan Richards. Thank you all for your mentorship and allowing me to get off my “island.” I have found friends in you all.

I want to thank the State of Nebraska for their financial support of the UNMC/Children's Hospital Pediatric Cancer Research Program. Thanks goes to the Technology Center for Genomics and Bioinformatics Core Facility at UCLA, TACGenomics and the Flow Cytometry, Electron Microscopy and Nanomaterials Characterization Core Facilities at UNMC for their assistance with these studies. Sincere thanks to the Child Health Research Institute and the Fred Pamela Buffet Cancer Center supported Core Facilities at UNMC. Furthermore, this research would not be possible without the support of the Pediatric Cancer Research Funds from the State of Nebraska (LB905; awarded to D.W. Coulter), UNMC Graduate Studies Assistantship/Fellowship and University of Nebraska Presidential Graduate Fellowship awards.

# **Exosomes Secreted under Hypoxia Enhance Stemness in Ewing's Sarcoma and Transform Microenvironment Cells**

Matthew J. Kling, Ph.D.

University of Nebraska Medical Center, 2020

Supervisor: Shantaram S. Joshi, Ph.D.

Intercellular communication between tumor cells and stroma within the hypoxic microenvironment promote aggressiveness and poor patient prognoses in ways that remain unclear. Here we show that hypoxic Ewing's sarcoma (EWS) cells release exosomes that promote sphere formation, a stem-like phenotype, in EWS cells by enhancing survival and a cancer-associated phenotype in fibroblasts (CAFs). Given that hypoxia enriches for stem-like cells, we exposed EWS cells to hypoxia and hypoxic EWS-derived exosomes and assessed the stem cell phenotype. Hypoxia and hypoxic EWS-derived exosome were found to enhance TIC formation *in vitro* and *in vivo* by reprogramming EWS cells. Analysis of the hypoxic exosomal miRNA cargo identified a HIF-1 $\alpha$  regulated miRNA, miR-210, as a potential mediator of sphere formation in cells exposed to hypoxic exosomes. Knockdown of HIF-1 $\alpha$  in hypoxic EWS cells led to decreased exosomal miR-210 levels and reduced the capacity of hypoxic exosomes to form spheres. Inhibition of miR-210 in hypoxic spheres attenuated sphere formation and overexpression of miR-210 in normoxic spheres significantly enhanced the number of EWS spheres. Our results indicate that hypoxic exosomal miR-210 targets the proapoptotic protein CASP8AP2 in recipient cells. Moreover, the suppression of CASP8AP2 led to a reduction in apoptotic cells and increased sphere formation.

Exosomes co-cultured with fibroblasts in a soft agar assay and 2D culture assessed induction of the CAF phenotype. Fibroblasts preconditioned with exosomes were injected into NSG mice to determine the effects of exosomes on tumorigenicity.

Exosomes increased expression of CAF markers and tumorigenicity in fibroblasts.

Network analysis of hypoxic-derived exosomes revealed enrichment of miRNA targeting the Akt pathway. Our observations suggest that hypoxic-derived exosomes enhance an aggressive phenotype in EWS and fibroblasts by increasing Akt signaling.

Together, the findings in this study suggest that hypoxic exosomes promote stemness in EWS cells by delivering enriched miR-210 that is capable of down-regulating apoptotic pathways, resulting in the survival of cells with increased sphere formation. Future studies will further investigate the effect of exosomal miRNA on target genes and the role these interactions play in driving aggressiveness in hypoxic EWS cells. Future work will investigate the role of exosomal miRNA on the Akt pathway in target cells.

## TABLE OF CONTENTS

<b>Acknowledgements</b> .....	i
<b>Abstract</b> .....	iii
<b>TABLE OF CONTENTS</b> .....	v
<b>List of Figures</b> .....	viii
<b>List of Tables</b> .....	x
<b>List of Abbreviations</b> .....	xi
<b>Chapter I: Introduction</b> .....	1
Ewing's sarcoma Introduction .....	1
EWS-ETS Fusion Proteins .....	2
<i>EWS</i> Gene .....	5
<i>FLI 1</i> Gene .....	6
EWS-FLI1 Targets .....	7
Role of miRNAs in EWS.....	9
Novel Therapeutic Targets in EWS .....	12
The Origin of Ewing's sarcoma and the discovery of the tumor-initiating cell .....	14
Tumor-Initiating Cells (TICs) Introduction.....	19
Defining Stemness .....	20
Heterogeneity and the TIC Model.....	22
Approaches to studying stemness and heterogeneity.....	24
The Hypoxic EWS Tumor Microenvironment Introduction.....	25
Overview of Hypoxia and Hypoxia Inducible Factors .....	27
Hypoxia, HIFs and Cancer Stem Cells .....	32
Hypoxia Regulated miRNAs in Cancer.....	33
miR-210, the Master Hypoxia Regulated miRNA.....	34
Role of miR-210 in Stemness.....	36
Intercellular Signaling in the Hypoxic Tumor Microenvironment.....	38
Exosome Biogenesis .....	41
Exosome Cargo .....	42
Exosome Secretion .....	44
Exosome Interactions with Recipient Cells .....	44
Function of Exosomes in the Hypoxic TME .....	45

Exosome Studies in EWS .....	47
Summary .....	48
Hypothesis and Specific Aims .....	49
<b>Chapter II: Materials and Methods .....</b>	<b>50</b>
Cell culture and hypoxia exposure .....	50
siRNA and miRNA transfection .....	50
MK-2206, Akt inhibitor, treatment .....	51
Exosome isolation .....	51
Nanoparticle tracking analysis (NTA).....	53
Electron microscopy.....	53
Sarcosphere assay .....	54
Colony formation assay.....	55
Western blot.....	55
RNA isolation, RNA-seq and analysis.....	56
Real-time quantitative PCR .....	57
Apoptosis Assay .....	57
Tumorigenicity Assays .....	57
Tumor dissociation and FACS analysis .....	58
Statistical analysis .....	59
<b>Chapter III: Characterization of EWS Normoxic<sup>EXO</sup> and Hypoxic<sup>EXO</sup> .....</b>	<b>60</b>
Introduction.....	60
Results .....	61
Discussion .....	81
<b>Chapter IV: Exosomes Secreted under Hypoxia Enhance Stemness and Tumorigenicity in EWS.....</b>	<b>86</b>
Introduction.....	86
Results .....	87
Discussion .....	104
<b>Chapter V: Exosomes Secreted under Hypoxia Activate Akt signaling in Ewing's Sarcoma Spheres and Cancer-Associated Fibroblasts .....</b>	<b>109</b>
Introduction.....	109
Results .....	110
Discussion .....	120
<b>Chapter VI: General Discussion .....</b>	<b>125</b>



Overview and Impact of Study .....	125
Limitations of Study and Future Work.....	128
Analysis of Pitfalls in EWS Hypoxia Studies .....	132
<b>Chapter VII: Bibliography .....</b>	<b>136</b>

## List of Figures

Figure 1.1: Schematic of most common EWS-FLI1 chromosomal translocation t(11;22)(q24;q12) .....	3
Figure 1.2: Outline of EWS and five ETS proteins (FLI1, ERG, FEV, ETV1, ETV4) that participate in Ewing's sarcoma translocations.....	4
Figure 1.3: General schematic of TIC model .....	21
Figure 1.4: Outline of hypoxia inducible factor protein domains and most common post- translational modifications .....	29
Figure 1.5: Schematic diagram of hypoxic effects on EWS tumor microenvironment (TME) .....	39
Figure 3.1: NanoSight tracking analysis (NTA) of SK-ES-1 exosomes isolated using different methods .....	67
Figure 3.2: Characterization of EWS Exosomes .....	68
Figure 3.3: Characterization of EWS-FLI1 in EWS exosomes .....	69
Figure 3.4: Representative electropherogram profile of total RNA in normoxic and hypoxic SK-ES-1 cells and exosomes .....	70
Figure 3.5: Differential expression of miRNAs in normoxic and hypoxic cells and exosomes .....	71
Figure 3.6: miR-210 expression in EWS exosomes.....	73
Figure 3.7: IPA analysis and interactome of exosomal miRs .....	74
Figure 3.8: Differential expression of miRNAs in normoxic and hypoxic cells and exosomes .....	76
Figure 3.9: Differential expression and IPA analysis of mRNAs in normoxic and hypoxic cells and exosomes.....	77
Figure 3.10: Differential expression of mRNAs in normoxic and hypoxic cells and exosomes .....	79
Figure 3.11: ESC gene expression in normoxic and hypoxic EWS cells .....	80
Figure 4.1: Hypoxia increases sphere formation, miR-210 and ESC genes in EWS cells .....	93
Figure 4.2: HypoxicEXO enhance sphere formation in EWS cells.....	94

Figure 4.3: HypoxicEXO increases stemness in EWS tumors .....	95
Figure 4.4: HIF-1 $\alpha$ Regulates HypoxicEXO miR-210 and mediates exosomal induced sphere formation .....	96
Figure 4.5: Akt regulates miR-210 in HIF-1 $\alpha$ dependent and dndependent ways and mediates HypoxicEXO-induced sphere formation .....	98
Figure 4.6: miR-210 regulates sphere formation by targeting CASP8AP2 .....	100
Figure 4.7: CASP8AP2 knockdown promotes sphere formation by enhancing survival .....	102
Figure 5.1: Hypoxia activates Akt in EWS spheres .....	114
Figure 5.2: HypoxicEXO increase Akt and ESC gene expression in EWS spheres .....	115
Figure 5.3: HypoxicEXO increase Akt in EWS tumors .....	116
Figure 5.4: HypoxicEXO enhances reprograming in NIH3T3 cells .....	117
Figure 5.5: HypoxicEXO enhance NIH3T3 tumorigenicity .....	118

List of Tables

Table 3.1: Hypoxia regulated miRNAs differentially expressed in SK-ES-1 Hypoxic<sup>EXO</sup> compared to Normoxic<sup>EXO</sup> ..... 72

## List of Abbreviations

1.	EWS	Ewing's sarcoma
2.	EWSR1	Ewing's sarcoma breakpoint region 1
3.	ETS	E26 transformation specific
4.	FLI1	Friend leukemia integration 1 transcription factor
5.	ERG	ETS-related gene
6.	FEV	Fifth Ewing variant protein
7.	ETV1	ETS variant transcription factor 1
8.	ETV4	ETS variant transcription factor 4
9.	TET	Ten-eleven translocation proteins
10.	TLS	Translocation in liposarcoma
11.	TAF15	TATA-binding protein-associated factor 15
12.	RRM	RNA recognition motif
13.	TFIID	Transcription factor II D
14.	Bcl2	B-cell lymphoma 2
15.	ChIP	Chromatin immunoprecipitation
16.	AP-1	Activator protein 1/FOS-JUN
17.	CBP	CREB-binding protein
18.	p300	Histone acetyltransferase p300
19.	BARD1	BRCA1 associated RING domain 1
20.	RHA	RNA helicase A
21.	NR0B1/DAX1	Nuclear receptor subfamily 0 group B member 1
22.	hRPB3	Human RNA polymerase II-p33 subunit
23.	TGF- $\beta$ RII	Transforming growth factor beta receptor II
24.	IGFBP-3	Insulin-like growth factor-binding protein 3
25.	ID2	Inhibitor of DNA binding protein 2
26.	PTPL1	Protein tyrosine phosphatase 1
27.	PLD2	Phospholipase D2
28.	PDGF	Platelet-derived growth factor
29.	GSTM4	Glutathione S-transferase Mu 4
30.	GLI1	glioma-associated oncogene 1
31.	EZH2	Enhancer of Zeste Homolog 2
32.	PDGF	Platelet derived growth factor

33.	CCND1	Cyclin D1
34.	CD	Cluster of differentiation
35.	hTERT	Human telomerase reverse transcriptase
36.	VEGF	Vascular endothelial growth factor
37.	MFNG	Beta-1,3-N-acetylglucosaminyltransferase manic fringe
38.	TASR	Translocation liposarcoma protein serine-arginine
39.	YB-1	Y box binding protein 1
40.	miRNA/miR	MicroRNA
41.	DGCR8	DiGeorge syndrome chromosomal region 8
42.	TRBP	TAR RNA binding protein
43.	RISC	RNA induced silencing complex
44.	hpMSC	Human pediatric mesenchymal stem cells
45.	HMGA2	High mobility group AT-Hook 2
46.	PI3K	Phosphatidyl inositol kinase 3
47.	siRNA	Silencing RNA
48.	IGF-1R	Insulin-like growth factor 1 receptor
49.	mTOR	Mammalian target of rapamycin
50.	Akt	AKR mouse strain that develops thymoma
51.	TIC	Tumor initiating cell
52.	PAS	Periodic acid schiff
53.	MPC	Mesenchymal progenitor cells
54.	FACS	Fluorescently activated cell sorting
55.	NSG	NOD scid gamma
56.	ESC	Embryonic stem cells
57.	CSC	Cancer stem cells
58.	TME	Tumor microenvironment
59.	HIF	Hypoxia inducible factor
60.	RNAseq	RNA sequencing
61.	ALDH	Aldehyde dehydrogenase
62.	CAF	Cancer associated fibroblast
63.	bHLH	Basic helix-loop-helix
64.	ODD	Oxygen-dependent degradation domain
65.	N-TAD	N-terminal transactivation domain
66.	C-TAD	C-terminal transactivation domain

67.	PHD	Prolyl hydroxylase
68.	VHL	Von Hippel-Lindau
69.	HRE	Hypoxia response element
70.	HRM	Hypoxia regulated miRNA
71.	GLUT1	Glucose transporter 1
72.	iPSC	Induced pluripotent stem cells
73.	HRM	Hypoxia regulated miRNA
74.	GPDH	Glycerol-3-phosphate dehydrogenase
75.	E2F3	E2F transcription factor 3
76.	FGFRL1	Fibroblast growth factor receptor like 1
77.	HOXA1	Homeobox A1
78.	ISCU	Iron-sulfur cluster assembly enzyme
79.	COX10	Cytochrome c oxidase 10
80.	SDHD	Succinate dehydrogenase complex subunit D
81.	EFNA3	Ephrin A3
82.	PTP1B	Protein tyrosine phosphatase 1B
83.	MNT	MAX network transcriptional repressor
84.	MAX	MYC associated factor x
85.	CASP8AP2	Caspase 8 associated protein 2
86.	HUVEC	Human umbilical vein cell
87.	BM-MSC	Bone-derived mesenchymal stem cells
88.	MVB	Multivesicular bodies
89.	ESCRT	Endosomal sorting complex required for transport
90.	TSG101	Tumor susceptibility gene 101
91.	FBS	Fetal bovine serum
92.	SOX2	SRY (sex determining region Y)-box 2
93.	OCT4	Octamer-binding transcription factor 4
94.	MYC	Myelocytomatosis
95.	siRNA	Silencing RNA
96.	hnRNP	Heterogeneous nuclear ribonucleoprotein
97.	GFP	Green fluorescent protein
98.	MMP	Metallomatrix protein
99.	$\alpha$ -SMA	Alpha smooth muscle actin
100.	IPA	Ingenuity pathway analysis

101.	NTA	NanoSight Tracking Analysis
102.	TEM	Transmission electron microscopy
103.	SEM	Scanning electron microscopy
104.	Normoxic <sup>EXO</sup>	Normoxic exosomes
105.	Hypoxic <sup>EXO</sup>	Hypoxic exosomes



# Chapter I

## Introduction

### Ewing's sarcoma Introduction

Ewing's sarcoma (EWS) is an aggressive and highly malignant tumor that belongs to a family of tumors that include primitive neuroectodermal tumors, Askin's tumors, and extrasosseous Ewing's sarcoma. The tumor was first described by James Ewing in 1921 as sheets of small round blue cells (1). In 85% of clinical cases, EWS tumors arise in bone localized primarily in the pelvis, diaphysis of long bones, the ribs and sternum. Fifteen percent of the cases are formed at extraosseous sites within soft tissues of the thoracic region, proximal limbs, bladder, kidney, prostate, paravertebral space and the meninges. The majority of patients afflicted with EWS are diagnosed between 10-20 years of age with a peak incidence of 15 years (2-4). The frequency of EWS are 1 to 3 per million per year and is more common in people of European descent with a minor predominance in males. Ewing's sarcoma is the second most prevalent malignant bone tumor in children and adolescents, but is considered to have the worst prognosis of the bone sarcomas (5, 6). The current 5-year survival rate has increased in recent years ranging from 59% to 78% in children under 15 years of age and 20% to 60% for adolescents over the age of 15 years, however, the 5-year survival rate patients diagnosed with metastasis or undergo relapse is less than a 25% (7).

Histologically, EWS tumors share the common round blue cell morphology with other tumors which include neuroblastoma, alveolar rhabdomyosarcoma and lymphoblastic lymphoma (8). The high expression of the cell adhesion transmembrane glycoprotein, CD99, in these tumors served as an immunohistochemical diagnostic

marker for EWS but had low specificity due to their common expression (9, 10). In the past, this led to diagnosis by exclusion until the discovery of the chromosomal translocation  $t(11;22)(q24;q12)$  and its EWS-FLI1 fusion protein which occurs in 85% of EWS (11, 12). This provided a more definitive diagnostic marker through molecular analyses. In the past, the correct cell of origin was a subject of great debate between primitive neuroectodermal cells (13) and mesenchymal stem cells. Studies supporting a mesenchymal origin indicated a primordial bone marrow derived mesenchymal stem cell (14). Riggi et al. demonstrated transformation of mesenchymal progenitor cells by introducing a retrovirus containing the fusion gene into murine MPC (15). In this study, the round blue cell phenotype was maintained along with upregulation of known EWS-FLI1 target genes.

This review will focus on the many aspects of ESFTs which include: the role of EWS-ETS fusion proteins and their constituents, the oncogenic role of the fusion proteins, the role of microRNAs and novel therapeutic targets in Ewing's sarcoma.

## **EWS-ETS Fusion Proteins**

ESFTs are characterized by a chromosomal translocation involving *the EWSR1* (Ewing's sarcoma breakpoint region 1) gene and the *ETS* (E26 transformation-specific) family of genes (11) (Figure 1.1). The most common translocation in 85% of patients afflicted with ESFT includes the fusion of *EWSR1* located on chromosome 22 band q12 and ETS family member *FLI1* (Friend leukemia integration 1 transcription factor) located on chromosome 11 band q24 (11). The result of this translocation,  $t(11;22)(q24;q12)$ , leads to the EWS-FLI1 chimera protein that functions as an aberrant oncogenic transcription factor (16-18). The N-terminal domain of EWS encompasses a potent transcriptional activation domain juxtaposed to the DNA-binding C-terminal domain of FLI1 (16, 19, 20). EWS-FLI1 isoforms exist in tumors which consist of translocations that combine a

**Figure 2.1: Schematic of most common EWS-FLI1 chromosomal translocation  $t(11;22)(q24;q12)$ .** Exons are denoted by black and white boxes. EWS and FLI gene breakpoint regions are indicated by EWSR1 and EWSR2, respectively. EWS-FLI1 fusion protein domains: SYQG, serine-tyrosine-glutamine-glycine rich regions (transactivation region); DNA-BD, DNA binding domain; Pro, proline-rich (activation domain). Image adapted from Delattre et al., 1994 New England Journal of Medicine 331:294-9 and Janknecht, 2005 Gene 363:1-14.

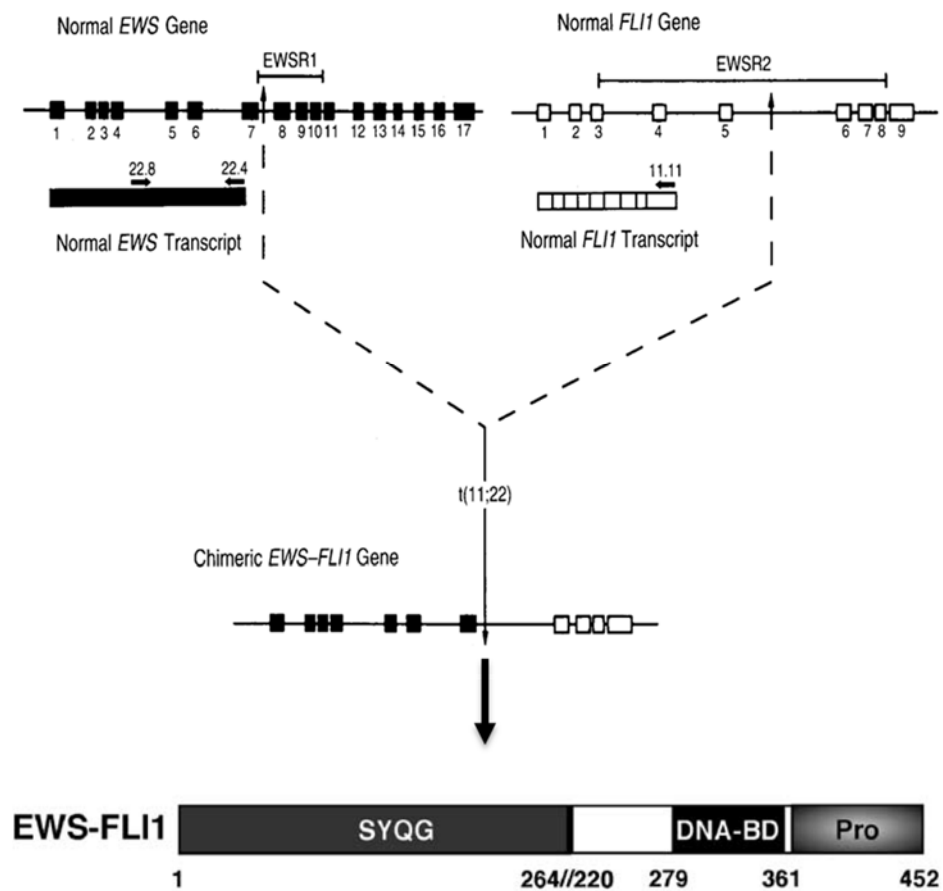
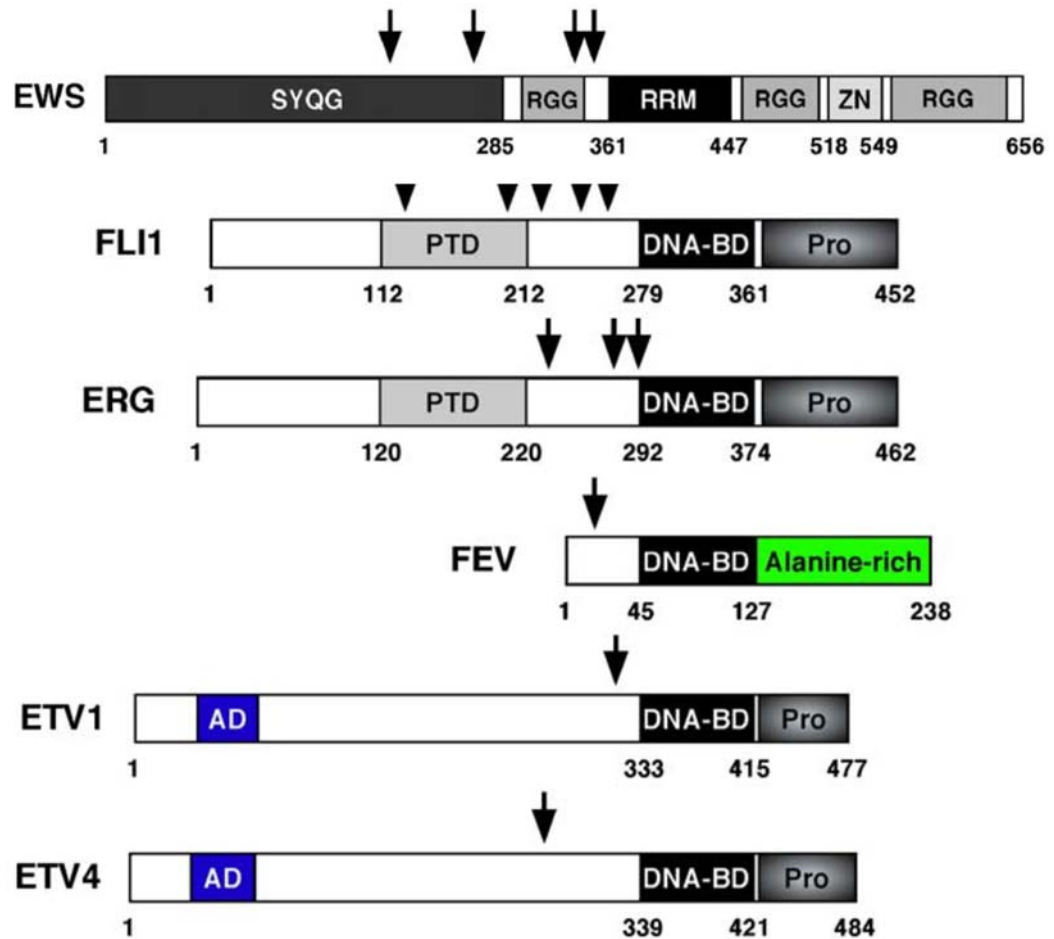


**Figure 1.2: Outline of EWS and five ETS proteins (FLI1, ERG, FEV, ETV1, ETV4)**

that participate in Ewing's sarcoma translocations. Arrows indicate observed breakpoints in EWS-ETS fusions. Image adapted from Janknecht, 2005 Gene 363:1-14.



truncated form of EWS at exons 7, 8, 9, or 10 to exons 5, 6, 7, or 8 of FLI1 (21), leading to chimeric variants which include the first 264 to 348 residues of EWS being fused to the last 191 to 324 residues of FLI1 (11). Breakpoints in the gene locus are in a small 8 Kb region in the *EWSR1* gene as opposed to the larger 35 Kb region in the *FLI1* gene (11). Research suggest that the amino and carboxy termini of EWS-FLI1 are integral for efficient cell transformation (16, 17). Different EWS-FLI1 isoforms have been shown to determine its transactivation potential which correlates with patient prognoses (21, 22). Tumorigenesis mediated by EWS-FLI1 has been shown to take place through DNA binding directly and indirectly, indicating that cell transformation was not completely dependent on DNA binding (23). Knockdown studies elucidated the oncogenic behavior of EWS-FLI1 showing growth inhibition, increased ability to undergo apoptosis, abolishment of anchorage-independent growth and attenuation of tumor formation in nude mice (8).

In EWS, other chromosomal translocations occur in 15 % of cases that involve the *ESWR1* gene binding ETS family members ERG (~10%) (24), ETV1 (<1%) (25), ETV2 (<1%) (26), FEV (<1%) (27) (Figure 1.2). These translocation variants result in fusion proteins that play a similar role as EWS-FLI1, but may vary in their ability to regulate gene transcription and transform cells (18).

### ***EWS* Gene**

*EWSR1* encodes the EWS protein which becomes fused to FLI1 in the majority of EWS cases (11). EWS contains an RNA recognition motif (RRM) and three regions rich in arginine-glycine-glycine (RGG) which are implicated in protein RNA-binding (11, 19). EWS has a zinc finger domain that may bind DNA, but most importantly, it contains a potent transcription activation N-terminal domain rich in serine-tyrosine-glutamine-glycine that is active when fused to a DNA-binding domain (16, 17, 28). EWS belongs to

the TET family of RNA-binding proteins that include TLS (translocated in liposarcoma) and TAF15 (TATA-binding protein associated factor 15) (29) TET family members have a high degree of homology and are involved in chromosomal translocations seen in various diseases such as EWS (EWS-ETS), myxoid liposarcoma (TLS-CHOP) and myxoid chondrosarcoma (TAF15-CHN) (11, 30). Multiple studies have shown that both TLS and EWS are post-translationally modified by Ser./Thr. protein kinases, such as PKC, and it is thought that this regulates their subcellular localization to the nucleus (31, 32). The N-terminus of EWS along with the other TET proteins are thought to function in RNA polymerase II (RNA pol II) transcription by interacting with RNA pol II subunits and TFIID (33). It has been shown that EWS-FLI1 may interact with similar RNA pol II subunits as EWS (34). Many experiments have suggested that TET proteins play a role in pre-mRNA splicing. This was confirmed by mass spec analyses. EWS and TLS carboxy terminal domains were found to interact with splicing activator YB-1. These studies suggest that TET proteins have a role as adapters between transcription and mRNA processing (35, 36).

### ***FLI1* Gene**

*FLI1* gene encodes the FLI1 protein which is the main fusion partner of EWS in EWS (11). FLI1 belongs to the highly homologous ETS family of transcription factors and is thought to have a role in oncogenesis (37). The N-terminal domain of FLI1 consists of the proline rich region that serves as a weakly- transactivating domain (NTA) that is displaced by EWS in the fusion protein. A strong DNA-binding domain is present at the C-terminal end of FLI1 along with another proline rich transcription activation domain (CTA) (38). Transcriptional activation or repression takes place in part when FLI1 or EWS-FLI1 recognizes a small core GGAA/T DNA sequence in the genome (39). Early on in embryonic development, FLI1 is expressed as a nuclear protein in mesenchymal

cells of neural crest and mesodermal origin (40-42). As an adult, FLI1 is expressed in hematopoietic cells located primarily in the thymus and the spleen due to expression in megakaryocyte, lymphocytes and erythroid precursors (43). Deletions of *FLI1* locus in mouse studies was embryonically lethal resulting in intra-cranial hemorrhaging and defective megakaryopoiesis (44, 45). These studies suggested that FLI1 plays a role in hematopoietic development. The oncogenic role of FLI1 was revealed in an animal model overexpressing FLI1 resulting in B cell proliferation, hypergammaglobulinemia and an autoimmune disorder (46). This confirmed FLI1's role in vasculogenesis. Further elucidation of FLI1's role in transformation and oncogenesis demonstrated FLI1 to inhibit expression of tumor suppressor retinoblastoma proteins (37). Cell survival is enhanced in erythroid cells by induction of Bcl2 expression by FLI1 (47). These studies show FLI1's ability to promote cell transformation and tumorigenesis.

### **EWS-FLI1 Targets**

The fusion protein is an oncogenic transcription factor with a potent transactivation domain fused to a DNA binding domain. EWS-FLI1 is able to modulate gene expression, thereby repressing or upregulating gene transcription leading to EWS formation (48). A myriad of genes have been identified through various knockdown studies and ChIP analysis demonstrating modulation by EWS-FLI1 (49). Binding to the gene promoter region by EWS-FLI1 can take place through direct DNA binding or through indirect binding via protein-protein interactions. To understand the mechanism of EWS-FLI1 driven pathogenesis, one must elucidate gene targets and protein-protein interactions. Target gene promoters have been shown to contain tandem binding sites for the ETS portion of the EWS-FLI1 and AP-1 proteins such as Fos-Jun dimers. The cooperative binding between the C-terminal portion of the fusion protein and Fos-Jun to promoter regions was found to be essential for EWS pathogenesis (50). This suggests

that the carboxy terminus of EWS-FLI1 not only interacts with DNA regulatory elements, but binds with other transcriptional regulators to promote oncogenesis. In addition to interacting with Fos-Jun, other basal transcriptional apparatus binding partners include CBP/p300 (51), BARD1 (52), RHA (53), NR0B1/DAX1 (54), TFIID (55) and RNA Pol II subunits hRPB3 and hRPB7 (34, 55).

Direct gene targets of EWS-FLI1 revealed by ChIP analysis contributes to EWS development. Downregulation of *TGF- $\beta$ RII* by the fusion protein at its promoter region has been shown to contribute to helping EWS cells evade growth inhibition (56). Knock-down studies revealed EWS-FLI1 transcriptional repression of *IGFBP-3* leading to increased cell survival by activating the Akt signaling pathway (57). Upregulation of Id2 by EWS-FLI1 may lead to the undifferentiated state of ESFT cells by interacting with the transcription factor E2A and, in turn, suppressing its DNA binding capability (58, 59). Cell growth and modulation of sensitivity to cytotoxic drugs is affected by the overexpression of *PTPL1* in EWS (60). Downregulation of *PLD2* by EWS-FLI1 correspondingly lead to decreased PDGF signaling, therefore, resulting in inhibited cell proliferation (61). Other direct targets of the fusion protein include Aurora kinase A, caveolin, GSTM4, GLI1, EZH2, uridine phosphorylase, *PDGF-C*, *CCND1*, MYC, *p21*, *p57*, hTERT, *VEGF*, *EAT-2*, *mE2-C*, *MFNG*, *DAX1* and *NKX2-2* (49).

The disordered nature of the fusion protein facilitates the formation of nuclear complexes that can modulate gene expression through both mRNA synthesis and splicing (62, 63). EWS-FLI1 interacts with part of the spliceosome and has been shown to regulate posttranscriptional splicing. The spliceosomal component U1C was identified as a protein partner in a yeast two hybrid approach experiment (62). In this study, EWS-FLI1 was demonstrated to alter the splicing site of E1A mRNA modifying its functionality. Other proteins such as TASR and YB-1 have been shown to be involved in the EWS-



FLI1 spliceosomal complex, but further research is needed to identify the spliceosome conformation (36, 64). A mechanism for modulation of gene expression may couple transcription initiation by the RNA Pol II interaction with mRNA splicing. EWS-FLI1 could potentially accompany RNA Pol II during transcription and simultaneously alter those transcripts through its interaction with the spliceosome.

### **Role of miRNAs in EWS**

MicroRNA (miRNA) are small, 20 to 30 nucleotide, non-coding RNAs that regulate gene expression through post-transcriptional modifications (65). One-third of the human genome has been estimated to be regulated by  $\approx 1500$  miRNAs (66). Silencing of mRNA translation occurs through miRNA selectively binding to a ~6-8 nucleotide sequence in the 3' UTR region on the target mRNA (65). miRNAs play a role in regulating normal cell function, development, embryogenesis, cell fate and maintenance of the cell (67-72). Due to miRNAs functions in carcinogenesis as tumor suppressors or oncomeres, therapeutically this presents a novel focus for determining prognostic markers and treatments for EWS patients (73, 74).

MiRNA processing begins with RNA polymerase II transcription resulting in long precursor miRNAs called pri-miRNAs. These pri-miRNA transcripts possess the sequence for one or more mature miRNAs that can arise from either protein coding genes or non-protein coding transcripts (75). Once pri-miRNA transcripts are generated, they fold into a stem-loop hairpin structure that is ~70 nucleotides long. This hairpin structure is stabilized by an RNA binding complex Drosha and DGCR8 where it is then cleaved by Drosha, generating pre-miRNA (75). The nuclear transporter, Exportin 5, assists in the diffusion of pre-miRNA from the nucleus to the cytoplasm (76). Dicer, with the help of TRBP, interacts with the pre-miRNA where further processing takes place resulting in a double-stranded miRNA (77). One of the two strands is selected to form

the RISC complex which contains the single miRNA strand bound to the Argonaute protein (78). This newly formed miRNA-RISC complex is able to inhibit protein expression through translational repression by targeting mRNAs 3'UTR or inducing mRNA degradation through an unknown mechanism (78). Understanding miRNA processing will most likely provide a window into how miRNAs are dysregulated in cancer and potentially lead to prevention and treatment of EWS. The interaction between the fusion protein and RNA pol II may lead to transcriptional repression of some miRNAs and potentially a gain of function of other miRNAs resulting in the oncogenic effects in EWS (79). Downregulation of TRBP, resulting in decreased levels of mature miRNA, has been shown in EWS and it has been theorized that TRBP may be a target of EWS-FLI1 (80).

EWS-FLI1 has been shown to potently induce miRNA expression profile differences, especially in miRNA-145 and let7a (80). Numerous miRNA expression profiling studies have been performed by knocking-down EWS-FLI1. In Ewing's sarcoma, miRNA expression was found to be deregulated in miRNA expression profile studies compared to controls (79, 81, 82). However, these studies revealed difference in expression profiles which may be a result of knock-down methods amongst other experimental design discrepancies. EWS-FLI1 and miRNA-145 were demonstrated to have an important role in EWS cell differentiation and tumor development (80). This was shown when EWS-FLI1 was introduced into human pediatric mesenchymal stem cells (hpMSC), resulting in miRNA-145 repression and induction of the EWS phenotype (80). Both EWS-FLI1 and miRNA-145 function in a reciprocating repressive feedback loop (80). SOX2, a target gene of EWS-FLI1 and miRNA-145 expressed in embryonic stem cells, was expressed in hpMSC upon induction of EWS-FLI1 (80). This may be a potential mechanism for EWS pathogenesis. Furthermore, Ban et al. confirmed EWS-

FLI1 and miRNA-145 are involved in a positive feedback loop and went on to show that miRNA-145 modulates the fusion protein by targeting the FLI1 3' UTR (81). Repression of let7a by EWS-FLI1 contributes to the tumorigenicity in EWS (80). Overexpression of let7a in *in vitro* studies revealed *HMGA2* translational repression resulted in decreased EWS cell proliferation (80). Synthetic delivery of let7a in EWS bearing mice inhibited EWS growth by regulating *HMGA2* (79). These studies demonstrated that a small group of downregulated miRNAs in EWS are responsible for reducing expression of pro-oncogenic targets in the IGF pathway (79).

Knock-down studies involving manipulation of EWS-FLI1 have demonstrated dysregulation of a myriad of miRNAs (79, 81, 82). This suggests that miRNAs have tumor suppressor and oncogenic functions that contribute to tumorigenesis of EWS. Functional analysis of miRNA34a, miRNA-31a, miRNA-125b and miRNA30a-5p have elucidated the impact that miRNA dysregulation can have on EWS pathogenesis. Overexpression of miRNA-34a in EWS cell lines demonstrated increased sensitivity to chemotherapy drugs and reduced the proliferative and malignant capabilities of the EWS cells (83). Nakatani et al. revealed miRNA-34a as an important prognostic marker in patient samples. Patients with increased miRNA-34a expression were relapse free for five years, but patients with downregulated levels of miRNA-34a were shown to have a recurrence within two years (83). Comparison of expression profiles of miRNA-31a in EWS cells and mesenchymal stem cells revealed decreased transcripts in EWS cells. When overexpressed in EWS cells, miRNA-31a contributes to increased apoptosis and decreased proliferation (84). MiRNA-125b has been shown to have both a tumor suppressive role and an oncogenic role. In A673 cells that have a type I fusion gene variant, miRNA-125b exhibits decreased expression levels. When overexpressed in A673 cell lines, there is a decrease in proliferation, migration, invasion, cell cycle arrest,

and increased apoptosis (79, 81, 82). MiRNA-125b was found to be upregulated in doxorubicin-resistant EWS cell lines. Knockdown of miRNA-125b increased sensitivity to doxorubicin in EWS cells; while studies overexpressing miRNA-125b demonstrated enhanced chemotherapeutic resistance (85). Franzetti et al. demonstrated the downstream effects of depleting EWS-FLI1 in A673 cells showing downregulation of miRNA-30a-5p (82). Overexpression of miRNA-30a-5p inhibited proliferation, invasion and CD99 in A673 cells (82). This study provided a link between the fusion protein and CD99.

### **Novel Therapeutic Targets in EWS**

Current treatment regimens of EWS include chemotherapy, radiation and surgery. The use of adjuvant chemotherapy following surgery and/or radiation resulted in significant improvements in outcomes (86). In the 1990s, ifosfamide and etoposide were added to the chemotherapeutic regimen, which already included vincristine, actinomycin D, cyclophosphamide and doxorubicin (87). Since then, the five year survival rate of EWS patients is ~60-70% when diagnosed with non-metastatic carcinomas and ~30% in patients that present with metastases at diagnosis (7). With these advances in treatment, EWS still has the worst prognosis of the bone sarcomas. The risk of developing a secondary malignancy, such as acute myeloid leukemia and myelodysplastic syndrome, is relatively high with the use of chemotherapy and radiation. The severity of these side effects using traditional therapies provides sufficient evidence that targeted therapeutic strategies must be developed.

The unique translocation resulting in EWS-FLI1 has been identified as a significant driver in EWS pathogenesis (16, 19, 88). Expression of EWS-FLI1 has not been demonstrated in any other cells other than EWS (89). Targeting EWS-FLI1 with antisense oligonucleotides, antisense RNA expressed from a vector and siRNA

delivered via nanoparticles inhibits EWS proliferation in cell lines and xenograft models (90, 91). Clinical implementation of this approach has proven to be a challenge due to a lack of efficient pharmacologic delivery mechanisms.

A more feasible approach may lie in disrupting interactions between EWS-FLI1 and its protein partners with small molecule inhibitors. The development of YK-4-279, a compound that blocks the interaction between EWS-FLI1 and RHA, was shown to decrease tumorigenic effects by inducing apoptosis in cell lines and inhibiting growth in xenograft models (92).

The use of small molecule inhibitors provides a novel approach to treating EWS. Overexpression of IGF-1R has been shown to promote cell growth and tumorigenesis. IGF-1R mediated signaling has been observed in EWS cell lines and tissue samples (93). The development of inhibitors targeting IGF-1R demonstrated toxicity in part because it acted on proximal portions of the signaling cascade. Combination of IGF-1R inhibitors and chemotherapy drugs may be a suitable therapeutic option. Knockdown studies inhibiting expression of the fusion protein in cell lines augmented p53 signaling activity (94, 95). This suggested EWS-FLI1 plays a role in repressing the tumor suppression activity of p53. Inhibitors Nutlin-3a, MI-219, Tenovins and actinomycin D have shown to stabilize and enhance p53 activity (96, 97). Rapamycin inhibits mTOR, the downstream effector of the PI3K-Akt signaling pathway, which mediates escape from apoptosis and cell proliferation (98). In EWS patients, the PI3K-Akt pathway may be over activated leading to disease development and progression (99). mTOR inhibitors block proliferation in EWS cell lines by arresting the cell cycle and concomitantly decreasing EWS-FLI1 levels (100). Inhibition of VEGF was shown to block the tumorigenic effects in EWS cell lines (101). Treatment with bevacizumab, a small molecule directed at the VEGF receptor, has been suggested, but the potential side effects to inhibiting VEGF signaling could disrupt angiogenesis in developing children

and adolescents, which could have deleterious effects during the maturation process. The receptor tyrosine kinase KIT and its ligand promote cell growth and cell survival in EWS cell lines (102, 103). The use of imatinib has been suggested to target the oncoprotein KIT. miRNA based therapeutics introduces promising candidate molecules such as miRNA-145, miRNA-143 and TRBP2 (80, 104).

The use of monoclonal antibodies targeting EWS-FLI1 has not been proven to be effective due to the disordered nature of the fusion protein. However, antibodies targeting proteins involved in EWS pathogenesis are a more likely therapeutic approach. Monoclonal antibodies directed at CD99 induce apoptosis in cell lines and slowed tumor progression in a xenograft model (105). A synergistic effect was seen when combined with doxorubicin and vincristine leading to enhanced growth inhibition (106). A less toxic approach targeting IGF-1R is being investigated using monoclonal antibodies Cixutumumab and Dalotuzumab. Both were both shown to inhibit IGF signaling and cell proliferation (107, 108).

### **The Origin of Ewing's sarcoma and the discovery of the tumor-initiating cell**

The cell of origin in EWS has remained elusive to investigators, however, along the path to determining a potential cell of origin, there have been some enlightening discoveries regarding cells permissive to EWS-FLI1 transformation and EWS subpopulations with TIC capabilities. In this section, I will describe the important studies that have contributed to determining the origin of EWS and the discovery of EWS TICs that partially resulted from this endeavor.

The largest gap in understanding EWS pathogenesis for the past two decades has been in elucidating a cellular origin that can be adapted to an animal model. Recently, a CRISPR/Cas9 approach was utilized to generate the chromosomal

translocation t(11;22) in stem cells resulting in the most common EWS fusion transcript (109), EWS-FLI1, however, the approach has not been translated to an animal model, nor has it lead to revealing a cell of origin that capitulates EWS tumorigenesis.

Histological observations of EWS tumors demonstrated a poorly differentiated phenotype with a morphology described as having sheets of round blue cells when stained with PAS (8). Early studies using immunohistochemistry indicated neuroectodermal and mesenchymal features based on surface marker expression profiles (8). Initially, NIH3T3 murine embryonic fibroblasts were transformed with EWS-FLI1 resulting in anchorage independent growth using a soft agar assay and increased tumorigenesis in mice compared to NIH3T3 control cells (110). In this model and others, functional IGF1R signaling was shown to be an early requirement for EWS-FLI1 mediated transformation (15, 110). Subsequent studies transducing human primary fibroblasts with the EWS-FLI1 fusion gene lead to induction of p53-dependent growth arrest and apoptosis. Further studies demonstrated that deletion of p53, p19<sup>ARF</sup> and p16<sup>INK4A</sup> allowed stable EWS-FLI1 expression in fibroblasts (15).

The continued search for a cell permissible to stable EWS-FLI1 expression found murine mesenchymal progenitor cells (MPCs) as a viable cell suitable for the fusion gene (15). Here, MPCs were isolated from the bone marrow of C57BL/6 mice and transduced with EWS-FLI1. MPCs expressing the fusion gene formed tumors in mice that had a round blue cell phenotype. The tumors expressed the EWS marker CD99 in the context of functional p53 and p19<sup>ARF</sup> expression. Stable expression of EWS-FLI1 in the presence of p53 and p19<sup>ARF</sup> previously prevented transformation and lead to apoptosis in primary fibroblasts. Similar to the findings in transformed NIH3T3 cells, these EWS-FLI1 expressing murine MPCs demonstrated significantly elevated IGF1 expression and upregulated IGF1R signaling. These findings provided the basis to proceed to transducing human MPCs with the fusion gene (15).

The findings in human mesenchymal stem cells (hMSCs) transduced with EWS-FLI1 (111) were very similar to the observations in transformed murine MPCs (15). Induction of CD99 was reported along with increased IGF1R signaling (111). Moreover, the studying found that these transformed cells maintained trilineage differentiation potential and upregulation of genes implicated in neural crest and neuronal development which supports the neuroectodermal origin hypothesis. A major roadblock to supporting hMSCs as the cell of origin for EWS was encountered when the EWS-FLI1 expressing hMSCs failed to form tumors in mice. However, there were significant similarities in the gene expression profile with primary EWS tumors. These observations demonstrated a shared gene program between EWS tumors and hMSCs induced with EWS-FLI1, which prompted this same group to explore permissibility in pediatric hMSCs, since EWS develops in children and young adults, and the hMSCs that they were using were from older patients. An interesting finding in this study, however, elucidated EZH2 expression was significantly increased in EWS-FLI1 expressing hMSCs . Importantly, EZH2 functions as a histone methyltransferase within the polycomb repressor complex 2 and has been described to be crucial for self-renewal and differentiation. This discovery suggested the potential emergence of a cancer stem cell phenotype that was pursued in subsequent studies by the Riggi lab.

The cancer stem cell population in EWS was discovered by probing for the cancer stem cell marker CD133 (14). The small EWS subpopulation expressing CD133 on their surface was sorted using a fluorescently tagged antibody recognizing the CD133 epitope on EWS primary cells. Serially xenotransplanting CD133+ and CD133- cells in a limiting dilution approach revealed that only CD133+ EWS cells could form tumors in mice. Tumors derived from CD133+ cells were analyzed by FACS and it was observed that the tumors retained their small subpopulation of CD133+ cells, while giving rise to a bulk tumor with a CD133- cell population. FACS analysis combined with serially



transplanting these cells two more times in NSG mice suggested that CD133+ EWS cells had the ability to self-renew and repopulate tumors with a differentiated cell type that comprises the bulk tumor. These findings are consistent with the current description of cancer stem cells. These findings were further supported, *in vitro*, by culturing CD133+ EWS cells in sphere assay that utilizes low adherence and serum free growth conditions. Only CD133+ cells formed spheres and they had significantly elevated levels of the stem cell factors OCT4 and NANOG, which suggested that these cells had a stem cell-like phenotype.

After discovering CD133+ EWS cells had bona fide cancer stem cell traits, this finding provided a phenotype to look for other cells that were transduced with EWS-FLI1 in order to determine a cell of origin. Human pediatric mesenchymal stem cells (hpMSCs) were the next logical cell to investigate. hpMSCs transduced with the fusion gene and cultured as spheres underwent reprogramming with a significantly greater induction of ESC genes compared to adult hMSCs (104). A strong induction of glycosylated CD133 was observed in transduced hpMSCs and an even greater induction in CD133 was reported in cells grown under sphere assay conditions as previously performed with primary EWS cells. Transduced hpMSCs expressing CD133 were analyzed by FACS and this revealed a small population, similar to EWS tumor cells. The CD133+ hpMSCs also had significant upregulation in OCT4, NANOG and SOX2 as seen previously with primary cells. Despite the permissiveness to EWS-FLI1 transduction and the remarkable similarities between the CD133+ hpMSCs and EWS primary CD133+ cells, hpMSCs transduced with the fusion gene were unable to form tumors in mice. The major finding in this paper revealed miR-145 to be significantly downregulated in CD133+ EWS-FLI1 expressing hpMSCs. miR-145 has been reported to maintain a differentiated phenotype by targeting virtually all of the known genes directly responsible for stemness.

Following the characterization of miR-145 in CD133+ hpMSCs expressing the fusion gene, De Vito et al. investigated the role of this miRNA in CD133+ primary EWS cells (80). They revealed that miR-145 was downregulated in CD133+ primary cells and the decrease in miR-145 expression contributed heavily to CSC properties in EWS. Moreover, TARBP2, a miRNA processing protein, was also downregulated and determined to be responsible for a global effect on miRNA dysregulation which included miR-145. An interesting finding in this study was that primary EWS cells grown as spheres, compared to adherent growth conditions, displayed tumorigenic capabilities and also had significantly decreased miR-145. This finding is particularly important because it described a mechanism to enrich for the stem cell population in EWS which is something that I took advantage of with EWS cell lines. Another study confirmed that primary EWS cells grown as spheres displayed a significant increase in expression of NANOG and OCT4 compared to adherent cells cultured with serum (112).

The cell of origin still remains elusive and it must be acknowledged that hMSC are very likely within the lineage of the cell of origin, but no conclusive evidence supports MSCs as the definitive cell. This is important because studies have used MSCs as a control for comparison, which is an approach that the evidence just doesn't support (113). The likely cell of origin is an early mesenchymal cell derived from the neuroectoderm that has multipotency towards both a neural crest cell and bone-derived mesenchymal cell fate. This assertion is supported by the literature. At this point, studies knocking down either CD99 or EZH2 in EWS cells drives differentiation towards a neural crest stem cell or neuronal stem cell fate (114-116). This is further supported in hMSCs and hpMSCs transduced with the fusion gene (104, 111). These transduced mesenchymal cells displayed neural crest stem cell gene expression profiles. On the other hand, EWS cells surviving EWS-FLI1 knockdown are driven towards a mesenchymal differentiation path that ends with cells representing osteocyte, adipocyte

or chondrocyte profiles (115). Studies knocking down CD99 and EWS-FLI1, separately and together, described a stoichiometric relationship between the two molecules that maintains a transformed oncogenic state capable of both neuronal and mesenchymal fates (115). With the use of generating chromosomal translocations using CRISPR/CAS9 and further investigations in cells derived from the neuroectoderm with both MSC and neural crest stem cell lineage potential, discovering a cell of origin that can be used to generate animal models for therapeutic studies is an attainable goal.

The role of EWS-FLI1 as the primary driver of tumor formation in EWS patients has provided insight into developing novel therapies to treat this highly malignant disease. Although progress is being made in developing small molecule inhibitors, further research is needed to elucidate the mechanisms whereby the fusion protein gene targets and protein partners initiate EWS pathogenesis. Evidence provided by Riggi et al. demonstrating EWS-FLI1 ability to transform mouse MPC advances the research field one step closer to developing a much needed animal model which would provide a platform for studying EWS development and drug testing. miRNA mediated tumorigenesis in EWS patients has led to the discovery in new prognostic markers and therapeutic targets which could eventually have a significant impact in disease treatment.

### **Tumor-Initiating Cells (TICs) Introduction**

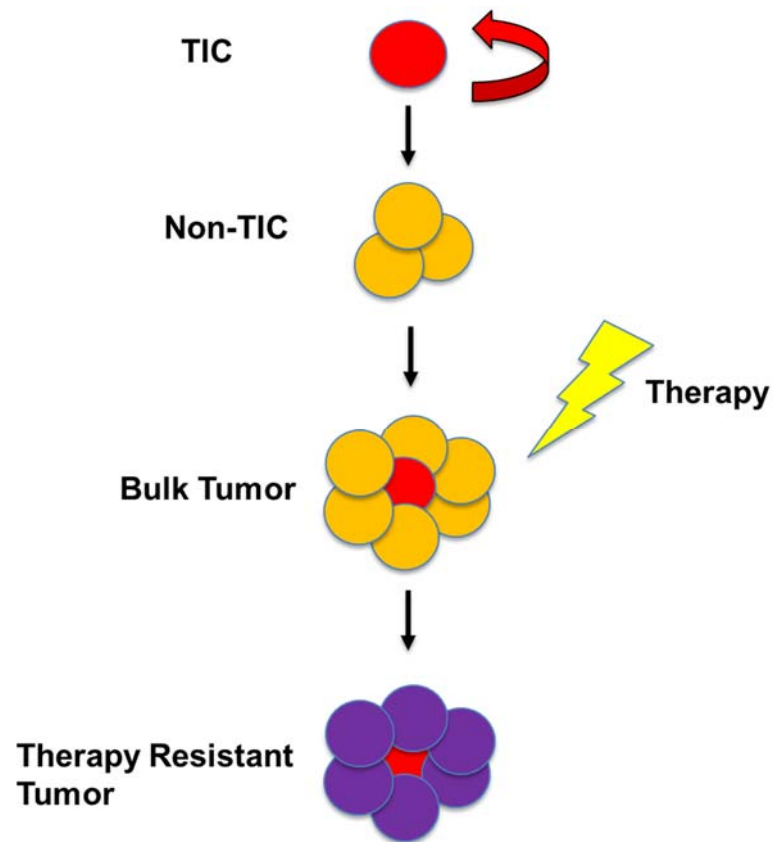
Aggressive tumors resulting from relapse and metastasis present a major therapeutic challenge that must be addressed to successfully cure cancer patients and until this challenge is met, patients with these advanced diseases will continue to have poor outcomes. Strategies utilizing conventional chemotherapy and radiotherapy currently remain ineffective when treating patients with aggressive malignancies and mounting evidence suggests this failure is the result of standard-of-care therapies

lacking the ability to target the heterogeneous population of tumor cells (Figure 1.3) (112, 117, 118). Tumor-initiating cells (TICs) contribute significantly to functional heterogeneity through a process of self-renewal leading to the preservation of a small tumor-initiating population, and by asymmetric division resulting in non-tumor forming daughter cells that compose the bulk of the tumor (119). This ability of TICs to maintain their own numbers through self-renewal and ability to give rise to a differentiated rapidly proliferating population is associated with embryonic stem cell (ESC) properties (119). Recent studies have shown that epigenetic modifiers along with the induction of ESC genes sustain self-renewal in TICs leading to long-term maintenance of tumors (104). Low oxygen (hypoxic) tumor microenvironments can induce an ESC expression profile in non-TICs representing a cellular reprogramming event into a TIC (120). Hypoxic tumor niches exploit this cancer cell plasticity phenomenon by promoting an aggressive phenotype by enriching for TICs (120).

### **Defining Stemness**

TICs comprise a small subpopulation of tumor cells that have the capacity for tumor initiation and demonstrate a phenotype similar to normal stem cells. Cells with stem cell-like properties can be defined as cells with the ability to self-renew while giving rise to cells that lack self-renewal potential and are unable to repopulate tumors. TICs possess these stem-like abilities by maintaining their small population through self-renewal and are able to give rise to a non-tumorigenic cell population that make up the bulk of many heterogeneous tumors including EWS. Self-renewal represents a key biological process where a TIC can preserve its population through either symmetric or asymmetric division. Symmetric division leads to the generation of two daughter cells that preserve the TIC phenotype, whereas, asymmetric division results in an

**Figure 1.3: General schematic of TIC model.** Cancer stem cells or TICs maintain their population through self-renewal (red arrow) and divide into differentiated non-TICS that populate the bulk tumor. Standard chemotherapy or radiation therapy (lightening symbol) results in therapy resistant tumor cells (purple cells) either through the selection of therapy resistant TICs or through mutational changes in TICs that results in therapy resistant subclones.



undifferentiated TIC and a differentiated non-tumor-initiating daughter cell that compose the bulk of the tumor (119).

Historically, much controversy has surrounded the terms TICs and cancer stem cells (CSC). CSCs along with normal stem cells both have self-renewal programs, however, the controversy lies in the uncertainty whether CSCs arise from normal stem cells or from differentiated cells that undergo a malignant transforming event. The term “CSC” suggests the former, but it is poorly understood if normal stem cells give rise to CSCs. To avoid this ambiguous and controversial terminology, it has been suggested by the field to refer to cells with stem cell programs that can initiate tumor formation as TICs. Characterization of TICs using functional tumor-initiating cell assays have been developed that define suspected TICs as demonstrating the following: (1) generation of tumors in an *in vivo* serial xenotransplantation assay, (2) demonstration of self-renewal using a xenograft assay by serial passaging at clonal cell doses, and (3) giving rise to proliferative daughter cells that comprise the bulk tumor but are unable to establish tumors by themselves (119).

### **Heterogeneity and the TIC Model**

Intratumoral heterogeneity is suspected to be a main contributor to relapse, metastasis and ultimately leading to therapy resistance. Mounting evidence suggests that intratumoral heterogeneity adopts a cellular hierarchical organization placing TICs at the apex (112, 117-119). As previously described, these cells are capable of self-renewal and have the ability to give rise to differentiated rapidly proliferating cells that compose the bulk tumor and are unable to form tumors. Contributing to this hierarchy includes variations in gene expression, epigenetic differences and tumor microenvironment (TME) influences (121). Genes that play a prominent role in self-renewal in TICs and are crucial for maintaining pluripotency, include SOX2, OCT4 and

NANOG (122). These embryonic stem cell factors have been demonstrated to be significantly upregulated in TIC populations compared to the differentiated cells (104). Recent studies have shown that epigenetic modifications including DNA methylation, histone modification and miRNAs sustain self-renewing in TICs leading to long-term maintenance of tumors (121). Key epigenetic repressors involved in TIC self-renewal include the Polycomb group repressor complexes, DNA methyltransferases and miRNA (123, 124). Hypoxic microenvironments have been shown to enrich for TICs and maintain this stem cell phenotype through stabilized HIF-2 $\alpha$  (120). Expression of HIF-2 $\alpha$  under chronic hypoxic conditions directly upregulates OCT4 by binding to its promoter and in turn is associated with maintaining stemness (125).

The classical approach to isolating and elucidating TIC populations utilized fluorescently activated cell sorting (FACS) for surface markers followed by serially passaging xenografts and confirmation of repopulating the tumor similar to the parental tumor. TIC surface markers for acute myeloid leukemia (CD34+ CD38-) (126), EWS (CD133+) (14) and breast cancer (CD44+ CD24-) (127) revealed TIC populations that were confirmed by an *in vivo* limiting dilution assay. However, in tumors that relapsed and underwent metastasis, particularly in EWS, the CD133- population was able to form tumors (112). This finding suggested heterogeneity within TIC populations and moreover, supports a needed genetic and epigenetic approach to determine intratumoral TIC populations.

Heterogeneity within the TIC subpopulations has been recently described in metastatic renal cancer where RNAseq revealed primary tumors with genetically and geospatially distinct subclones (128). These subclones gave rise to metastatic lesions in the lung and liver within the same patient. This study was limited by bulk sequencing, which fails to elucidate intratumoral diversity within TIC populations. To better

understand lineage maps that describe the hierarchical organization and branching evolution within tumors, sequencing at single cell resolution is required. Recently in breast cancer, single cell-seq was used to determine the small subpopulation in primary tumors that gives rise to metastatic cells (129). This finding elucidated the hierarchical organization and intratumoral TIC heterogeneity in breast cancer.

### **Approaches to studying stemness and heterogeneity**

To develop targeted therapies for TICs, studies utilizing multiple approaches to identify and isolate TICs must be used to improve therapies in this resistant subpopulation. Assays currently being employed to identify TICs, measure the following: sphere-formation, *in vivo* growth using serial xenotransplantation, dye efflux, chemoresistance, embryonic stem cell expression, aldehyde dehydrogenase activity (ALDH), cell surface marker expression and more recently, single cell sequencing (129, 130).

In EWS, cells expressing the suspected TIC surface marker CD133 were isolated from EWS tumors and demonstrated to be a viable TIC subpopulation (14). In this study they cell sorted CD133+ cells and serially xenotransplanted these cells in NOD/SCID mice. Using this limiting dilution approach, Suva et al. demonstrated that primary CD133+ cells could initiate tumors and give rise to heterogeneous populations of CD133+ TICs and differentiated CD133- daughter cells. These findings suggested that CD133+ cells could self-renew and give rise to differentiated cells that repopulated the bulk tumor. Moreover, in this study and others, CD133+ cells could form spheres in an *in vitro* sphere assay where CD133- cells could not. Sphere assays assess the cells ability to behave like TICs in an *in vitro* setting. Multiple studies measured the expression of embryonic stem cell factors OCT4, SOX2 and NANOG in primary CD133+ cells and CD133+ spheres (14, 104, 112). They observed, under both conditions, that CD133+



cells expressed significantly elevated levels of OCT4 and NANOG compared to both primary CD133<sup>-</sup> cells and cells grown under adherent conditions. Upregulation of these stem cell genes in the CD133<sup>+</sup> EWS cells further supports a TIC phenotype. Expression of stem cell genes have been widely reported to be crucial for maintaining self-renewal, pluripotency and an undifferentiated state (122).

Labs investigating chemoresistance in EWS TICs found that both primary EWS cells and cell lines expressing high levels CD133, ALDH and dye efflux activity demonstrated enhanced resistance to chemotherapies (112, 131). In addition to CD133 serving as a TIC marker in EWS, cells with high ALDH activity have been observed in hematopoietic and neural stem cells (132, 133). ALDH is a detoxifying enzyme that oxidizes intracellular aldehydes and it's been suggested that this function plays a role in maintaining stemness (134). Cells with high dye efflux capabilities have been described to have elevated ATP-binding cassette transporter activity and these efflux pumps are suggested to underlie a mechanism for drug resistance (130).

A remaining challenge to studying TICs in EWS lies in determining the geographically separated genetic subclones that contribute the heterogeneity in EWS. Multiple regional tumor biopsies coupled with single cell sequencing will lead to the next major advancements in understanding the cancer. Functional screening will be needed to confirm suspected TICs and further elucidate intratumoral TIC heterogeneity.

### **The Hypoxic EWS Tumor Microenvironment Introduction**

Recently, importance has been placed on the role of the tumor microenvironment (TME) in promoting tumor formation and how the interaction between cancer cells and the TME can lead to relapse, metastasis and ultimately, therapy resistance (135, 136). Targeting the TME in patients with aggressive malignancies is an emerging area and

remains an opportunity to develop new therapies. EWS tumors display a diverse TME where 85% of patients are diagnosed with malignancies primarily localized within bone, but in 15% of patients, EWS arises within extra-osseous soft tissues (7). Moreover, aggressive tumors develop metastatic lesions in the lungs and at distant bony sites (137). This TME consists of tumor cells, osteoblasts, osteoclasts, immune cells, endothelial cells, mesenchymal cells, cancer-associated fibroblasts (CAFs), etc. Acellular components of the TME consists of extracellular matrix, various soluble factors and extracellular vesicles that support the tumor niche . Importantly, low oxygen levels or hypoxia is a critical feature of the TME and is associated with an aggressive phenotype and poor prognosis in cancer patients.

Developing tumors demonstrate proliferation rates that depend significantly on an adequate blood supply. Rapidly proliferating cells often outgrow their vascular supply leading to periods of acute hypoxia (138). Tumor cells undergoing hypoxia adapt to these low oxygen levels by upregulating and stabilizing hypoxia inducible factors (HIFs) HIF -1 $\alpha$  and -2 $\alpha$  (138). Tumor cells undergoing a transient decrease in oxygen delivery stabilize HIF-1 $\alpha$  (139), which drives downstream gene expression programs involved in shifting metabolic function from oxidative phosphorylation to glycolysis and stimulating angiogenesis (138). This cycling pattern results in a reciprocal relationship between proliferation rates and vessel growth that significantly contributes to the expanding tumor. The nature of this regional fluctuation in tumor growth has been primarily attributed to HIF -1 $\alpha$  activity mediating the adaptive response to acute hypoxia. However, in some contexts, HIF -2 $\alpha$  has been demonstrated to have an overlapping and compensatory role in the absence of HIF -1 $\alpha$  (138). As a consequence of rapidly proliferating tumor cells and the formation of abnormal vasculature, aggressive tumors develop regions within the core and throughout the tumor mass that experience limited

oxygen perfusion for extended periods of time. The initial cellular response in these areas is mediated by HIF -1 $\alpha$  which is maximally stabilized between 5-8 hours and then decreases its expression as it reaches homeostasis within the hypoxic TME (138). In addition to upregulating genes involved with angiogenesis and metabolism, HIF -1 $\alpha$  induces antiapoptotic gene programs to enhance survival (140). After prolonged or chronic exposure to the hypoxic microenvironment, HIF -2 $\alpha$  becomes stable and is maximally expressed generally between 24 and 48 hours (139). Genes mainly associated with an oncogenic phenotype, especially ESC programs that contribute to generating TICs, is driven by HIF -2 $\alpha$ , however, in some contexts, overlap exists between HIF -1 $\alpha$  and HIF -2 $\alpha$  (138). These chronic hypoxic TMEs are associated with necrotic regions and substantial evidence correlates these regions with aggressive tumors and poor outcomes (141).

In EWS, a clinical study reported primary tumors from patients with necrosis demonstrated a strong correlation with the worst overall survival and had an increased chance for metastasis (142). A separate study observed significant expression of HIF -1 $\alpha$  in 18/28 EWS patient tumors, however, no data was presented that linked patient outcomes with HIF expression (143). Studies investigating hypoxia in EWS have mainly focused on the role of hypoxia on metabolism, survival, anchorage-independent growth, migration and invasion and the effects of HIF -1 $\alpha$  on EWS-FLI (143-147). Few studies have documented the expression of HIF-2 $\alpha$  in hypoxic EWS cells and currently, the temporal expression of HIF -1 $\alpha$  and HIF -2 $\alpha$  remains unknown.

## **Overview of Hypoxia and Hypoxia Inducible Factors**

Hypoxia is an essential feature of the microenvironment in many solid tumors. Tumor cells adapt to low oxygen environments by stabilizing HIFs that can induce gene expression involved with metabolism, angiogenesis and cell survival (138). HIFs belong

to the (P)ER-(A)RNT-(S)IM family that function as basic helix-loop-helix DNA binding proteins (bHLH-PAS) (148-150). These transcription factors consist of oxygen sensitive  $\alpha$  subunit isoforms (HIF-1 $\alpha$ , HIF-2 $\alpha$  and HIF-3 $\alpha$ ) and a constitutively active  $\beta$  subunit (HIF-1 $\beta$ ) that forms a heterodimer (Figure 1.4) (150-152). Under normoxia (21% O<sub>2</sub>), the HIF  $\alpha$  subunits are constitutively transcribed and translated, however, their stability is inhibited by hydroxylation of specific proline and arginine residues that mark the protein for proteasomal degradation (153-155). In hypoxic conditions, the  $\alpha$  subunits are stabilized and translocate to the nucleus where they dimerize with HIF-1 $\beta$  and go on to stimulate transcription in a DNA binding dependent manner (156, 157).

The HIF family consists of conserved protein domains throughout both the  $\alpha$  and  $\beta$  subunits. The HIFs have an N-terminal bHLH domain (required for DNA binding) and PAS-A and PAS-B domains (required for heterodimerization). Homology between HIF-1 $\alpha$  and HIF-2 $\alpha$  bHLH and PAS domains is roughly 85% and 70%, respectively. The high degree of sequence similarities in these domains results in the potential for significant overlap in DNA binding (158). Both HIF-1 $\alpha$  and HIF-2 $\alpha$  contain N- and C-terminal transactivation domains (N-TAD and C-TAD) that are required for HIF target gene activation. Within the HIF  $\alpha$  subunits, the oxygen-dependent degradation (ODD) domain confers oxygen dependent stabilization (153, 154, 159-161). The ODD domain contains proline and asparagine residues that are hydroxylated during normoxic conditions (162). HIF-3 $\alpha$  contains the N-terminal bHLH, PAS and N-TAD domains, but lacks the C-TAD domain. Many HIF-3 $\alpha$  splice variants have been reported and the most common isoform, HIF-3 $\alpha$ 4, lacks both TAD domains and functions as a negative regulator of HIF-1 $\alpha$ . (163, 164) Target gene specificity for both  $\alpha$  subunits is regulated by the TAD domains. Target gene overlap between HIF-1 $\alpha$  and HIF-2 $\alpha$  is regulated by the C-TAD while gene specificity is conferred by the N-TAD (165-167). Selectivity is suggested to be facilitated



by distinct transcriptional cofactors that recognize the N-TAD in a specific  $\alpha$  subunit (167).

Regulation of the HIF-1 $\alpha$  and HIF-2 $\alpha$  under normoxia occurs through posttranslational modifications. In normoxic conditions, the  $\alpha$  subunits are transcribed and translated, however, stable expression is not maintained in the presence of higher oxygen tension levels, resulting from their proteasomal degradation. Prolyl-4-hydroxylases (PHD 1-4) hydroxylate proline residues in the ODD domain of the  $\alpha$  subunits (168, 169) leading to recognition of the hydroxyl groups by the von Hippel Lindau (VHL) E3 ubiquitin ligase complex. Upon binding to VHL, the  $\alpha$  subunits are poly-ubiquitinated, marking them for proteasomal degradation (153, 170, 171). PHD2 has a stronger effect on HIF-1 $\alpha$  while PHD3 has more of an influence on HIF-2 $\alpha$  (169). To catalyze the hydroxylation of the proline residues (Pro-402 and Pro-564 in HIF-1 $\alpha$ ; Pro-405 and Pro-531 in HIF-2 $\alpha$ ; Pro-492 in HIF-3 $\alpha$ ), the PHDs require iron,  $\alpha$ -ketoglutarate, ascorbate and oxygen (155, 172). LXXLAP motifs within the ODD domains contain the proline residues targeted by the PHD's (163, 173). In addition to regulation of HIF stability by the PHDs, inhibition of HIF transactivation potential is another means to downregulate HIF function. Factor Inhibiting HIF (FIH) disrupts HIF transactivation potential by hydroxylating asparagine (Asn-803 in HIF-1 $\alpha$ ; Asn-847 in HIF-2 $\alpha$ ) residues within the C-TAD domains in both  $\alpha$  subunits (174, 175). Hydroxylation in the C-TAD domain blocks the interaction between the HIFs and co-factors involved in mediating target gene specificity (176). Major oxygen independent regulators of HIF stability include proteins involved with E3 ubiquitin ligase activity such as receptor of activated protein kinase C (RACK 1), hypoxia associated factor (HAF) and carboxyl terminus of Hsp70-interacting protein (CHIP) (177-179).

HIF target genes contain hypoxia-response elements (HRE) with a consensus sequence of 5'-(A/G)CGTG-3' that are located near the proximal promoter in open chromatin regions (180, 181). Mounting evidence suggests functional HREs require interactions between the HIFs and other DNA-binding proteins such as FOS, CREB, CEBPB and SP1 (181, 182). Luciferase reporter assay experiments mutating HRE and proximal binding sites revealed a significant decrease in transcription, suggesting the HIFs ability to induce transcription either through cooperative DNA-binding or through recruitment of (183) HIF1 $\alpha$  cooperatively recruit RNAPoIII to HREs (184).

The most well-known HIF target genes regulate biological processes involved with metabolism and oncogenesis (162). Extensive research has investigated the role of HIF1 $\alpha$  in upregulating genes central to the metabolic shift from oxidative phosphorylation to glycolysis and regulation of oxygen supply and consumption (162). In addition to modulating oxygen homeostasis, other HIF targets directly influence pro-oncogenic pathways such as autophagy, cell survival, migration and invasion, stemness and resistance to chemotherapy (181, 185, 186). Target gene selectivity between HIF-1 $\alpha$  and HIF-2 $\alpha$  underlies a complex mechanism that depends on cell type, culture conditions, hypoxia severity and duration, and the mutational landscape of HIF regulatory proteins and miRNAs. Much attention has been focused on the severity and duration of hypoxic exposure relative to HIF-1 $\alpha$  and HIF-2 $\alpha$  expression. HIF-1 $\alpha$  is typically expressed under acute hypoxia (6-24 hrs) in more severe hypoxic conditions (0.1-1% O<sub>2</sub>), and targets genes involved in metabolism (PFK, LDHA, MCT4 and CA-IX)) and apoptosis (BNIP3). Temporal expression of HIF-2 $\alpha$  ranges from 24 hrs-days under moderate hypoxic conditions (1-5% O<sub>2</sub>) and target genes involved in stemness (OCT4) and oncogenesis (LOX, MMP1 and TWIST) (187). Common genes expressed by both HIFs include VEGFA and GLUT1 (187), however, the overlap between HIF-1 $\alpha$  and HIF-2 $\alpha$  is

dependent on the cellular context. Additional factors that influence HIF transactivation specificity include the recruitment of coactivators such as CBP and p300 (151).

### **Hypoxia, HIFs and Cancer Stem Cells**

Hypoxia is required for embryogenesis and maintenance of stem cell pluripotency (187). In solid tumors, hypoxia is an essential feature of the microenvironment and it is suggested that cancer stem cells (CSC) are enriched in hypoxic regions within the tumor (188). CSCs are suspected to underly the driving force behind tumor initiation and progression and is associated with aggressive therapy resistant tumors (112, 189, 190). Induction of ESC genes, SOX2, OCT4 and NANOG, consistent with CSCs have been demonstrated to be directly increased by hypoxia (120). Furthermore, iPSC reprogramming efficiency has been enhanced by hypoxia (191). Recently, mounting evidence suggests that the HIFs regulate the CSC subpopulation. Both HIF-1 $\alpha$  and HIF-2 $\alpha$  have been shown to promote de-differentiation through Notch signaling (192). In normal ESCs, HIF-1 $\alpha$  has been suggested to play a more important role, while in glioblastoma CSCs, both HIF-1 $\alpha$  and HIF-2 $\alpha$  were essential for maintaining the undifferentiated state (193). Other studies have reported that HIF-2 $\alpha$  was exclusively expressed in CSCs and HIF-1 $\alpha$  was stabilized under severe hypoxia in both stem and non-stem cells (194). These findings are further supported given that necrotic regions within tumors represent areas exposed to severe hypoxia or anoxia for prolonged periods of time (142). In addition, tumor necrosis and HIFs are both associated with poor patient outcomes, however, necrosis has been associated with aggressive tumors in EWS, but it remains unknown what role the HIFs play in these patients (143). A key gene target of HIF-2 $\alpha$  is the ESC gene OCT4 and as a result, functions to maintain the CSC subpopulation and promote oncogenesis (125). In prostate cancer, SOX2 knockdown lead to decreased sphere formation. SOX2 was



observed to be directly upregulated by both HIF-1 $\alpha$  and HIF-2 $\alpha$  and silencing of either HIF resulted in a decrease in SOX2 expression. Interestingly, sphere formation in shHIF-2 $\alpha$  cells was significantly inhibited compared to shHIF-1 $\alpha$  and control cells (120). These findings suggest overlapping or potentially interdependent roles between HIF regulation of stemness. In glioma, similar findings were observed where both HIF-1 $\alpha$  and HIF-2 $\alpha$  knockdown cells demonstrated comparable deficits in *in vitro* sphere formation and *in vivo* tumor formation (194). Another study in glioma revealed activation of Akt signaling leading to enrichment of the CD133+ CSCs when cultured under hypoxia, however, HIF-1 $\alpha$  was suspected to drive this process, but this study did not account for HIF-2 $\alpha$  (195).

### **Hypoxia Regulated miRNAs in Cancer**

Emerging evidence suggests that miRNAs participate in mediating the hypoxic response in normal and oncogenic cells (196). Recently, miRNAs were found to be consistently upregulated across multiple studies in different cancer models (Table 3.1) (197-199). These hypoxia regulated miRNAs (HRM) are differentially expressed in hypoxic conditions under the control of HIF-1 $\alpha$ -dependent and -independent mechanisms (197, 200). HRMs regulated directly by HIF-1 $\alpha$  contain hypoxia response elements (HRE) in their promoter region and can be bound by the HIF-1 dimerized complex (197). In addition, stabilized HIF-1 $\alpha$  under hypoxia can elevate expression of transcription factors that can directly increase HRM expression (201). HIF-1 $\alpha$ -independent induction of HRMs have been shown to be regulated by signaling cascades, such as Akt/mTOR, with elevated activity under hypoxic conditions (200). Previous reports have demonstrated increased miRNA biogenesis under hypoxia as result of Ago2 accumulation, however, these studies remain unclear and implicate both HIF-1 $\alpha$ -dependent and -independent pathways that require further investigation (202, 203).

## **miR-210, the Master Hypoxia Regulated miRNA**

miR-210 is considered a master HRM due to its consistent enrichment and phenotype in normal and oncogenic cells exposed to hypoxia (204). Accumulation of miR-210 in hypoxic cells is regulated by HIF-1 $\alpha$ -dependent and -independent pathways previously mentioned. The miR-210 stem-loop is located in the intronic region of the long noncoding RNA, AK123483, on chromosome 11p15.5. MiR-210 contains a HRE in the proximal promoter that is located 400 bp upstream of the stem-loop (205). Both HIF-1 $\alpha$  and HIF-2 $\alpha$  bind to the HRE and activate miR-210 transcription (205, 206). Following transcription and integration into the RISC complex, miR-210-3p functions as the guide-strand, while the miR-210-5p passenger strand is degraded by argonaute (207). In addition, NF $\kappa$ B has been shown to induce miR-210 expression by binding to a conserved  $\kappa$ B consensus sequence in the core promoter region (208). Recently, Akt signaling has been shown to increase miR-210 expression in a HIF-independent manner, however, the mechanism remains unclear (209). miR-210 expression is elevated in many solid tumors and is correlated with hypoxic tumors with poor outcomes and moreover, makes miR-210 a suitable biomarker for prognosis (210). In hypoxic cancer cells, miR-210 targets mRNA involved in stabilizing HIF-1 $\alpha$ , cell cycle progression, metabolism, DNA repair, angiogenesis, differentiation and stem cell survival (210).

Since miR-210 contains a HIF-1 $\alpha$  binding site and is one of the most highly expressed miRNA in hypoxic cells, early reports hypothesized a feedback mechanism where miR-210 enhances HIF-1 $\alpha$  stability and thereby increases its own expression. The initial investigation into this potential feedback loop revealed the miR-210 mediated silencing of glycerol-3-phosphate dehydrogenase 1-like (GPD1L) protein, an enhancer of prolyl-hydroxylation (211). miR-210 and knocking down GPD1L confirmed the feedback

mechanism whereby miR-210 functions to stabilize HIF-1 $\alpha$  under hypoxic conditions (211).

The impact of miR-210 on cell proliferation has, at first glance, contradictory effects in hypoxic cancer cells, however, upon deeper analysis, miR-210 mediated effects on cell proliferation appear to be dependent on growth conditions (208, 212). As previously discussed, hypoxic cells grown under adherent conditions in the presence of FBS, demonstrate a decrease in their proliferative capacity. On the other hand, hypoxic spheres form larger spheres as a result of increased proliferation compared to normoxic spheres. Consistent with these findings, miR-210 repressed cellular proliferation in adherent cells by targeting cell cycle regulators E2F3 (213), FGFR1 (212) and HOXA1 (197). In hypoxic spheres, miR-210 targeted a Myc antagonist protein, MNT, resulting in cell cycle progression (208).

A common hallmark in hypoxic cancer cell metabolism is marked by the shift in mitochondrial respiration or oxidative phosphorylation to glycolysis (214). miR-210 has been observed to mediate this metabolic shift in hypoxic cells by targeting enzymes involved in oxidative phosphorylation such as ISCU1/2 (215), COX10 (216) and SDHD (217). Interestingly, after prolonged hypoxia, miR-210 can sustain the glycolytic shift even after the cells are returned to normoxia (218). This phenomenon has been observed in aggressive tumors experiencing oxygen cycling.

Developing tumors undergoing transient or acute hypoxia represent an oxygen tension cycling event that involves continuous blood vessel formation in order for the tumor to grow. Stimulation of angiogenesis requires VEGF signaling to support the vascular growth needs of the developing tumor. miR-210 contributes to this angiogenic need by targeting negative regulators of the VEGF signaling pathway (218). These key regulators include EFNA3 (218) and PTP1B (219). Given HIF-1 $\alpha$  directly increases

VEGF expression, stabilization of HIF-1 $\alpha$  by miR-210 represents an indirect pathway influencing angiogenesis. This mechanism has been observed in the angiogenic response to ischemic renal ischemia/reperfusion injury (220).

The role of hypoxia in maintaining stem cell pluripotency and promoting dedifferentiation is an area of ongoing research that is constantly evolving. miR-210s role in hypoxia regulated stemness remains an emerging field of research that has identified newly discovered mechanisms that contribute to the cancer stem cell phenotype.

### **Role of miR-210 in Stemness**

Under hypoxic conditions, miR-210 has been demonstrated to facilitate dedifferentiation and support stem cell survival (221, 222). In osteosarcoma, miR-210 dedifferentiated Stro<sup>-</sup>CD117<sup>-</sup> non-osteosarcoma stem cells into Stro<sup>+</sup>CD117<sup>+</sup> osteosarcoma stem cells (221). In this study, miR-210 increased sphere formation by targeting, a negative regulator of Slug, NFIC resulting in increased SLUG expression and Stro<sup>+</sup>CD117<sup>+</sup> expression. In another osteosarcoma study, miR-210 knockdown resulted in decreased colony formation, cell proliferation, migration and invasion, survival and tumor formation.

In glioma stem cells, hypoxia led to increased sphere formation and was associated with elevated miR-210 levels (223). Knockdown of miR-210 inhibited the formation of spheres and decreased CSC markers, survival and cell cycle progression. Underlying the hypoxic enrichment of glioma stem cells, miR-210 was demonstrated to directly target MNT, a negative regulator of the MYC/MAX interaction. Silencing MNT resulted in increased MYC and MAX expression which is associated with an enhanced CSC phenotype in glioma.

In BM-MSCs, hypoxia induced a HIF-1 $\alpha$  mediated prosurvival program that upregulated Akt signaling and miR-210 levels (222). Knockdown of HIF-1 $\alpha$  resulted in decreased survival and miR-210 expression. Further investigation revealed miR-210 targets CASP8AP2, decreasing apoptosis in hypoxic BM-MSCs. CASP8AP2 is an integral member of the apoptotic signaling complex that activates caspase-8, facilitating Fas-induced apoptosis (224). Currently, CASP8AP2 has been demonstrated to interact with the caspase-8 death effector domain (224), however, CASP8AP2 has not been extensively studied and its exact role in apoptosis remains unclear. A similar mechanism has been outlined in HUVECs where miR-210 targets CASP8AP2, protecting HUVECs from oxidative damage (225). In another study, miR-210 protected hypoxic cardiomyocytes from apoptosis by targeting, the proapoptotic protein, AIFM3 (209). Interestingly, miR-210 expression was shown to be induced by both Akt signaling and HIF-1 $\alpha$ . Inhibition of Akt phosphorylation in normoxic cells resulted in decreased miR-210, indicating a HIF-1 $\alpha$  independent role in miR-210 regulation. In the hypoxic cardiomyocytes, the data indicated that miR-210 was under the dual regulation of both Akt and HIFs (209). In EWS and other studies, Akt signaling has been shown to stabilize and amplify HIF-1 $\alpha$  expression but it remains unknown if miR-210 expression is directly linked to the Akt mediated stabilization HIF-1 $\alpha$  (226, 227).

Currently, miR-210 has been suggested as a biomarker for aggressive hypoxic tumors, however, no link has been made between miR-210 and tumors with increased stem cell populations. A recent study demonstrated that miR-210 contained in small extracellular vesicles or exosomes reflected the primary tumor in mice and moreover, these vesicles could be harvested from the peripheral vasculature as a liquid biopsy (228). In this same study, exosomes carrying miR-210 increased angiogenesis and

tumor formation in a xenograft mouse model. Further studies are needed to explore the role of exosomal miR-210 on stemness.

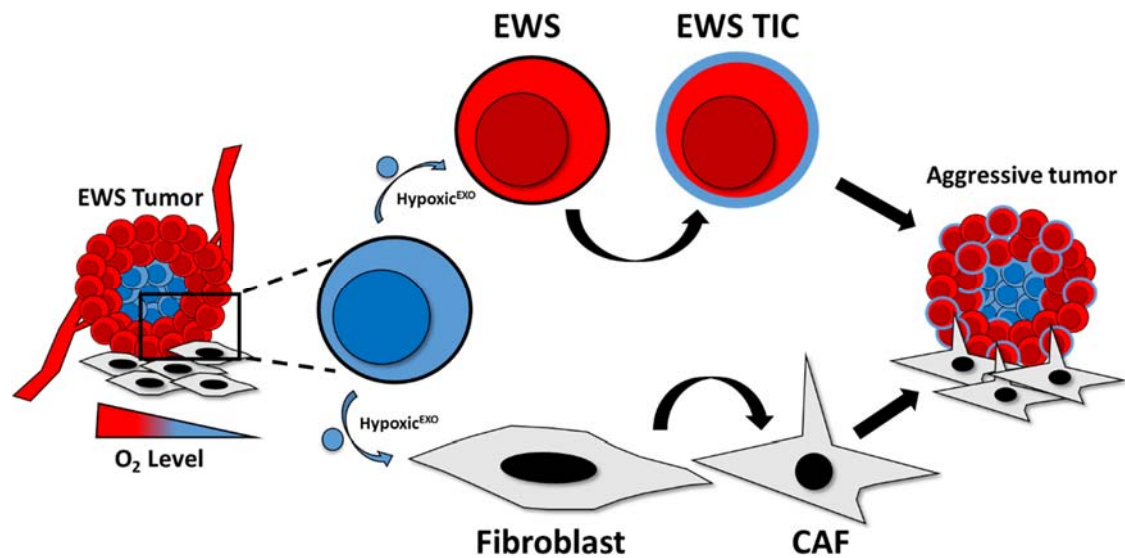
### **Intercellular Signaling in the Hypoxic Tumor Microenvironment**

Mounting evidence suggests that tumor cells rely on the TME for survival, proliferation, invasion and metastasis, and maintenance of the TIC subpopulation (229, 230). Studies indicate that the TME induces phenotypic and functional differences in tumor cells throughout the developing tumor resulting in niches with unique properties that can contribute to resistance to cytotoxic drugs and radiotherapy (231). Hypoxia is a key feature of the TME that is thought to underly the aggressive phenotype observed in cancer patients. Necrotic regions in tumors often result in the worst overall outcomes in many cancers, including EWS (142). These regions are subject to severe and prolonged hypoxia that is associated with aggressive tumor progression (231). It has been demonstrated that cells undergoing chronic hypoxia in these regions can communicate with cancer cells and stroma in normoxic regions of the tumor (230). This mechanism is suggested to underly a major contributing factor to aggressive tumors.

Recently, small extracellular vesicles (exosomes) have been described as important mediators of cell-to-cell communications in the TME (Figure 1.5) (232, 233). Exosomes have been shown to function as a bridge between neighboring cancer cells and stromal cells by delivering bioactive lipids, protein, mRNAs, miRs and gDNA that can be horizontally transferred to cells within the local TME or cells at distant sites (230). Uptake of exosomes derived from cancer cells induces epigenetic changes in target cells that play a significant role in tumor growth, progression, metastasis, drug resistance, angiogenesis and induction of pre-metastatic niches (230). These protumorigenic effects are mediated not only through cross-talk between cancer cells, but between cancer cells and their surrounding stroma (230). More recently, Ramteke et

**Figure 1.5: Schematic diagram of hypoxic effects on EWS tumor**

**microenvironment (TME).** Hypoxic EWS-derived exosomes (Hypoxic<sup>EXO</sup>) enhance Ewing's sarcoma (EWS) tumor initiating-like cell (TIC) phenotype and reprogram cancer-associated fibroblasts (CAF) with enhanced tumor forming capabilities.



al. reported that exosomes secreted from hypoxic prostate cancer cells transformed fibroblasts into CAFs and enhanced stemness in naïve prostate cancer cells, however, the effect that hypoxic exosomes had on inducing TIC-like cells remains unclear (234). Interestingly, CAFs have been observed in multiple cancer models to promote tumor growth and metastasis in the local TME and support the pre-metastatic niche at distant sites (235). Mounting evidence suggests exosomes play a significant role in reprogramming fibroblasts and mesenchymal stem cells into CAFs that are capable of supporting both the local TME and at metastatic sites (236, 237). In EWS, the role of exosomes in reprogramming cancer cells into TICs and transforming fibroblasts is unknown. Here, we will discuss the process of exosome biogenesis and how these small extracellular vesicles are secreted and their uptake in recipient cells. Moreover, I will explore the function of exosomes in the hypoxic TME and the current understanding of the role of exosomes in EWS.

Exosomes are small extracellular vesicles (40-150 nm) that originate from the multivesicular endosome (238, 239). These vesicles are thought to arise from all cell types and are present in all body fluids (239). The heterogeneity of exosomes is extensive and is largely attributed to the size, phenotypic state of their derived cell and their diverse cargo that includes proteins, RNA and DNA (240-242). Initially, exosomes were thought to function as “cellular garbage bags” that remove excess or unwanted cellular waste. However, this function was been supported in cancer cells that shuttle chemotherapy drugs out of the cell and confer chemoresistance (243). Recently, exosomes have been demonstrated to function in intercellular cross-talk in both physiological and pathophysiological conditions in an autocrine, paracrine and endocrine manner (244). Clinically, cancer patients have been observed to contain roughly double the amount of circulating exosomes in their peripheral vasculature (245, 246) and the



mechanism of action underlying the cause of enhanced exosome secretion in cancer patients is unknown. Furthermore, liquid biopsy studies have taken advantage of this phenomenon by isolating exosomes in these patients to uncover biomarkers that can be used for detection, prognosis and personalized therapy approaches in cancer patients (244).

## **Exosome Biogenesis**

Exosome biogenesis begins with the inward budding of the plasma membrane to form the early endosome. Invagination of the endosome results in the formation of multivesicular bodies (MVBs) that contain the exosomes. The MVBs have two common fates: degradation of the MVBs and their contents undergo lysosomal degradation or fusion with the plasma membrane resulting in release of the exosomes into the extracellular space (239). This process differentiates exosomes from other extracellular vesicles such as apoptotic or microvesicles that emerge from evagination of the plasma membrane. Key components involved in exosome biogenesis include the endosomal sorting complexes required for transport complexes (ESCRT) (247, 248). Studies in the exosome biogenesis have revealed ESCRT-dependent and -independent pathways that appear to be context dependent. ESCRT-independent mechanism have been reported in oligodendroglial cells that secrete exosomes dependent on the enzymatic activity of sphingomyelinase (249). The ESCRT machinery composes a multiprotein complex that includes ESCRT-0, -I, -II, and -III, along with accessory proteins such as ALIX (247, 248). These proteins localize on the cytoplasmic side of the invaginating endosomes where they recognize ubiquitinated proteins marked for sorting into the developing exosomes (ESCRT-0,-I and -II) and facilitate membrane budding and scission (ESCRT-III), forming the individual exosomes (250). Additional proteins involved with exosome biogenesis include TSG101, annexin A2, RAB5, RAB7 and RAB27.

## Exosome Cargo

Exosomes contain a diverse molecular cargo that affects the biogenesis pathway, exosome secretion, targeting and uptake into target cells, and functional alterations in the recipient cell's phenotype (239). The exosomal payload includes lipids, proteins, RNA and DNA (239). The lipid composition in exosomes imparts a more rigid and durable membrane that is suggested to resist degradation during transport throughout the body. Enrichment of cholesterol, sphingomyelin, hexosylceramides, phosphatidylserine and saturated fatty acids compose exosomal membranes (251-254).

Exosomes contain proteins that are generally considered markers for exosomes that participate in the exosome biogenesis pathway, and proteins that reflect the cell of origin and its physiological conditions (240). Currently, no single marker exists to distinguish between exosomes and other extracellular vesicles, however, protein commonly used to confer the presence of exosomes include: tetraspanins (CD9, CD63, CD81 and CD82), MHC molecules, heat shock proteins, Alix and TSG101 {Colombo, 2014 #1245, 255-257}. Exosomes are abundant in proteins that compose the plasma membrane, cytoskeleton, cytosol and proteins involved in vesicular trafficking (250, 258, 259). Protein content can vary dramatically under different environments such as hypoxia, and when cells undergo apoptosis resulting in apoptotic bodies (260).

The RNA profile typically observed in exosomes consists of small RNAs <700 nucleotides compared to cellular RNA profiles ranging from 400-12,000 nucleotides. These bioactive RNAs include mRNA, lncRNA, miRNA, piwiRNA, tRNA and Y-RNA (242, 261-263). Ribosomal RNA has been reported in exosomes but it is suggested that the presence of rRNA is the result of microvesicle contamination (263). miRNAs are the most widely studied RNA in exosomes due to their functional ability to silence target mRNAs once delivered to recipient cells via exosomes. Interestingly, the Kalluri lab

demonstrated that miRNA are bound to Argonaut forming a stable RISC in exosomes and moreover, this discovery was the first to convincingly show miRNA biogenesis continues within exosomes which supports previous claims of the selective sorting of miRNAs into exosomes (264). Mounting evidence suggests that miRNA loading into exosomes is a deliberate and selective process rather than by passive loading (264). The selective loading of miRNA into exosomes has been demonstrated to be regulated by the heterogeneous nuclear ribonucleoprotein (hnRNP) A2B1 (265). A2B1 belong to a family of hnRNPs that facilitate the trafficking of RNA. A2B1 recognizes a GGAG motif in miRNA that directs loading into exosomes (265). The selective loading of mRNA into exosomes is suggested to occur through a similar mechanism where A2B1 recognizes a 25 nt motif containing a CTGCC sequence (266). Intact functional exosomal mRNA was shown to be translatable in recipient cells in a study that co-culture human mast cells with exosomes derived from mouse mast cells resulting in murine proteins expressed in human mast cells (242). Further supporting this finding, another study GFP-tagged mRNA and observed that exosomal delivery of this tagged mRNA expressed green fluorescence in the exosome treated cells. Moreover, an important control in this study reported the absence of the GFP tagged protein in the exosomes (267). Hypoxia has been shown to induce the selective sorting of both miRNA and mRNA reflecting the RNA expression profile observed in the hypoxic cells (232, 233).

The DNA content in exosomes is far less explored but has significant potential for use as a biomarker in the detection of tumors and other pathophysiological conditions . Exosomes derived from MYC amplified tumors contained the oncogene MYC dsDNA and reflected the overall mutational landscape of the parental tumor cells. Fibroblasts treated with these exosomes revealed the transfer of MYC DNA in the cytosol and nucleus, however, no functional observations were made (268).

## **Exosome Secretion**

Once the exosomes are packaged, the MVBs migrate to and fuse with the plasma membrane releasing the exosomes into the extracellular space (239). The mechanism involving the trafficking, docking and fusion of the MVBs with the plasma membrane is not well understood and is an area of ongoing research. Proteins required for this process include actin and myosin (cytoskeleton), myosins and kinesins (molecular motors), and GTPases and SNAREs (targeting and fusion) (269). Rab GTPase family members Rab11, Rab27 and Rab 35 have been demonstrated to be involved with exosome secretion in different contexts (270-272), however, selective knockdown of the GTPases result in partial decreases in exosome release. Proteins implicated in MVB fusion to the plasma membrane include SNARE complex members VAMP7 and synaptotagmin VII (273, 274). These proteins have been shown to have cell type dependent roles in either exosome secretion or lysosomal fusion.

## **Exosome Interactions with Recipient Cells**

Interactions between exosomes and recipient cells occur via autocrine, paracrine and endocrine mechanisms in both physiological and pathophysiological conditions. The ability of exosomes to deliver its cargo to target cells depends on their interactions with recipient cells (239). The mechanism underlying the cellular specificity of exosomal targeting remains unknown, however, studies investigating how exosomes bind to target cells are becoming clearer. Uptake of exosomes into cells involves ligand-receptor interactions that can trigger either receptor mediated endocytosis or signal transduction (115), membrane fusion (252, 275) and phagocytosis (276). Ligand-receptor interactions between exosomes and target cells include exosomal proteins MHC I/II (277) and

tetraspanin receptors (115) capable of binding to integrins on the cell surface triggering signaling pathways or endocytosis.

### **Function of Exosomes in the Hypoxic TME**

Exosomes are enriched in the TME and function in the cross-talk between cancer cells and their surrounding stroma. In cancer, exosomes have been demonstrated to play a significant role in invasion and migration, proliferation, angiogenesis, therapy resistance, metabolism, immune evasion and stemness. Exosomes alter the phenotype in recipient cells largely through the delivery of their cargo (230). Currently, exosomal delivery of bioactive proteins and miRNA have received the greatest attention, however, these studies are in their nascent stages. In hypoxia studies, cancer-derived exosomal proteins play an important role in promoting cancer progression. Observations in hypoxic nasopharyngeal carcinoma cells revealed transcriptionally active HIF-1 $\alpha$  present within their hypoxic derived exosomes (115). Recipient cells treated with exosomes carrying HIF-1 $\alpha$  demonstrated an invasive and EMT phenotype associated with decreased E-cadherin expression coupled with increased N-cadherin levels. Interestingly, HIF-1 $\alpha$  delivered to target cells accumulated in the recipient cell's nucleus and maintained its stability in these cells with functional PHDs and Von Hippel Lindau E3 ligases (260). It was suggested that HIF-1 $\alpha$  was protected from proteasomal degradation by an undefined mechanism where internalization of exosomal HIF-1 $\alpha$  mediated shuttling directly to the nucleus (260). In prostate cancer, delivery of hypoxic derived exosomes increased invasion, migration and stemness in normoxic prostate cancer cells, and reprogrammed prostate fibroblasts into CAFs (234). IPA network analysis of the proteomic profile in hypoxic exosomes indicated enrichment of proteins involved in targeting adherens junctions. This network was suggested to underly the observations of the hypoxic exosome mediated effects on invasion and migration, however, these

networks were not validated and do not explain the effects associated with induction of stemness in normoxic prostate cancer cells or reprogramming of fibroblasts into CAFs. Proteins elevated in the hypoxic exosomes included MMP-2, MMP-9 (associated with metastasis) and various molecules involved in cancer signaling pathways such as TGF- $\beta$ 2, TNF1 $\alpha$ , IL6, Akt, ILK1 and  $\beta$ -catenin (234).

Increasing efforts are being made to elucidate the mechanisms underlying the exosome mediated transfer of miRNAs to target cells and the pro-oncogenic effects that result from this process. Recent studies in breast cancer revealed exosomal miRNA promoted tumorigenesis in a Dicer-dependent manner and moreover, Dicer was demonstrated to facilitate miRNA processing from pre-miRNAs to mature miRNAs in exosomes resulting in stable miRNA capable of exerting long lasting pro-tumorigenic effects in recipient cells (264). It is well established that the internalization of cancer derived exosomes into recipient cells introduces a myriad of miRNA with overlapping targets capable of interacting with the same mRNA in the host cell and eliciting similar oncogenic effects (244, 264, 278). Currently, most studies have focused on single miRNA and their targets, however, the authors noted that their observed effects were modest in most cases and could be attributed to other miRNAs with overlapping mRNA targets. Hypoxic oral squamous cell carcinoma cells were reported to secrete exosomes with enriched miR-21 capable of promoting a metastatic phenotype in a HIF-1 $\alpha$  and HIF-2 $\alpha$  dependent manner (233). Upon overexpression and knockdown of miR-21 using mimics and inhibitors, the authors reported a modest effect on tumor formation, suggesting a more complex miRNA network contributing to the hypoxic exosome effects (233).

Cancer-associated fibroblasts participate in the TME by supporting cancer cell invasion, proliferation and metastasis (279) CAFs overexpress  $\alpha$ -SMA compared to

normal fibroblasts and detection of  $\alpha$ -SMA is generally used as a reliable CAF marker (279). The mechanism describing how normal fibroblasts are reprogrammed into CAFs is still unclear. However, mounting evidence suggests the CAFs arise from exosomes secreted from cancer cells in the local TME (234) and currently, no studies in EWS have reported an exosome mediated induction of the CAF phenotype. Exosomes secreted from hypoxic prostate cancer cells induced expression of  $\alpha$ -SMA in prostate fibroblasts, suggesting that hypoxia enhances CAF reprogramming via an exosome mediated process (234). Recently, breast cancer derived exosomes delivering miR-9 to human breast fibroblasts was demonstrated to enhance the switch to CAFs (236). Another study in breast cancer revealed the miRNA cargo in breast cancer derived exosomes transformed endothelial cells with tumorigenic capabilities (264). In a previous report, exosomes derived from colorectal cancer cells induced  $\alpha$ -SMA expression and anchorage-independent growth in recipient fibroblasts (280). Recently, gastric cancer derived exosomes were shown to mediate CAF induction by increasing Akt signaling (281) and in several other reports, activated Akt signaling was observed to underly development and progression of malignant fibrosarcoma (282, 283).

### **Exosome Studies in EWS**

The role of exosomes in EWS has not been extensively explored. Initial reports focused on the mRNA profile in exosomes isolated from EWS cell lines and patient plasma where they identified a common transcript signature that could be used as biomarkers for detection of minimal residual disease (113). Other reports demonstrated that shCD99 EWS-derived exosomes could transfer enriched miR-34a to recipient EWS cells and stimulate neural differentiation (114) while in another study, EWS-derived exosomes carrying *EZH2* mRNA could be delivered intact to mesenchymal stem cells (284).

## Summary

Hypoxia is a critical feature of tumors and is associated with poor patient prognoses. The hypoxic TME is suggested to enrich for stem-like cancer cells and stromal cells that are protumorigenic. However, the mechanism underlying how hypoxia promotes an aggressive phenotype in EWS remains unclear. Exosomes are small nano-sized vesicles secreted from cancer cells that function within the TME as important intercellular communicators that induce a malignant phenotype, both locally and throughout the developing tumor. Exosomes carry bioactive lipids, protein, mRNAs, miRs and gDNA that can be horizontally transferred to cells within the local TME or cells at distant sites. Uptake of the exosomal RNA cargo derived from hypoxic cancer cells has been shown to mediate protumorigenic effects in cancer cells and reprogramming of fibroblasts into CAFs. In EWS, the role of exosomal miRNA in reprogramming cancer cells into stem-like cells and transforming fibroblasts is unknown.



## Hypothesis and Specific Aims

### Hypothesis

I hypothesize that EWS-derived exosomes secreted under hypoxic conditions enhance stemness in EWS cells and reprogram stromal cells of the tumor microenvironment through miRNA delivery.

#### **Aim 1: Determine the molecular role of hypoxia in mediating EWS-derived exosome enhancement of EWS stem-like cells.**

In this aim, my working hypothesis is that the transfer of hypoxic exosomal miRNAs to normoxic recipient cells target mRNAs that contribute to sphere formation. In our approach to this aim, we will knockdown HIF-1 $\alpha$  in hypoxic EWS cells and assess the exosomal RNA content and their impact in recipient cells using *in vitro* sphere formation and *in vivo* tumorigenesis assays. The impact of this aim will establish a molecular mechanism through which hypoxia can promote stemness in EWS.

#### **Aim 2: Determine the role of hypoxic EWS-derived exosomes on Akt signaling in EWS spheres and cancer-associated fibroblasts.**

In this aim, our working hypothesis is that hypoxic EWS cells secrete exosomes that activate Akt in EWS spheres and reprogram NIH3T3 fibroblasts into tumorigenic CAFs. In our approach to this aim, we will analyze the RNA content in hypoxic exosomes and determine the miRNA and mRNA that may stimulate Akt signaling in EWS spheres and transformed CAFs. The impact of this aim will establish a novel mechanism by which hypoxic exosomes can reprogram neighboring EWS and microenvironment cells into tumor initiating cells.

## Chapter II

### Materials and Methods

#### Cell culture and hypoxia exposure

EWS cell lines A673 and SK-ES-1, and the mouse embryonic fibroblast cell line NIH3T3 were obtained from the American Type Culture Collection (ATCC, Manassas, VA, USA). All cells were cultured in RPMI-1640 medium supplemented with 10% fetal bovine serum and 1% penicillin/streptomycin (Invitrogen, CA, USA) as adherent monolayers in a humidity-controlled incubator at 5% CO<sub>2</sub> and 21% O<sub>2</sub> at 37°C. Hypoxia experiments for adherent cell growth and sphere formation were performed with a Thermo Scientific™ Heracell™ VIOS CO<sub>2</sub> trigas incubator (Thermo Fisher Scientific, Waltham, MA, USA) at 5% CO<sub>2</sub>/95% N<sub>2</sub> and oxygen levels maintained at 1% O<sub>2</sub> at 37°C. For exosome isolation, A673 and SK-ES-1 cells were cultured in RPMI-1640 media containing 10% exosome-free FBS (System Biosciences, Palo Alto, CA, USA), 1% glutamine and 5% penicillin/streptomycin (Gibco, Carlsbad, CA, USA). In all studies, cell lines were maintained in culture for no more than 10 passages.

#### siRNA and miRNA transfection

Pre-designed HIF-1 $\alpha$ , CASP8AP2 and Non-Targeting Control (NTC) ON-TARGET *plus* siRNAs in SMARTpool format were obtained from Dharmacon (Horizon Discovery, Waterbeach, UK). miR-210-3p mimics, miR-210-3p inhibitor and negative control (miR-scramble) mimics were purchased from Ambion (Thermo Fisher Scientific, Waltham, MA, USA). All transient transfections were performed with Lipofectamine RNAiMAX (Invitrogen, Waltham, MA, USA) according to the manufacturer's instructions

Following transfections, cells were used in downstream exosome isolations, sarcosphere assays and/or immunoblotting.

### **MK-2206, Akt inhibitor, treatment**

A673 and SK-ES-1 cells were seeded at a density of  $5 \times 10^5$  per well in 6-well plates and allowed to adhere overnight. Following cell adherence, the EWS cells were treated with DMSO or MK-2206 (Selleckchem, Pittsburgh, PA) [ $IC_{50}$ ] indicated in the figure legend. The cells were cultured under normoxic or hypoxic conditions for 48 hrs in exosome-free media. After 48 hrs, the cells were lysed for immunoblotting or PCR and the conditioned media was processed for exosome isolation, followed by PCR or co-culturing assays.

### **Exosome isolation**

Exosomes were prepared from the cell culture supernatant of A673 and SK-ES-1 EWS cells using ultracentrifugation and filtration protocols as described previously (285). Briefly, EWS cells cultured to 70% confluency were washed with PBS and cultured in RPMI 1640 media containing 10% exosome-free FBS (System Biosciences, Palo Alto, CA, USA) under normoxia (21%  $O_2$ ) and hypoxia (1%  $O_2$ ) for 48 hrs. The conditioned media was collected and centrifuged for 10 min at 300 x g, 20 min at 2000 x g to remove cell debris, and 30 min at 10,000 x g to remove microvesicles larger than 200 nm.

For standard ultracentrifugation, the raw exosomes were collected by ultracentrifugation at 100,000 x g for 90 min in a SW 28 rotor (Beckman Coulter, Chaska, MN, USA). Exosome pellets were washed with PBS and passed through a 0.2  $\mu$ m SFCA filter (Thermo Fisher Scientific, Waltham, MA, USA) to remove large contaminating lipid and vesicular aggregates.

For exosome isolation using an OptiPrep™ (Sigma Aldrich, St. Louis, MO, USA ) solution density gradient, the raw exosomes were added to the top of discontinuous gradient. The OptiPrep™ (iodixanol) gradients were prepared from a 60% (w/v) iodixanol stock and diluted with 0.25 M sucrose, 10 mM Tris-HCL at a pH of 7.5 to make the following solutions: 40%, 20%, 10% and 5% (w/v). The gradient was prepared by layering 3 ml of each solution, beginning with 40%, to the bottom of a 10 ml Ultraclear polypropylene tube (Beckman Coulter, Chaska, MN, USA). The prepared OptiPrep™ solution was centrifuged at 100,000 x g for 90 min in a SW40Ti swinging bucket (Beckman Coulter, Chaska, MN, USA). Following centrifugation, twelve 1 ml fractions were manually collected and placed individually into polycarbonate tubes (Beckman Coulter, Chaska, MN, USA).

For exosome isolation using a sucrose cushion, the raw exosomes were overlaid on top of a 30% sucrose/D2O cushion and centrifuged at 100,000 x g for 90 min in a SW28 swinging bucket (Beckman Coulter, Chaska, MN, USA).

Following the exosome isolation preparations using standard ultracentrifugation, OptiPrep™ and sucrose cushion methods, the final solutions were ultracentrifuged at 100,000 x g for 90 min in a 70.1 Ti rotor (Beckman Coulter, Chaska, MN, USA). The exosome pellets were resuspended in 200 µl PBS and used immediately for co-culture assays or stored at -80°C.

Exosomes derived from cells transfected with HIF-1α siRNAs and NTCs were isolated using the Exoquick™ reagent (System Biosciences, Palo Alto, CA, USA) with modifications to the vendor instructions. Briefly, conditioned media was centrifuged for 20 min at 2000 x g and 30 min at 10,000 x g. Next, Exoquick™ was added to the conditioned media and the remaining exosome precipitation steps were followed

according to the manufacturer's instructions. The exosome pellet was resuspended in 200  $\mu$ l PBS and used immediately for co-culture assays or stored at  $-80^{\circ}\text{C}$ .

### **Nanoparticle tracking analysis (NTA)**

Exosomes were analyzed using a NanoSight NS300 (NanoSight Ltd, Navato, CA, USA). A red laser beam was used to visualize particles and assess their movement under Brownian motion. Illuminated particles were recorded and analyzed using the NTA software (NTA 3.1 Build 3.1.54) which applies the two-dimensional Stokes-Einstein equation to calculate size distribution and concentration of nano-sized particles.

### **Electron microscopy**

Transmission electron microscopy (TEM) imaging of exosomes was performed as previously described (286), with some modifications. Briefly, exosomes were fixed for 1 hr in a mixture of 2% paraformaldehyde, 2% glutaraldehyde in 0.1 M Sorensen's phosphate buffer. Following fixation, the exosome sample was layered on a formvar/silicon monoxide-coated 200 mesh grid and air-dried for 2 min. Grids were then stained with Nanovan negative stain (Nanoprobes, Yaphank, NY, USA) and air-dried for an additional 2 min. Samples were observed at 80Kv with a Tecnai G2 Transmission Electron Microscope (FEI Company, Hillsboro, OR, USA). For scanning electron microscopy (SEM), exosome samples were fixed using the same Sorensen's fixation cocktail. Samples were washed three times with Sorensen's phosphate buffer prior to and after fixation with 1% osmium tetroxide. Next, samples were dehydrated in a graded ethanol series (50%, 70%, 90%, 100%) three times per steps. Following dehydration, exosome samples were kept in hexamethyldisilazane overnight to air dry and then placed on a glass coverslip. A 50 nm layer of gold/palladium was sputter coated

(Hummer VI Anatech, Sparks, NV) onto each sample. Samples were observed at 30Kv with a Quanta 200 Scanning Electron Microscope (FEI Company, Hillsboro, OR).

### **Sarcosphere assay**

A673 and SK-ES-1 parental cells and cells transfected with CASP8AP2 siRNAs, NTCs, miR-210 mimics, miR-210 inhibitors and negative control mimics were cultured in serum-free media in non-adherent conditions. To prevent cell aggregations resulting in false positives, cells were seeded at low densities (20 cells/ $\mu$ L) in 6-well or 24-well Corning ultra-low attachment plates in sphere media composed of DMEM/F12 supplemented with 20 ng/mL EGF, 40 ng/mL bFGF, 2  $\mu$ g/mL Heparin, 0.1 mM  $\beta$ -mercaptoethanol, 1% B27, 1% N2 and 1% penicillin/streptomycin. Sphere formation was assessed, microscopically, in cells grown under normoxia (21% O<sub>2</sub>) and hypoxia (1% O<sub>2</sub>) after 5 days. To assess sphere formation in EWS and NIH3T3 cells pre-treated with exosomes, EWS cells (1000 cells/well) were cultured at a low density (1 cell/ $\mu$ L) in 24-well low attachment plates with serum-free sphere media (as previously mentioned). Exosomes (20  $\mu$ g/mL) derived from EWS cells cultured under normoxic and hypoxic conditions were added to A673 and SK-ES-1 cells, respectively. Sarcospheres were counted using a microscope after 5 days. All experiments were performed in triplicate.

For siRNA experiments, exosomes derived from EWS cells transfected with siHIF-1 $\alpha$  or NTC were cultured with parental EWS cells and assessed for sphere formation after 5 days.

For miRNA experiments, EWS cells transfected with miR-210 inhibitors were co-cultured with hypoxic exosomes derived from their parental cell line as previously mentioned. Sphere formation and immunoblotting was assessed after 5 days.

## Colony formation assay

NIH3T3 fibroblasts ( $2 \times 10^3$  cells/well) were co-cultured with SK-ES-1 Normoxic<sup>EXO</sup> and Hypoxic<sup>EXO</sup> (20 $\mu$ g/mL) in 0.3% agar semisolid RPMI 1640 media containing 10% exosome-free FBS (System Biosciences, Palo Alto, CA, USA) and plated in triplicate in 12-well plates. Following 3 weeks, colony formation with  $\geq 50$  cells was counted using an inverted microscope.

## Western blot

EWS cells ( $2 \times 10^4$  cells/well) were seeded in a 6-well ultra-low adherent plate (Corning) and pretreated with exosomes (0 or 20  $\mu$ g/mL) in a sphere assay. Following 5 days, cells were harvested and lysed for use in western blot. NIH3T3 fibroblasts ( $1 \times 10^6$  cells/well) were plated in an adherent 6-well plate and co-cultured with SK-ES-1 Normoxic<sup>EXO</sup> and Hypoxic<sup>EXO</sup> (20  $\mu$ g/mL) for 24, 28 and 72 hours. Total protein was isolated from cells and exosomes using RIPA lysis buffer (Thermo Fisher Scientific, Waltham, MA, USA). Protein from cells was quantified using the BCA method (Pierce, Waltham, MA, USA) and the amount of protein in exosomes was estimated by measuring protein content with the Bradford assay (Bio-Rad, Hercules, CA, USA). SDS-PAGE was conducted under reducing or non-reducing conditions followed by immunoblot as previously described (287). Antibodies used in this experiment were Myc, Oct 3/4, TSG101, CD63, MIC2 (CD99), FLI (EWS-FLI1), Calnexin (1:500, all Santa Cruz Biotechnology, Dallas, TX, USA), HIF-1 $\alpha$  (1:1000, BD Biosciences, San Jose, CA, USA), CASP8AP2/FLASH (1:1000, Abcam, Cambridge, UK),  $\alpha$ -SMA, phospho-AKT, AKT, mTORC1, phosphor-mTORC1, EZH2, Sox2, Nanog, IGF-1R (1:1000, all Cell Signaling, Danvers, MA), CD133 (1:50, Miltenyi Biotec, Waltham, MA) and  $\alpha$ -Tubulin (1:4000, Sigma Aldrich, St. Louis, MO, USA). Blots were incubated with appropriate horseradish

peroxidase-tagged secondary antibodies and visualized using the  $\text{myECL}$  Imager (Thermo Fisher Scientific, Waltham, MA, USA).

### **RNA isolation, RNA-seq and analysis**

EWS cell and exosome total RNA was isolated using miRCURY™ RNA Isolation Kit according to the manufacturer's protocol. RNA concentrations and quality were determined by ND-1000 (Nanodrop Technologies, Wilmington, DE, USA) and Fragment Analyzer automated CE systems (Agilent, Santa Clara, CA, USA). Electropherograms were generated using the Fragment Analyzer. Library preparation RNA-seq and miRNA-seq were performed using KAPA Stranded mRNA-Seq Kit (Roche Company) and QIAseq miRNA Library Kit (Qiagen, Hilden, Germany), respectively. Sequencing was performed using the Illumina HiSeq3000 system (Illumina, San Diego, CA, USA). For the mRNA read counts, the reads were first mapped to the latest UCSC transcript set using Bowtie2 version 2.1.0 and the gene expression level was estimated using RSEM v1.2.15. TMM (trimmed mean of M-values) was used to normalize the gene expression. Differentially expressed genes were identified using the edgeR package of Bioconductor. Genes showing altered expression with  $p < 0.05$  and more than 1.5 fold changes were considered differentially expressed. The miRNA count was calculated using the QIAseqmiRNA platform (<http://ngsdataanalysis.sabiosciences.co-m/QIAseqmiRNA/>). The cutoff of differential miRNA was a fold-change threshold of 1.5 and maximum p-value of 0.05. Ingenuity Pathway Analysis (IPA) software (Ingenuity® Systems, [www.ingenuity.com](http://www.ingenuity.com)) was used to identify biological functional pathways and networks associated with differentially expressed mRNAs and miRNAs. Network score presented as  $-\log(p \text{ value})$  and statistical significance ( $p < 0.05$ ) was performed using Fisher's exact test.



## Real-time quantitative PCR

For mRNA quantification, cDNA was obtained using the iScript Advanced cDNA Kit for RT-qPCR (BIO-RAD, Hercules, CA). Typically, 2 µg of total RNA was used as template per reaction. Real-time PCR amplification was performed using a Taqman Gene Expression Master Mix and Taqman primers *EWS-FLI1*, *SOX2*, *OCT4*, *NANOG* and *MYC* (Applied Biosystems, Waltham, MA, USA) and each target gene was normalized to *GAPDH* (Applied Biosystems, Waltham, MA, USA). For miRNA quantification, miRNA was reverse transcribed and amplified using a Taqman MicroRNA assay kit (Applied Biosystems, Waltham, MA, USA). The Taqman probe based primers included has-miR-145, has-miR-210 and endogenous controls RNU6B and has-miR-16 (Applied Biosystems, Waltham, MA, USA). Both mRNA and miRNA RT-qPCR amplification was performed using the QuantStudio 3 instrument (Applied Biosystems, Waltham, MA, USA). Relative quantification was calculated using a comparative Ct method.

## Apoptosis Assay

To detect apoptosis in EWS spheres transfected with NTC or siCASP8AP2, spheres were dissociated and fluorescently stained using an Annexin-V-FITC/PI flow cytometry assay kit (BD Biosciences, San Jose, CA) according to the manufacturer's instructions. Quantification of apoptotic cells were performed with the FACSCalibur system (BD Biosciences, San Jose, CA).

## Tumorigenicity Assays

Four-to-six week old NOD-SCID with common gamma chain deletion (NSG) mice were purchased from Jackson Laboratories (Bar Harbor, ME). All animal studies were

performed under an Institutional Animal Care and Use Committee (IACUC) approved protocol in accordance with federal, state and UNMC guidelines.

SK-ES-1 cells ( $1 \times 10^5$ ) were inoculated subcutaneously into the right flank of NSG mice ( $n=7/\text{group}$ ). On the day of injection, SK-ES-1 cells were suspended in a 2:1 mixture (PBS:Matrigel) (BD Biosciences, San Jose, CA, USA) and with either (i) PBS (control), (ii) Normoxic<sup>EXO</sup> or (iii) Hypoxic<sup>EXO</sup> (20  $\mu\text{g}/\text{mL}$ ). Mice were injected intratumorally with PBS, Normoxic<sup>EXO</sup> or Hypoxic<sup>EXO</sup> (20  $\mu\text{g}/\text{mL}$ ) twice per week for six weeks.

NIH3T3 cells ( $1 \times 10^5$  cells/well) were pretreated with Normoxic<sup>EXO</sup> and Hypoxic<sup>EXO</sup> (20  $\mu\text{g}/\text{mL}$ ) for 72 hrs. Following incubation period, NIH3T3 cells were harvested and  $1 \times 10^5$  cells were mixed respectively with PBS, Normoxic<sup>EXO</sup> and Hypoxic<sup>EXO</sup> (20  $\mu\text{g}$ ) in 150  $\mu\text{L}$  PBS and then injected into the right flank of NSG mice ( $n=5/\text{group}$ ).

Tumor formation was measured three times a week using the Bioptron TumorImager (Princeton, NJ). When the tumor volume reached the end of their time course or 1  $\text{cm}^3$ , the experiment was concluded and mice were euthanized using  $\text{CO}_2$  and cervical dislocation. Tumors were removed and processed for either FACS analysis, western blot, H&E staining or immunohistochemistry. Briefly, IHC staining was performed using  $\alpha\text{-SMA}$  antibody (1:1000, Cell Signaling, Danvers, MA) and ImageJ was used to quantify staining density.

### **Tumor dissociation and FACS analysis**

After removal of SK-ES-1 tumors treated with either PBS, Normoxic<sup>EXO</sup> or Hypoxic<sup>EXO</sup>, tumor samples were mechanically dissociated and enzymatically digested with collagenase II (56  $\text{mg}/\text{L}$ ) and IV (170  $\text{mg}/\text{L}$ ) (Sigma, St. Louis, MO, USA) in a shaking incubator for 45 min at 37  $^\circ\text{C}$ . Samples were pipetted vigorously and passed through a 70  $\mu\text{m}$  nylon cell strainer (Miltenyi Biotec, Waltham, MA). Erythrolysis was carried out using

1X RBC lysis buffer (Miltenyi Biotec, Waltham, MA) according to manufacturer's instructions. Viability was assessed in disaggregated single cells using trypan blue staining. Samples with ~90% viability were analyzed by fluorescence-activated cell sorting (FACS) using CD133/1 phycoerythrin (AC133), 1/10) antibody (Miltenyi Biotec, Waltham, MA), isotype control mouse IgG1 phycoerythrin (1/10, BD Pharmingen, San Jose, CA, USA) and LIVE/DEAD (Invitrogen, Waltham, MA, USA) viability stain in a LSRII apparatus (BD Biosciences, San Jose, CA, USA).

### **Statistical analysis**

Statistical analysis between groups were calculated using Student *t* test or one-way ANOVA with Tukey's multiple comparisons test. A value of  $p \leq 0.05$  was considered statistically significant. All data is presented as mean  $\pm$  standard error of the mean (SEM).  $\Delta\Delta C_q$  method was used to calculate relative gene expression from qRT-PCR data. All experiments were replicated a minimum of three times unless otherwise indicated.

## Chapter III

### Characterization of EWS Normoxic<sup>EXO</sup> and Hypoxic<sup>EXO</sup>

#### Introduction

Small extracellular vesicles (exosomes) have been described as important mediators of cell-to-cell communicators in the TME (230). Exosomes arise from the early endosome and are trafficked through the cell within multivesicular bodies (MVBs). MVBs fuse with the plasma membrane releasing these exosomes into the extracellular space. These small vesicles range in size from 30-150 nm and carry bioactive lipids, protein, mRNAs, miRs and gDNA that can be horizontally transferred to cells within the local TME or cells at distant sites (239). Exosomes enter the peripheral vasculature to reach distant target cells and given this ability, cancer-derived exosomes may serve as a novel diagnostic and prognostic marker that can be assessed through liquid biopsy (244).

The role of exosomes in EWS is currently unclear. Initially, exosomes isolated from EWS cell lines and patient serum identified mRNA (113) and miRNA (115) profiles. These reports investigated the functional (115) and biomarker (113) significance of EWS exosomes. Studies in other cancer models investigating the role of hypoxic exosomes have provided insight into how hypoxic tumors can secrete exosomes that propagate an aggressive phenotype in cells outside the hypoxic niche (233). Exosomes released from hypoxic prostate cancer cells enhanced sphere formation in normoxic cells and induced a cancer-associated fibroblasts (CAF) phenotype in normal prostate fibroblasts (234), but they were unable to elucidate a mechanism describing how hypoxic exosomes promoted stemness in normoxic cells and reprogrammed CAFs. CAFs have been observed in multiple cancer models to promote tumor growth and metastasis in the local TME and support the pre-metastatic niche at distant sites (279).

The role of exosomes in promoting stemness and induction of the CAF phenotype in EWS is unknown and highlights a major gap in scientific knowledge. In this study, we sought to characterize the protein, mRNA and miRNA content in EWS exosomes, furthermore, we performed RNA-seq followed by IPA analysis in order to identify miRNAs and mRNAs that may play a role in promoting sphere formation in EWS cells and reprogramming fibroblasts into CAFs.

## Results

To determine an optimal exosome isolation method for downstream functional assays, we cultured SK-ES-1 cells in exosome-free media for 48 hours and processed the conditioned media using the following methods: Opti-Prep gradient, discontinuous sucrose gradient and ultracentrifugation followed by microfiltration (Figure 3.1). All of the methods isolated particles within the acceptable size range for exosomes. The sucrose isolation method yielded the smallest average exosome size (117.8 nm) while the Opti-Prep and ultracentrifugation methods resulted in much bigger particle sizes (152.6 nm and 142.6 nm, respectively). As expected however, the ultracentrifugation technique yielded a significantly greater particle concentration compared to the other isolation methods. Together, these results indicate that the ultracentrifugation exosome isolation method is an acceptable isolation method and will yield adequate exosomes for downstream functional assays.

To investigate the role of hypoxia on exosome secretion in EWS, A673 and SK-ES-1 cells, we first measured the expression of HIF-1 $\alpha$  in A673 and SK-ES-1 EWS cells cultured under 1% O<sub>2</sub> for an increasing duration (310). In both EWS cell lines, HIF -1 $\alpha$  expression stabilized at 6 hrs (Figure 3.2A). Since HIF-1 $\alpha$  expression was stable at 48 hours and exosome isolations typically require 48 hour incubations in exosome-depleted media, we proceeded to culture our EWS cells in exosome-free media under normoxic

(21%O<sub>2</sub>) and hypoxic (1%O<sub>2</sub>) conditions for 48 hours. EWS-derived exosomes were isolated by collecting the supernatant and performing multiple centrifugation and ultracentrifugation steps, followed by microfiltration. The exosomes were analyzed using Nanosight tracking analysis (NTA) to measure particle size and concentration. NTA revealed both A673 and SK-ES-1 exosomes with particle sizes within the expected size range of 30-150 nm (Figure 3.2B) (310). In both cell lines, the total particle concentration of hypoxic EWS-derived exosomes (Hypoxic<sup>EXO</sup>) secreted was lower than normoxic EWS-derived exosomes (Normoxic<sup>EXO</sup>) following normalization to cell numbers. Proliferation rates in hypoxic EWS cells were decreased ~30% compared to normoxic cells which was consistent with the differences observed in particle concentration between normoxic and hypoxic cells (310). Total exosomal protein was also similar to total particle concentration and together, our findings suggest that EWS exosome secretion is dependent on proliferation rates which is consistent with the effects of hypoxia on cell proliferation (310).

EWS Normoxic<sup>EXO</sup> and Hypoxic<sup>EXO</sup> were visualized using transmission and scanning electron microscopy. TEM confirmed small vesicles ranging from 30-150 nm (Figure 3.2C) (310) while SEM revealed aggregates of vesicles larger than 150 nm (Figure 3.2D). These observations may explain the NTA results detecting particles outside the range of exosomes. We confirmed the presence of EWS-derived exosomes by immunoblotting for protein markers involved in exosome biogenesis. Western blotting demonstrated decreased levels of CD63 and TSG101 in SK-ES-1 Hypoxic<sup>EXO</sup> compared to Normoxic<sup>EXO</sup>. The endoplasmic reticulum protein calnexin served as a negative control and was not observed in either exosome lysates (Figure 3.2E) (310). Next, we probed for proteins crucial in EWS pathogenesis. We identified CD133, EZH2, IGF-1R, EWS-FLI1 and CD99 in both SK-ES-1 exosomes. Interestingly, SK-ES-1 Hypoxic<sup>EXO</sup> had

increased levels of the fusion protein EWS-FLI1 and EWS proteins, CD99 and EZH2, which are involved in maintaining a transformed phenotype (Figure 3.3B). Total protein isolated from Normoxic<sup>EXO</sup> and Hypoxic<sup>EXO</sup> lysates was reflected in similar levels of  $\alpha$ -tubulin. Previously, EWS-FLI1 mRNA was detected in EWS exosomes, we wanted to see if hypoxia modulated EWS-FLI1 mRNA in Hypoxic<sup>EXO</sup>. Interestingly, EWS-FLI1 levels were significantly elevated in Hypoxic<sup>EXO</sup> (Figure 3.3A). Together, we concluded that our isolation method reliably captured vesicles consistent with exosome characteristics and contained proteins and mRNA important in EWS pathogenesis.

Recently, hypoxia was demonstrated to alter mRNA and miRNA profiles in cancer-derived exosomes. Furthermore, exosomes have been shown to genetically and metabolically reprogram cancer cells through the delivery of their RNA payload (233). We sought to identify mRNAs and miRNAs in our Hypoxic<sup>EXO</sup> that may play a role in promoting stemness. First, total RNA was isolated from normoxic and hypoxic SK-ES-1 cells and their derived exosomes. Capillary electrophoresis revealed a broad composition of RNA with enrichment of small RNAs in the exosomes compared to their respective cells (Figure 3.4) (310). Cellular RNA profiles demonstrated typical ribosomal subunit peaks (28S and 18S), but were not seen in the exosomal lysates (288). The presence of these ribosomal RNAs have been reported in both microvesicles and apoptotic bodies which further supports the high quality of the exosome isolation (310).

RNAseq was performed using the Illumina HiSeq3000 to identify exosomal miRNAs. Unsupervised hierarchical clustering identified miRNA clusters that were significantly different between normoxic and hypoxic cells, and Normoxic<sup>EXO</sup> and Hypoxic<sup>EXO</sup> (Figures 3.5A,B) (310). We observed 467 miRNAs to be differentially expressed between normoxic and hypoxic cells threshold for comparison of 1.5 fold with a significance of  $P < 0.05$  (Figure 3.5C) (310). Hypoxic cells displayed 94 increased

and 373 decreased miRNAs compared to normoxic cells. In Hypoxic<sup>EXO</sup>, we observed 75 enriched and 90 depleted miRNAs compared to Normoxic<sup>EXO</sup> (Figure 3.5D) (310). In Table 3.1, miRNA that are positively and negatively regulated by the HIFs are listed in their respective columns. We plugged-in our miRNA values based on differential miRNA expression between Hypoxic<sup>EXO</sup> and Normoxic<sup>EXO</sup>. Our results were consistent with previous studies characterizing up- and downregulated miRNAs in Hypoxic<sup>EXO</sup>. Using real-time PCR, we validated the top regulated miRNA observed in both the cellular and exosomal miRNA-seq results and found miR-210 expression to be consistently elevated in Hypoxic<sup>EXO</sup> compared to Normoxic<sup>EXO</sup> for both EWS cell lines (Figure 3.6) (310). This data identifies a hypoxically regulated exosomal miRNA, miR-210, that may influence cellular function in normoxic EWS target cells and could potentially serve as a reliable prognostic marker for hypoxic EWS tumors.

Next, we used Ingenuity Pathway Analysis (IPA) software to determine the top experimentally verified diseases and biological functions related to these 165 miRNAs and their predicted cellular target mRNAs. The top three categories included “Organismal Injury and Abnormalities, Reproductive System Disease and Cancer” (Figure 3.7A). IPA network analysis of these differentially expressed miRNAs allowed us to gain insight into particular miRNA-mRNA interactions and narrow the predicted biological effects that these exosome-derived miRNAs have within target cells. The top network identified miRNAs targeting mRNA nodes involved in “Cancer Biology” (score=23) centering on indirect interactions between significantly expressed oncogenic miRNAs and hyperactivation of Akt signaling (Figure 3.7B). These experimentally validated miRNAs involved in modulating Akt activity include miR-19b-3p, miR-92a-3p, miR-25, miR-181-5p, miR-27a-3p, miR-29b-3p and miR-30c-5p. Interestingly, many of these miRNAs (miR-9-5p, miR-27a-3p, miR-210-3p, miR-181a-5p and miR-25) are



involved in maintaining stemness in cancer cells, however, these functions are independent from the interactome converging on Akt signaling. Together, IPA analysis of the miRNA cargo in Hypoxic<sup>EXO</sup> identifies key miRNAs that converge on a common pathway that has been previously demonstrated to drive a stem-like phenotype in cancer cells.

Unsupervised hierarchical clustering identified miRNA clusters that were significantly different between normoxic cells and Normoxic<sup>EXO</sup>, and hypoxic cells and Hypoxic<sup>EXO</sup> (Figures 3.8A,B). We observed 1,139 miRNAs to be differentially expressed between normoxic cells and Normoxic<sup>EXO</sup> and 1052 differentially expressed miRNAs between hypoxic cells and Hypoxic<sup>EXO</sup>, threshold for comparison of 1.5 fold with a significance of  $P < 0.05$ ) (Figure 3.8C,D). Normoxic<sup>EXO</sup> displayed 640 increased and 449 decreased miRNAs compared to normoxic cells (Figure 3.8C). In Hypoxic<sup>EXO</sup>, we observed 496 enriched and 556 depleted miRNAs compared to hypoxic cells (Figure 3.8D).

Cluster analysis identified mRNAs that were significantly different between Normoxic<sup>EXO</sup> and Hypoxic<sup>EXO</sup> (Figures 3.9A). We observed 586 mRNAs to be differentially expressed, at threshold for comparison of 1.5 fold with a significance of  $P < 0.05$ ) (Figure 3.9B). In Hypoxic<sup>EXO</sup>, we observed 292 enriched and 294 depleted miRNAs compared to Normoxic<sup>EXO</sup>. IPA analysis was used to determine the top experimentally verified diseases and biological functions related to these 586 mRNAs and their predicted pathways. The top three categories included “Cancer, Organismal Injury and Abnormalities, and Gastrointestinal Disease” (Figure 3.9C). IPA network analysis of these differentially expressed mRNAs revealed predicted biological pathways that these exosome-derived mRNAs have within target cells. The top network identified mRNAs targeting mRNA nodes involved in “Post-Translational Modification, Hereditary Disorder,

Neurological Disease” (score=54) converging on direct interactions between significantly expressed mRNAs and activation of Akt signaling (Figure 3.9D).

Cluster analysis between normoxic cells and Normoxic<sup>EXO</sup>, and hypoxic cells and Hypoxic<sup>EXO</sup> revealed 11,374 and 11,729 mRNAs to be differentially expressed, respectively (threshold for comparison of 1.5 fold with a significance of  $P < 0.05$ ) (Figure 3.10A,B). Normoxic<sup>EXO</sup> displayed 4,810 increased and 6,564 decreased mRNAs compared to normoxic cells (Figure 3.10C). In Hypoxic<sup>EXO</sup>, we observed 5,038 enriched and 6,691 depleted mRNAs compared to hypoxic cells (Figure 3.10D). mRNA-seq revealed elevated levels of the ESC genes in exosomes compared to their respective parental cells. Validation of the ESC mRNA using qRT-PCR demonstrated significantly increased expression of SOX2, OCT4 and NANOG in exosomes compared to their derived cells, respectively, (Figure 3.11A,B), however, MYC was enriched in, Normoxic<sup>EXO</sup> and significantly depleted in Hypoxic<sup>EXO</sup> when compared to their respective cells. Interestingly, MYC was significantly increased in Normoxic<sup>EXO</sup> when compared to Hypoxic<sup>EXO</sup>, but no significant difference was observed in SOX2, OCT4 and NANOG expression between normoxic and hypoxic exosomes.

**Figure 3.1: NanoSight tracking analysis (NTA) of SK-ES-1 exosomes isolated using different methods.** NTA of Opti-Prep, discontinuous sucrose, ultracentrifugation methods showing particle size and relative concentration.

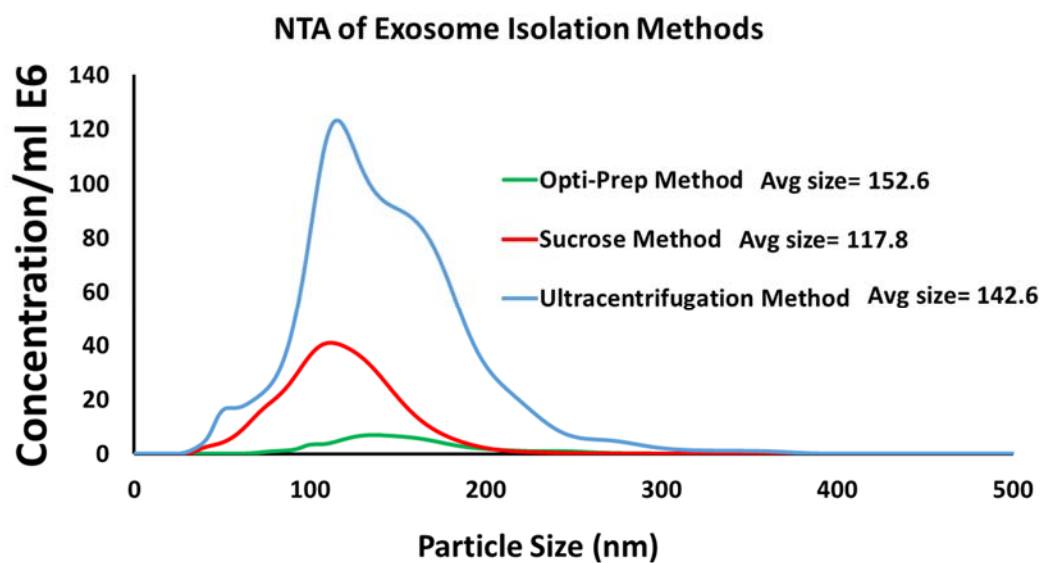


**Figure 3.2: Characterization of EWS Exosomes.** (A) Western blot of HIF-1 $\alpha$  in A673 and SK-ES- cells cultured under hypoxia (time points: 0, 6, 24, 48 and 72 hrs.). (B) NanoSight tracking analysis (NTA) of normoxic and hypoxic A673 and SK-ES-1 exosomes showing particle size and relative concentration. (C) Transmission electron micrograph (TEM) of normoxic and hypoxic A673 and SK-ES-1 exosomes. (D) Scanning electron micrograph (SEM) of normoxic and hypoxic SK-ES-1 exosomes (magnification, X30,000; scale bar, 1  $\mu$ ). (E) Western blot of key EWS proteins EWS-FLI1, CD99, CD133, EZH2 and IGF1R involved in EWS pathogenesis. Loading controls and exosomes markers  $\alpha$ -Tubulin and TSG101 were assessed respectively.

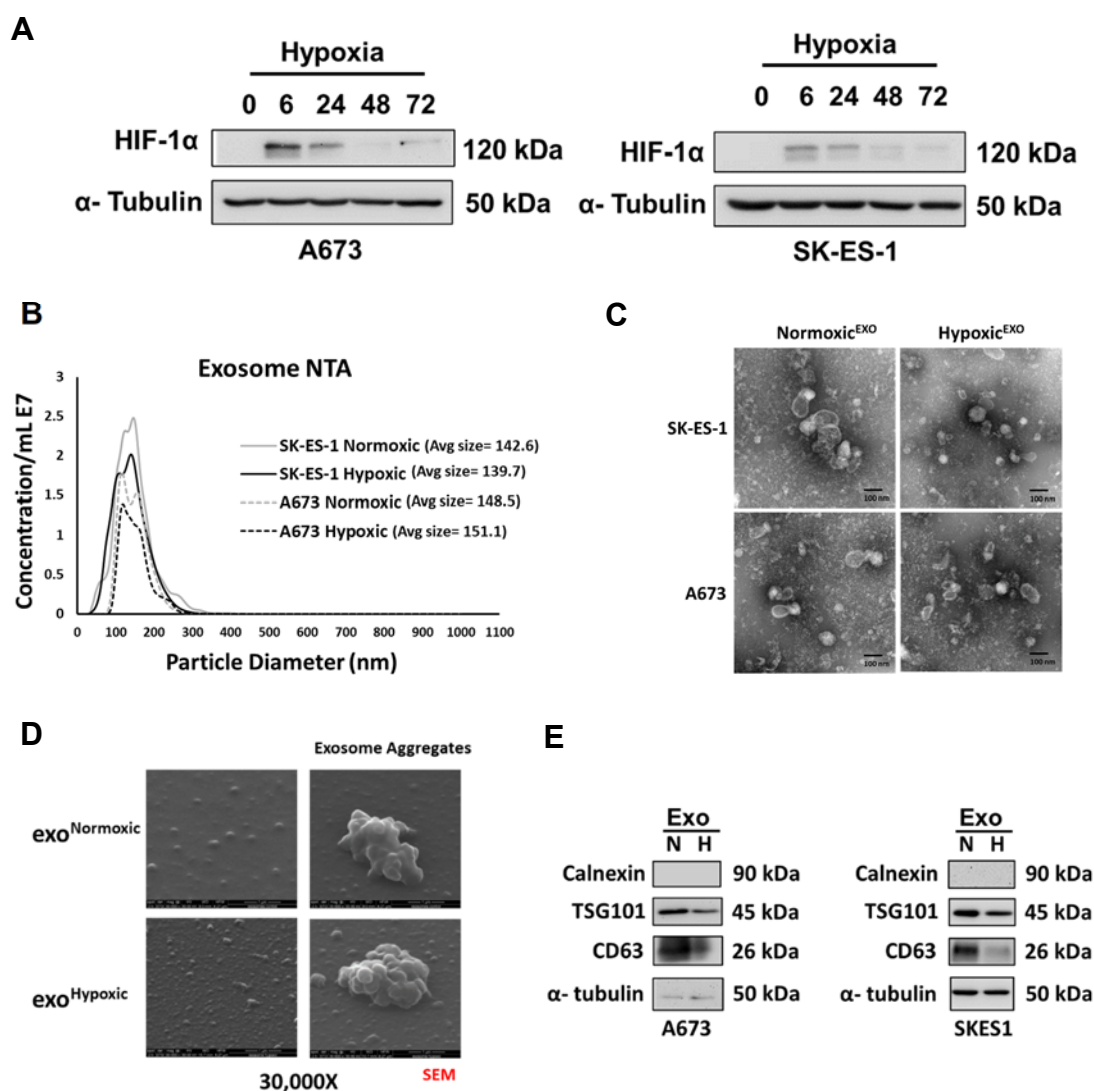


**Figure 3.3: Characterization of EWS-FLI1 in EWS exosomes.** (A) Assessment of EWS-FLI1 mRNA in SK-ES-1 Normoxic<sup>EXO</sup> and Hypoxic<sup>EXO</sup> using qRT-PCR (Mean  $\pm$  SEM, n=3 \*,  $P \leq 0.005$ , \*\*,  $P \leq 0.0005$ ). RNU6B was used as a control to normalize expression. (B) Western blot of key EWS proteins CD133, EZH2, IGF-1R, EWS-FLI1, CD99 involved in EWS pathogenesis. Loading controls and exosomes markers  $\alpha$ -Tubulin and TSG101 were assessed respectively.

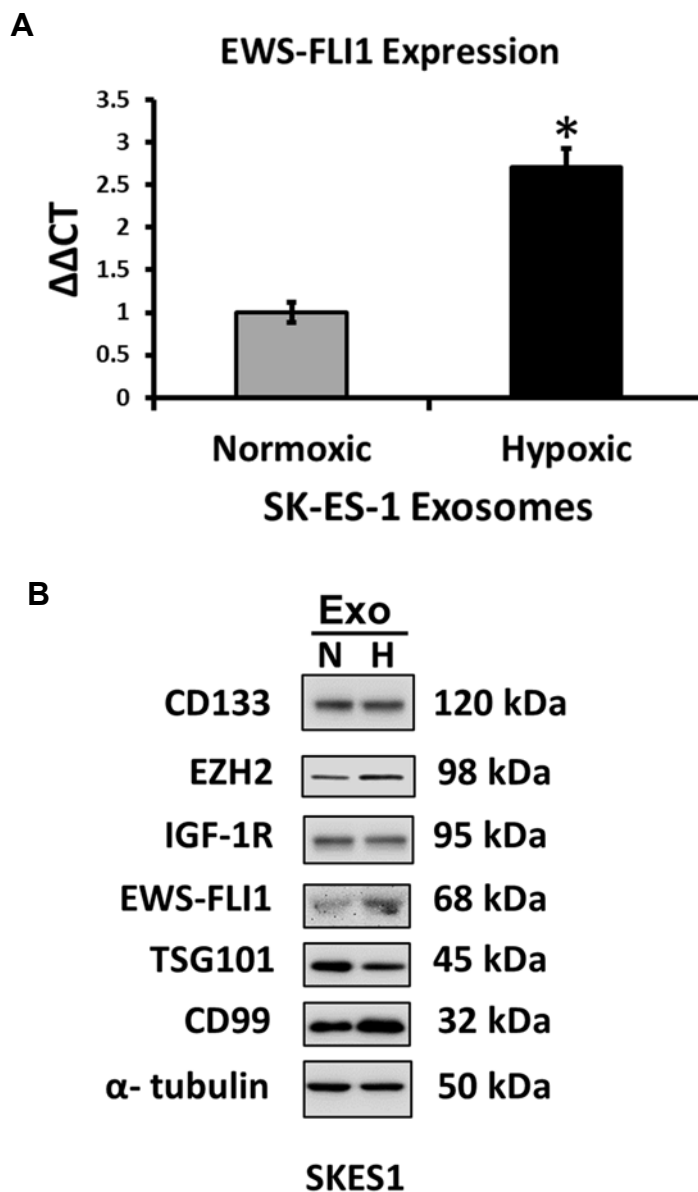


**Figure 3.4: Representative electropherogram profile of total RNA in normoxic and hypoxic SK-ES-1 cells and exosomes.** Ribosomal subunits 28S and 18S were observed in cellular RNA profiles and were absent in exosomal RNA.

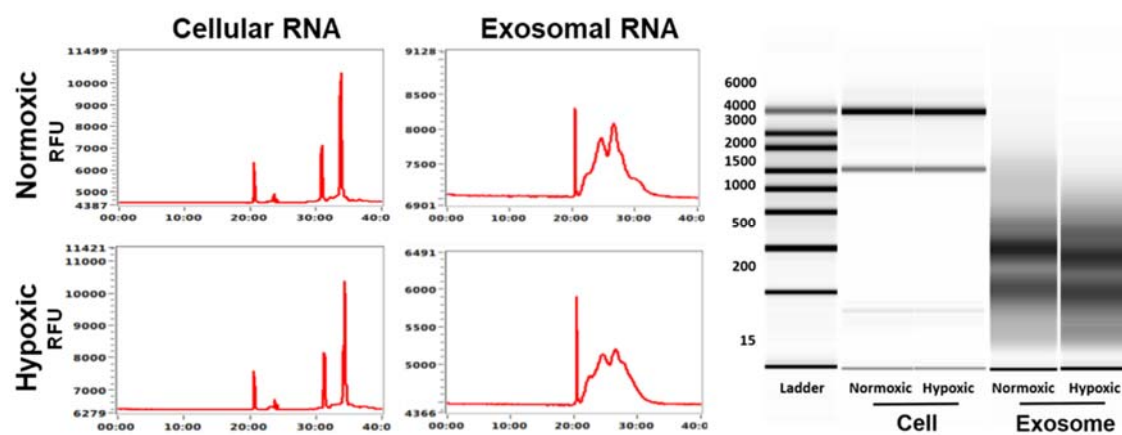


**Figure 3.5: Differential expression of miRNAs in normoxic and hypoxic cells and exosomes.** Unsupervised cluster analysis of SK-ES-1 miRNAs in (A) normoxic and hypoxic cells and (B) Normoxic<sup>EXO</sup> and Hypoxic<sup>EXO</sup>. Each column represents a biological replicate and every row denotes an individual miRNA. The Z-score color scale indicates high expression represented by red ranging to low expression denoted by green. Volcano plot of miRNA differentially expressed ( $\geq 1.5$  fold threshold) in SK-ES-1 (C) normoxic compared to hypoxic cells and (D) Hypoxic<sup>EXO</sup> compared to Normoxic<sup>EXO</sup>. Significance ( $-\log_{10}$  p-value) was plotted versus fold change ( $\log_2$  fold change) along the y and x axis, respectively.

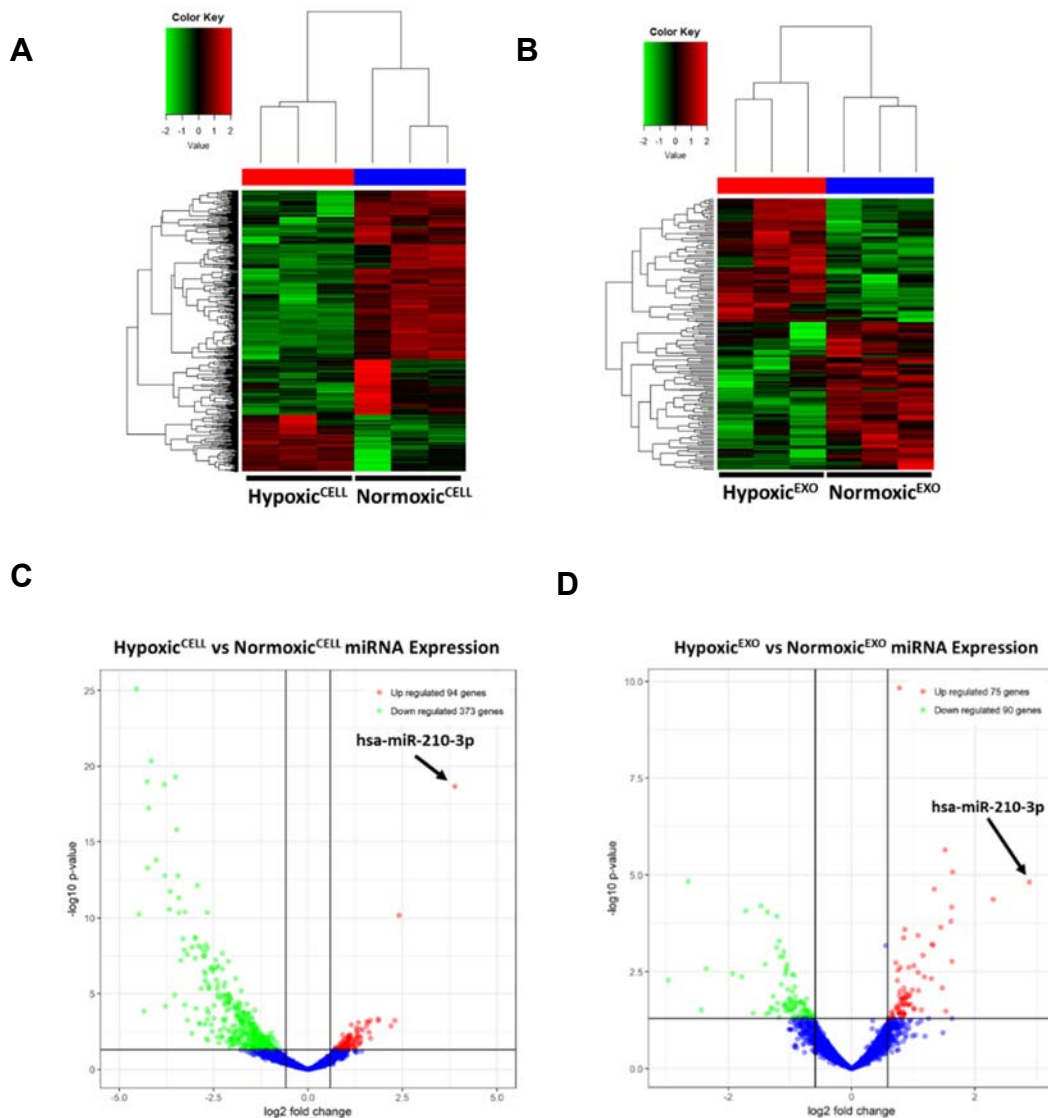


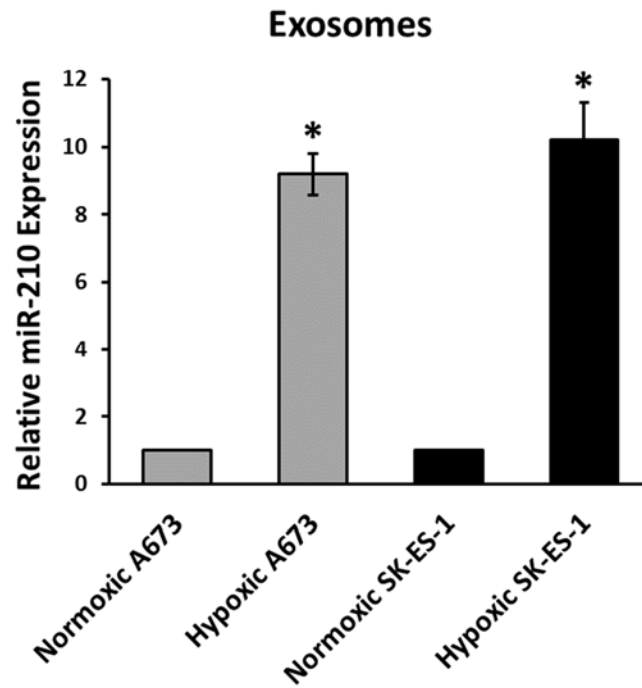
**Table 3.1: Hypoxia regulated miRNAs differentially expressed in SK-ES-1**

**Hypoxic<sup>EXO</sup> compared to Normoxic<sup>EXO</sup>.** Fold change was calculated using miRNA-seq read counts.

<u>Upregulated</u>		<u>Downregulated</u>	
<u>miRNA</u>	<u>Fold Change</u>	<u>miRNA</u>	<u>Fold Change</u>
miR-210	3.1	miR-25	-1.7
miR-30d	1.9	miR-181d	-1.5
miR-10b	1.8	miR-489	-1.48
miR-27	1.7	miR-200b	-1.44
miR-339	1.6	miR-22	-1.43
miR-206	1.5	miR-449	-1.34
miR-21	1.5	miR-424	-1.27
miR-23	1.5	let-7f	-1.25
miR-125a	1.49	miR-196b	-1.2
miR-181b	1.43	miR-30	-1.18
miR-373	1.4	miR-200a	-1.17
miR-93	1.4	miR-150	-1.1
miR-26	1.3	miR-20b	-1.005
miR-30a-5p	1.3		
miR-497	1.25		
miR-103	1.2		
miR-193b	1.2		
miR-30c	1.2		
miR-188	1.1		

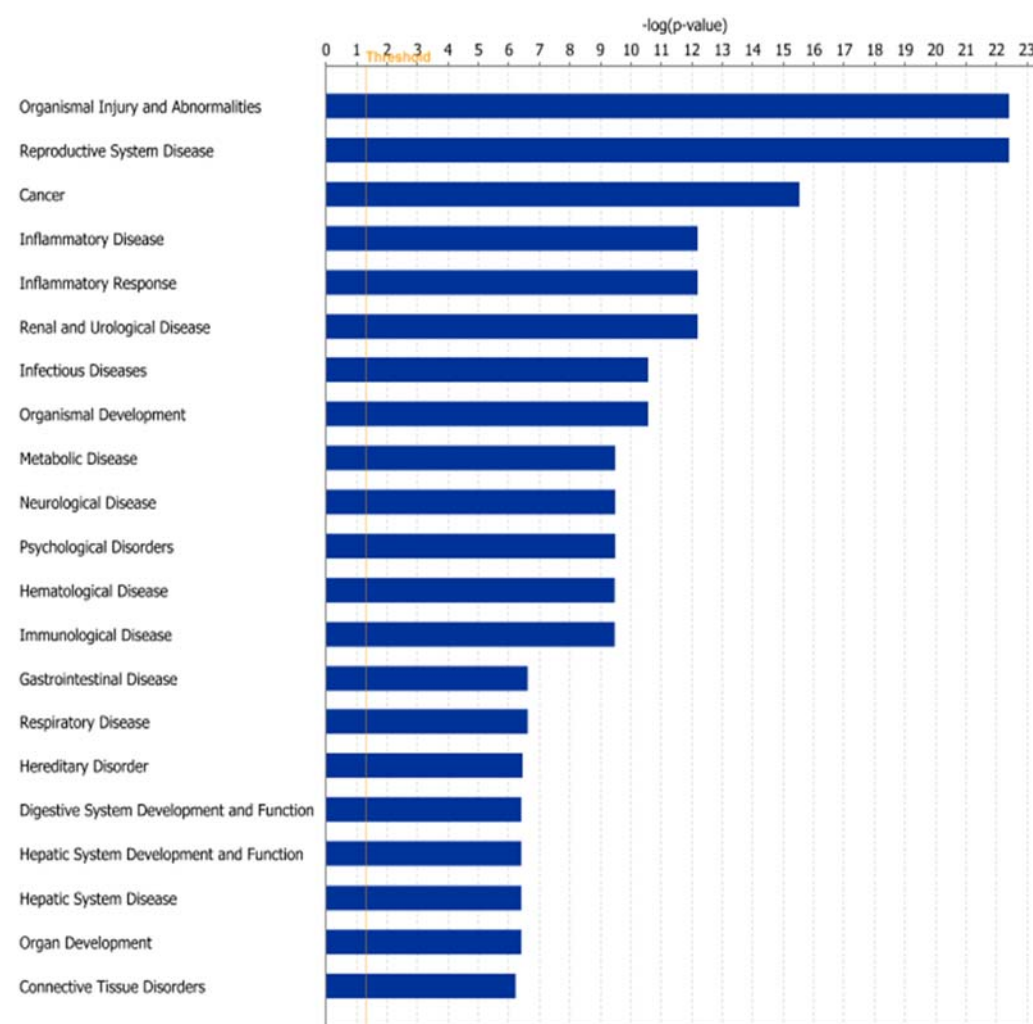


**Figure 3.6: miR-210 expression in EWS exosomes.** Validation of hypoxia regulated miRNAs miR-210 A673 and SK-ES-1 Normoxic<sup>EXO</sup> and Hypoxic<sup>EXO</sup> using qRT-PCR (Mean  $\pm$  SEM, n=3, \*,  $P \leq 0.05$ ). miR-16 was used as a control to normalize miRNA expression.



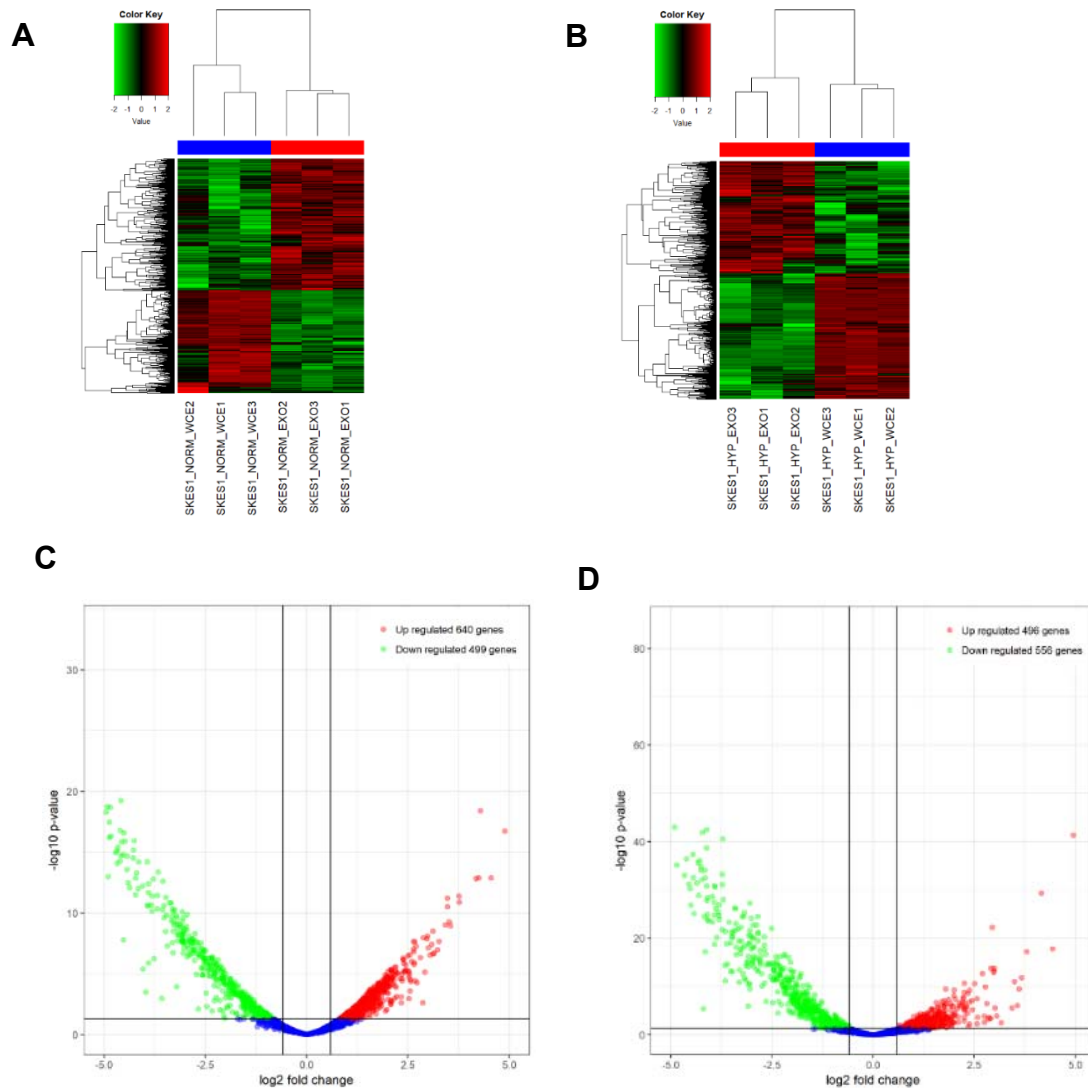
**Figure 3.7: IPA analysis and interactome of exosomal miRs.** (A) IPA analysis of the top 15 significantly represented diseases and biological function categories for miRNA differentially ( $\geq 1.5$  fold) expressed in Hypoxic<sup>EXO</sup> compared to Normoxic<sup>EXO</sup>. (B) Top network generated by IPA software indicating differentially expressed Hypoxic<sup>EXO</sup> derived miRNAs and their predicted targets. Direct interactions are denoted by solid lines and indirect interactions are represented by dotted lines. Red and green indicates high and low miRNA expression, respectively.

**A**

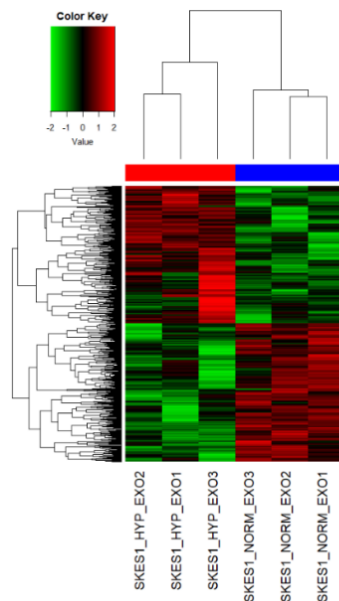
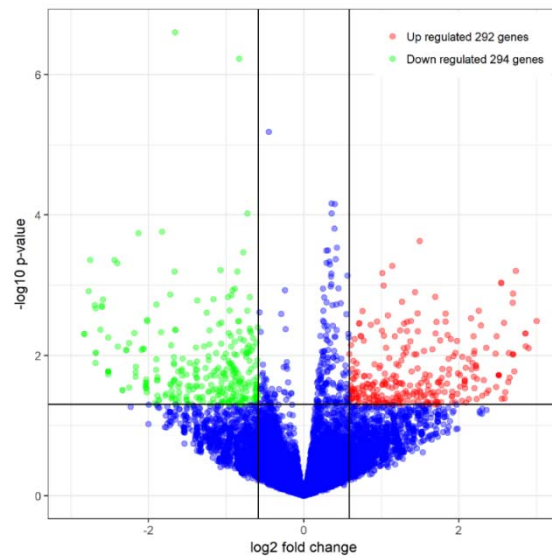




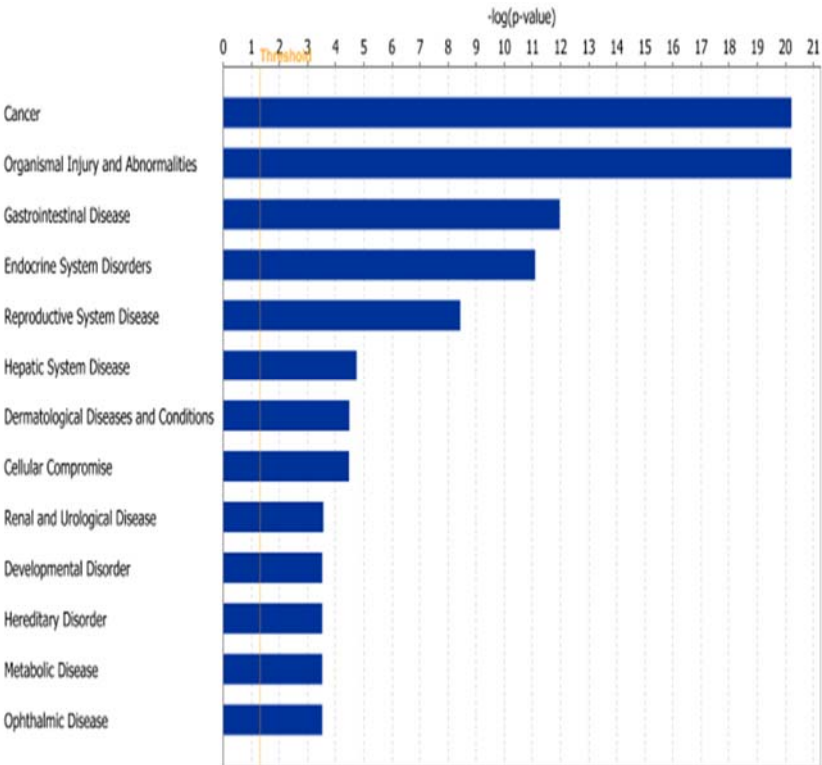
**Figure 3.8: Differential expression of miRNAs in normoxic and hypoxic cells and exosomes.** Heatmap of differentially expressed miRNAs in SK-ES-1 (A) Normoxic<sup>EXO</sup> compared to Normoxic cells and (B) Hypoxic<sup>EXO</sup> compared to Hypoxic cells. Each column represents a biological replicate and every row denotes an individual miRNA. The Z-score color scale indicates high expression represented by red ranging to low expression denoted by green. Volcano plot of miRNA significantly upregulated or downregulated ( $\geq 1.5$  fold threshold) in SK-ES-1 (C) Normoxic<sup>EXO</sup> compared to Normoxic cells and (D) Hypoxic<sup>EXO</sup> compared to Hypoxic cells. Significance ( $-\log_{10}$  p-value) was plotted versus fold change ( $\log_2$  fold change) along the y and x axis, respectively.



**Figure 3.9: Differential expression and IPA analysis of mRNAs in normoxic and hypoxic cells and exosomes.** (A) Cluster analysis of mRNAs in SK-ES-1 Normoxic<sup>EXO</sup> and Hypoxic<sup>EXO</sup>. Each column represents a biological replicate and every row denotes an individual mRNA. The Z-score color scale indicates high expression represented by red ranging to low expression denoted by blue. (B) Volcano plot of top differentially expressed ( $\geq 1.5$  fold threshold) mRNA significantly upregulated or downregulated in SK-ES-1 Hypoxic<sup>EXO</sup> compared to Normoxic<sup>EXO</sup>. Significance ( $-\log_{10}$  p-value) was plotted versus fold change ( $\log_2$  fold change) along the y and x axis, respectively. (C) IPA analysis of the top 15 significantly represented diseases and biological function categories for mRNA differentially ( $\geq 1.5$  fold) expressed in Hypoxic<sup>EXO</sup> compared to Normoxic<sup>EXO</sup>. (D) Top network generated by IPA software indicating differentially expressed Hypoxic<sup>EXO</sup> derived mRNAs and their predicted targets. Direct interactions are denoted by solid lines and indirect interactions are represented by dotted lines. Red and green indicates high and low mRNA expression, respectively.

**A****B**

C



D

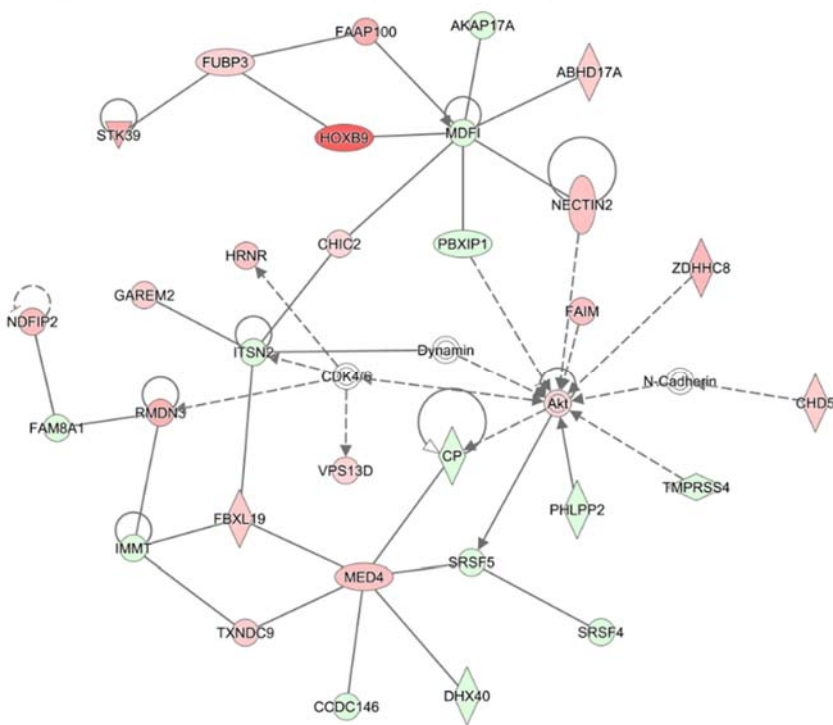


**Figure 3.10: Differential expression of mRNAs in normoxic and hypoxic cells and exosomes.** Heatmap of differentially expressed mRNAs in SK-ES-1 (A) Normoxic<sup>EXO</sup> compared to Normoxic cells and (B) Hypoxic<sup>EXO</sup> compared to Hypoxic cells. Each column represents a biological replicate and every row denotes an individual mRNA. The Z-score color scale indicates high expression represented by red ranging to low expression denoted by green. Volcano plot of mRNA significantly upregulated or downregulated ( $\geq 1.5$  fold threshold) in SK-ES-1 (C) Normoxic<sup>EXO</sup> compared to Normoxic cells and (D) Hypoxic<sup>EXO</sup> compared to Hypoxic cells. Significance ( $-\log_{10}$  p-value) was plotted versus fold change ( $\log_2$  fold change) along the y and x axis, respectively.

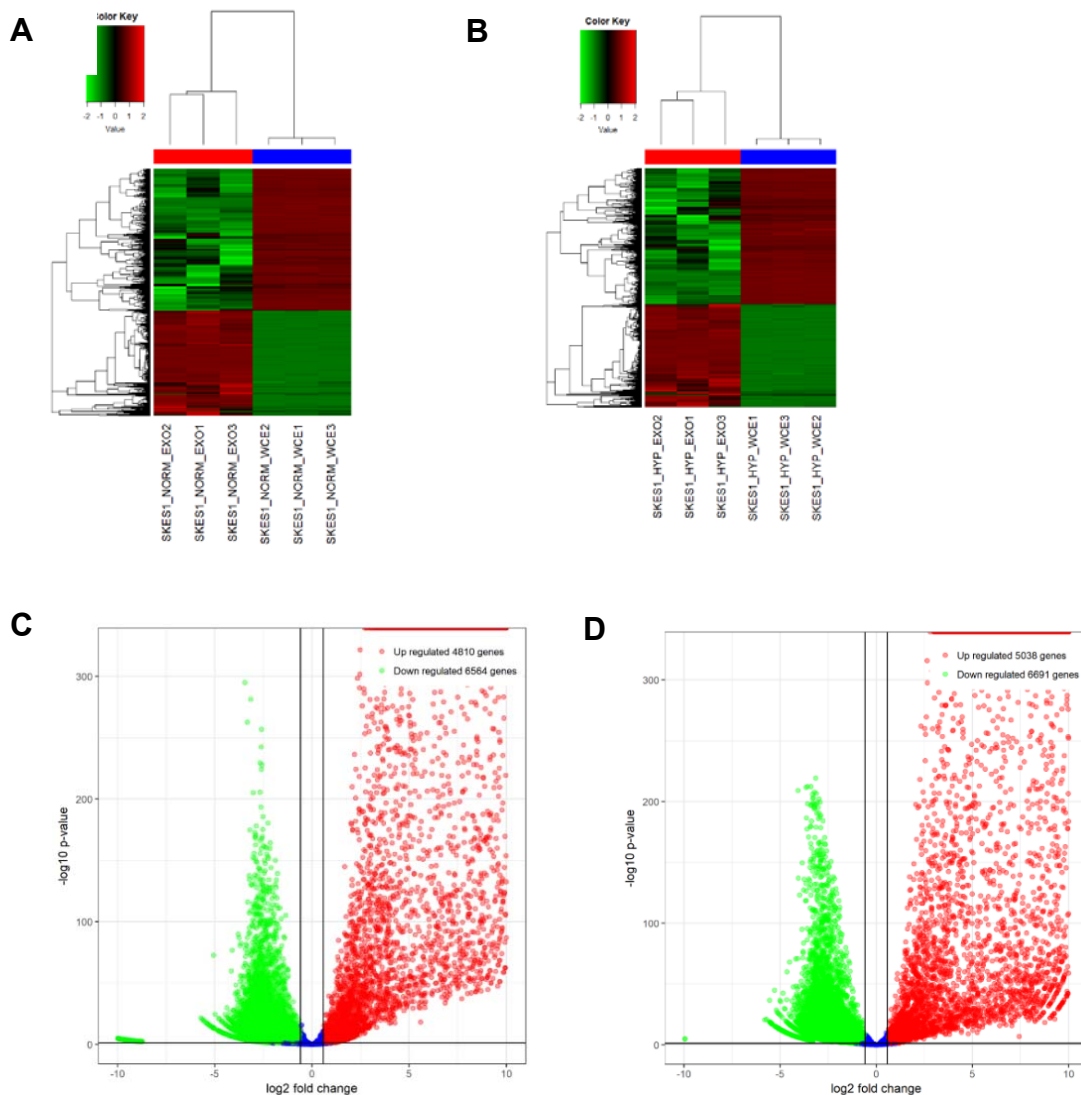
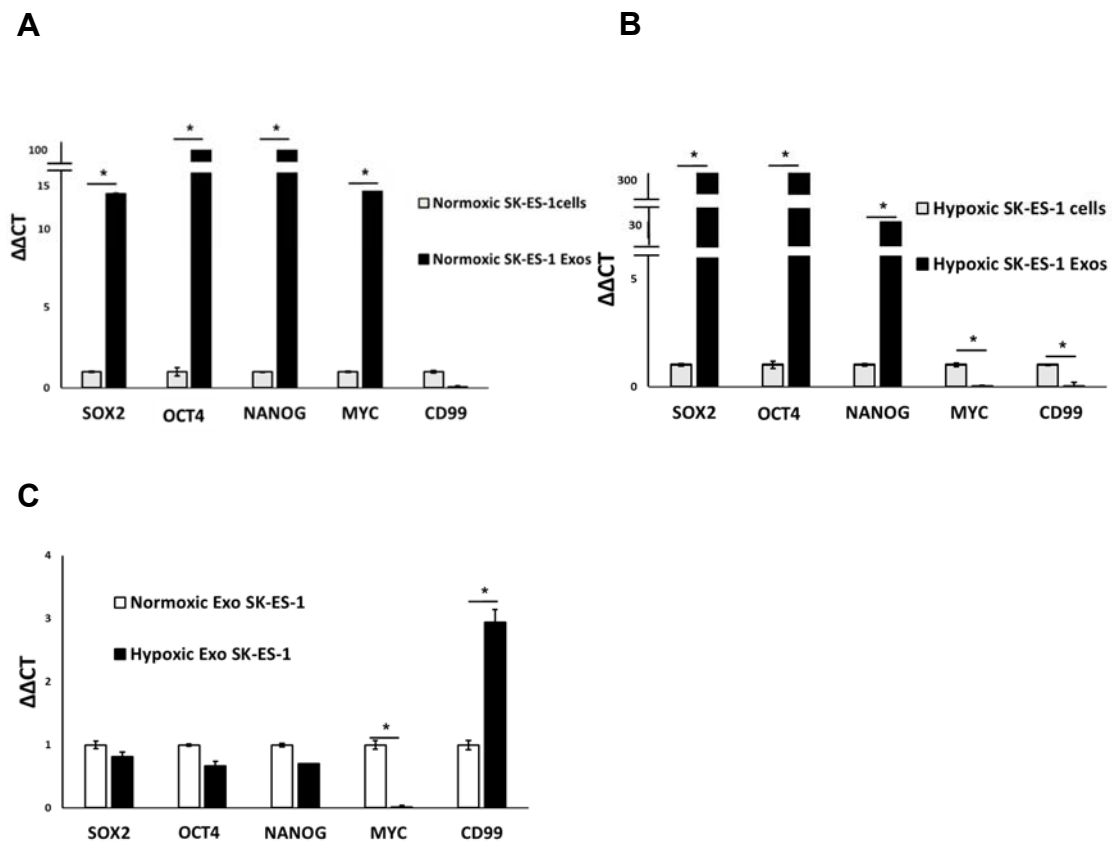


**Figure 3.11: ESC gene expression in normoxic and hypoxic EWS cells.**

Differential expression of ESC genes *SOX2*, *OCT4*, *NANOG* and *MYC* in (A) Normoxic<sup>EXO</sup> compared to Normoxic cells, (B) Hypoxic<sup>EXO</sup> compared to Hypoxic cells and (C) Normoxic<sup>EXO</sup> compared to Hypoxic<sup>EXO</sup> assessed by qRT-PCR. *GAPDH* was used as the endogenous control (Mean  $\pm$  SEM, n=3 \*,  $P \leq 0.05$ , \*\*).





## Discussion

The major challenge facing exosome research is the ability to differentiate between exosomes and other extracellular vesicles such as microvesicles. The methods to discriminate between exosomes (~40-150 nm) and microvesicles (~100-1000 nm) assess size, morphology, protein content, and buoyant density, however, these parameters remain insufficient (285). Until the mechanisms involved in exosome biogenesis and the selective packaging of exosomal cargo can be elucidated, current techniques remain insufficient to fully characterize exosomes and their functional affects. Presently, the guidelines for characterizing exosomes are based on the previously mentioned parameters, but consideration of the pitfalls is promoted when drawing conclusions from exosome studies (289).

The persistent difficulties in exosome studies arise from the challenges in exosome preparations that are unable to strictly enrich for exosomes. The predominant methods utilized in the field include exosome isolation kits, ultracentrifugation with microfiltration, and ultracentrifugation approaches implementing Opti-Prep (iodixanol) or sucrose gradients to isolate particles based on their buoyant density, however, each method is associated with its own advantages and disadvantages (289). Our findings indicated that the sucrose gradient method produced particles with the smallest average size compared to the standard ultracentrifugation and Opti-Prep isolation methods. The standard ultracentrifugation approach yielded significantly more particles than the other methods and were within the acceptable size range for exosomes. Interestingly, the Opti-Prep approach, often considered the gold standard method, yielded the greatest particle size but produced the lowest concentration compared to the other isolation techniques. The Opti-Prep method dilutes iodixanol into a sucrose solution. Both Opti-Prep and sucrose isolations were setup as discontinuous gradients creating density

barriers. Opti-Prep gradient solutions are iso-osmotic and prevent the rupturing of vesicles, unlike sucrose solutions that are hyper-osmotic. Since both solutions contain sucrose, this can often result in the aggregation of particles due to the “sticky” nature of the hydroxyl groups on the sucrose molecules. This can cause aggregated particles to form pellets at the bottom of tubes and therefore, defeat the purpose of the gradient. Sucrose is also suspected of inhibiting uptake of exosome into recipient cells. Together this would explain the low yield in both approaches using density gradient solutions and thereby, provided us with the rationale to utilize the standard ultracentrifugation and microfiltration method for downstream analysis and functional studies. SEM analysis of our particles isolated using standard ultracentrifugation confirmed that aggregation of exosome-like particles was occurring and immunoblotting of proteins involved in the exosome biogenesis pathways further supports the standard isolation protocol as a reliable preparation method for exosomes.

Initial studies suggested that Hypoxic<sup>EXO</sup> were being secreted at an elevated rate compared to normoxic cells (290). Our findings and others (234) indicate that exocytosis of exosomes is dependent on cellular proliferation. A likely explanation for these discrepancies could be attributed to the use of exosome isolation methods that utilize polyethylene glycol to pulldown exosomes during the centrifugation process. This approach wouldn't be able to discriminate exosomes from microvesicles or apoptotic bodies, and isolations significantly contaminated with these vesicles would explain the differences in hypoxia mediated exosome secretion. No isolation approach can totally eliminate microvesicles or apoptotic bodies, however, our method utilizes multiple ultracentrifugation and microfiltration steps which have been overwhelming described as a superior method. Furthermore, RNA analysis in our exosomes failed to reveal

ribosomal peaks which are commonly observed in microvesicles and apoptotic bodies. It also is very plausible that these differences are merely context dependent observations.

Detection of increased protein levels of EWS-FLI1, EZH2 and CD99 in Hypoxic<sup>EXO</sup> provides insight into a potential mechanism responsible for the enhanced effects observed in cells treated with Hypoxic<sup>EXO</sup>. However, in addition to elevated levels of EWS-FLI1, EZH2 and CD99, Hypoxic<sup>EXO</sup> had relatively equal levels of CD133 and IGF-1R compared to Normoxic<sup>EXO</sup>. Studies transducing the EWS-FLI1 fusion gene into mesenchymal stem cells, the hypothesized cell of origin, were able to elicit a similar phenotype observed in primary EWS TICs but were unable to demonstrate tumor formation in mice with these transformed cells (15, 49, 104, 111). This suggested that EWS-FLI1 alone is unable to recapitulate the EWS phenotype. In separate contexts, both CD99 and EZH2 had demonstratable roles in maintaining stemness in EWS and together, forced expression of these proteins may reveal the necessary conditions underlying EWS tumorigenesis (111, 115, 116). Further studies are needed to determine the role of these proteins in EWS cells and the potential exosome mediated effect on EWS TICs and CAF formation.

In cancer patients, exosomes are reportedly elevated within the systemic vasculature compared to normal healthy control patients and carry biomarkers with the potential to detect and monitor the development of tumors (244). Characterization of mRNA in EWS cells and their derived exosomes was previously performed in order to identify an RNA profile that could be used to detect minimal residual disease following therapy (113). We advanced this approach by reporting differential expression of mRNAs and miRNAs in hypoxic and normoxic EWS exosomes and in addition, we compared RNA expression profiles between normoxic and hypoxic cells, and between cells and their respective exosomes. Importantly, the differential expression of our

exosomal miRNA cargo revealed selective sorting of small RNAs in Hypoxic<sup>EXO</sup> that in part reflected the miRNA profile in our hypoxic cells, that could be used to assess prognosis in EWS patients with hypoxic tumors.

Detection of hypoxia regulated miRNAs in circulating exosomes have played a major role as prognostic and predictive markers that correlate with metastasis and chemoresistance (290, 291). We validated the top miRNA, miR-210, that was differentially expressed in our hypoxic cells and Hypoxic<sup>EXO</sup>. Furthermore, we identified a miRNA profile consistent with findings in exosomes derived from hypoxic breast cancer cells and patient samples (290, 292). Moreover, breast cancer patients with elevated exosomal miR-210 were associated with tumor metastasis (293). In EWS patients, EWS-FLI1 is the sole diagnostic marker that distinguishes EWS from other sarcomas and bone cancers (8). In our study, we are the first to show a miRNA profile in EWS exosomes that could serve as biomarkers and assist in the prediction of outcomes in EWS patients with aggressive hypoxic tumors (310).

The effects of exosome mediated transfer of miRNAs to target cells has garnered the most attention in the exosome field (244). Internalization of cancer derived exosomes into recipient cells introduces a myriad of miRNAs with overlapping targets capable of interacting with the same mRNA in the host cell and eliciting similar oncogenic effects. Most studies have focused on the function of a singular miRNA and the effects it has on an individual mRNA, while few studies have taken an integrated approach to profiling the broad miRNA expression in exosomes by utilizing software to analyze cancer pathways and networks describing predicted interactions between miRNA and their validated targets. This approach would take into consideration the large amount of miRNAs in exosomes and their potential overlapping targets that contribute to a known phenotype. Analysis of our miRNA cargo revealed 75 enriched and 90 depleted

miRNAs in Hypoxic<sup>EXO</sup> compared to Normoxic<sup>EXO</sup> (310). IPA analysis of these differentially expressed miRNAs revealed enrichment of Hypoxic<sup>EXO</sup> miRNAs with experimentally observed and predicted diseases and biological functions within the categories of Organismal Injury and Abnormalities, Reproductive System Disease and Cancer. The top network displayed protein targets associated with aggressive EWS tumors and maintenance of stemness under hypoxic conditions. Analysis of this interactome depicts Akt as the most significantly targeted protein node and notably, 7 miRNAs were revealed to interact with Akt signaling pathway. These candidate miRNAs have been previously reported to indirectly activate Akt by silencing repressors of this signaling pathway. In addition, IPA analysis of the mRNA in Hypoxic<sup>EXO</sup> converged on the Akt signaling pathway. These findings suggest a broader regulatory network which may affect Akt signaling in cells treated with EWS Hypoxic<sup>EXO</sup>.

Future work validating and matching the molecular profiles between exosomes and their parental EWS tumors is needed in order to identify EWS patients with hypoxic tumors and to devise new approaches that can overcome therapy resistant tumors. Based on our findings, the subsequent chapters will focus on the Hypoxic<sup>EXO</sup> mediated effect on stemness by delivering exosomal miR-210 to recipient EWS cells and the effects of exosomal miRNA on reprogramming fibroblasts into CAFs with enhanced tumorigenicity by targeting the Akt signaling pathway.

## Chapter IV

# Exosomes Secreted under Hypoxia Enhance Stemness and Tumorigenicity in EWS.

### Introduction

Hypoxia is an essential feature of the tumor microenvironment (TME) in many solid tumors and it is suggested that enrichment of stem-like cells occurs within the hypoxic niche (120, 294), however, this mechanism remains poorly understood in EWS. Stabilization and activation of the hypoxia inducible factor HIF -1 $\alpha$  in hypoxic tumor cells plays a major role in mediating the adaptive response to low oxygen levels (140). HIF -1 $\alpha$  has been demonstrated to regulate tumor formation and stem cell survival in hypoxic cancer cells by inhibiting apoptosis (194). Emerging evidence indicates intercellular communication between tumor cells in hypoxic and normoxic regions contributes to functional differences associated with hypoxic tumors (233, 234, 295).

Recently, small extracellular vesicles called exosomes have been described as important mediators of cell-to-cell communication that transduce signals to neighboring cells and cells outside the local TME (233). This function may provide a mechanism for how hypoxic cells communicate beyond their hypoxic niche and promote aggressive tumors. In the TME, exosomes range in size from 30-150 nm and carry bioactive lipids, protein, mRNAs, miRNAs and gDNA that can be horizontally transferred to cancer cells that drive tumor growth, progression, metastasis, drug resistance, angiogenesis and induction of pre-metastatic niches (244).

The role of hypoxic exosomes have provided insight into how hypoxic tumors can secrete exosomes that propagate an aggressive phenotype in cells outside the hypoxic niche. Exosomes released from hypoxic prostate cancer cells enhanced sphere

formation in normoxic cells (234), but they were unable to elucidate a mechanism describing how hypoxic exosomes promote stemness in normoxic cells. More recently, hypoxia was demonstrated to alter miRNA profiles in cancer-derived exosomes. Furthermore, exosomes have been shown to reprogram cancer cells, genetically and metabolically, through the delivery of their miRNA payload (233). In breast cancer, hypoxic exosomes containing elevated levels of miR-210 increased migration and proliferation in recipient cancer cells (228). In hypoxic tumors, miR-210 is directly regulated by HIF -1 $\alpha$  at its HRE and is involved in driving metabolic changes, angiogenesis, cell proliferation, migration, invasion, apoptosis and stemness (210).

The role of hypoxia regulated exosomes and miRNA in EWS is currently unknown and highlights a major gap in scientific knowledge. Therefore, we sought to evaluate the role of hypoxic EWS-derived exosomes on the formation of stem-like cells and tumorigenicity in EWS. We hypothesized that the transfer of hypoxic derived exosomal miR-210 to normoxic cells targets the proapoptotic member caspase-8-associated protein 2 (CASP8AP2), resulting in increased sphere formation and survival.

## Results

To determine whether hypoxia promotes stemness in EWS cells, we measured the effects of hypoxia on sphere formation and induction of stemness markers in EWS cells. EWS cells cultured under hypoxic conditions formed significantly more spheres than cells cultured under normoxia (21% O<sub>2</sub>) (Figure 4.1A) (310). Hypoxic spheres expressed significantly elevated levels of miR-210 (Figure 4.1B) (310) and ESC genes *SOX2*, *OCT4* and *NANOG* compared to normoxic spheres (Figure 4.1C). Upregulation of the ESC program in hypoxic spheres indicates an enrichment of stem-like cells. In hypoxic spheres, the observed decrease in MYC is supported by a previous report in hypoxic prostate cancer cells demonstrating similar inhibition in MYC expression (120).

Previously, miR-145 was shown to be epigenetically repressed in primary EWS CSCs and spheres compared to non-CSCs and cells grown in adherent cultures with FBS (104). Consistent with recent findings, we observed miR-145 to be significantly decreased in our EWS spheres compared to adherent cells (Figure 4.1D). Together, these findings suggest that hypoxia enhances the stem-like phenotype in EWS cells.

We next investigated whether hypoxic exosomes promoted stemness in EWS cells outside of a hypoxic environment, we co-cultured EWS Normoxic<sup>EXO</sup> and Hypoxic<sup>EXO</sup> with normoxic cells in a sphere-forming assay. EWS cells cultured under normal oxygen tension levels demonstrated enhanced sphere formation after adding Hypoxic<sup>EXO</sup> (Figure 4.2) (310). SK-ES-1 Hypoxic<sup>EXO</sup> enhanced sphere formation 3.7-fold while A673 Hypoxic<sup>EXO</sup> increased sphere formation by 2.2-fold compared to the effect of their respective Normoxic<sup>EXO</sup> on normoxic cells. These results suggest that Hypoxic<sup>EXO</sup> could enhance stemness in normoxic EWS cells (310).

Based on our previous finding demonstrating that Hypoxic<sup>EXO</sup> can enhance sphere formation (234), we hypothesized that Hypoxic<sup>EXO</sup> can increase tumor formation. This rationale is supported by earlier studies showing EWS cells that are capable of forming spheres *in vitro* to have enhanced *in vivo* tumor initiating abilities. To determine if Hypoxic<sup>EXO</sup> can enhance tumor formation, we injected NSG mice subcutaneously with EWS ( $1 \times 10^5$ ) cells. Normoxic and hypoxic exosomes (20  $\mu$ g) were injected bi-weekly into the tumor site. Xenograft mice injected with Hypoxic<sup>EXO</sup> formed significantly bigger tumors than the other groups (Figure 4.3A). Interestingly, there was no difference in tumor growth between normoxic control and Normoxic<sup>EXO</sup> mice. To determine if this Hypoxic<sup>EXO</sup> mediated affect on tumor formation correlated with an increase in EWS CSCs, we disaggregated our tumors and assessed the EWS CSC marker, CD133, using FACS analysis (Figure 4.3C). Hypoxic<sup>EXO</sup> exosomes increased the CD133 population



1.5-fold compared to PBS control tumors. No difference in CD133<sup>+</sup> cells was observed between PBS controls and Normoxic<sup>EXO</sup> treated mice. Recently in breast cancer studies, hypoxic exosomes carrying miR-210 increased angiogenesis and proliferation in xenograft mice (228). Consistent with these findings, we observed increased CD31 and Ki67 staining in mice injected with Hypoxic<sup>EXO</sup> (Figure 4.3B). Together, our findings suggest Hypoxic<sup>EXO</sup> can enhance tumor formation and moreover, this effect on tumor growth may be the result of exosomal miR-210 stimulating EWS tumor initiating cells and angiogenesis.

Since HIF-1 $\alpha$  has been shown to regulate the expression of miR-210 in hypoxic cells, we evaluated whether miR-210 levels in hypoxic EWS cells and their Hypoxic<sup>EXO</sup> were HIF-1 $\alpha$  dependent by knocking down HIF-1 $\alpha$  using siRNAs (siHIF-1 $\alpha$ ) (Figure 4.4A) (310). In our HIF-1 $\alpha$  knockdown cells, we observed a significant decrease in HIF-1 $\alpha$  under hypoxic conditions. Knockdown of HIF-1 $\alpha$  significantly decreased miR-210 in both our hypoxic cells (Figure 4.4B) and in their Hypoxic<sup>EXO</sup> (Figure 4.4C) (310). In addition, miR-210 levels in the HIF-1 $\alpha$  knockdown cells and exosomes were similar to their normoxic controls. These results indicate that miR-210 expression in hypoxic EWS cells and Hypoxic<sup>EXO</sup> is regulated by HIF-1 $\alpha$ . Next, we assessed the effect of Hypoxic<sup>EXO</sup> derived from siHIF-1 $\alpha$  cells on sphere formation (Figure 4.4D) (310). Here, Hypoxic<sup>EXO</sup> derived from siHIF-1 $\alpha$  cells failed to increase sphere formation compared to control Hypoxic<sup>EXO</sup>. Together, these findings suggest that the stabilization of HIF-1 $\alpha$  in hypoxic cells play a significant role in the Hypoxic<sup>EXO</sup> mediated effects on sphere formation (310).

Recent EWS studies implemented PI3K inhibitors to show that Akt signaling stabilized HIF-1 $\alpha$  and promoted chemoresistance (226). In another study, activated Akt was demonstrated to regulate miR-210 in hypoxia dependent and independent ways (209), however, it remains unclear how Akt regulates miR-210 under normoxic

conditions. To determine the role of Akt signaling in regulating HIF-1 $\alpha$  and miR-210, we first treated our EWS cells with an Akt inhibitor at sub-IC50 concentrations. A673 and SK-ES-1 were treated with MK-2206 (3  $\mu$ M and 1  $\mu$ M, respectively) for 48 hours under normoxic and hypoxic conditions. In both cell lines, MK-2206 treatment groups demonstrated complete inhibition of Akt phosphorylation compared to their normoxic and hypoxic DMSO controls (Figure 4.5A). Consistent with previous studies (226), we observed partial knockdown of HIF-1 $\alpha$  in our hypoxic EWS cells treated with MK-2206. MK-2206 treatment significantly decreased miR-210 expression in our EWS cells under both normoxic and hypoxic conditions (Figure 4.5B). Hypoxic EWS cells treated with MK-2206 only partially decreased miR-210 levels compared to their hypoxic controls, and moreover, hypoxic A673 and SK-ES-1 treatment groups displayed ~20- and ~15-fold increases in miR-210 compared to their normoxic controls. These findings are supported by previous reports showing Akt regulation of miR-210 in HIF-1 $\alpha$  dependent and independent ways. Interestingly, miR-210 levels were unaffected in Normoxic<sup>EXO</sup> derived from MK-2206 treated cells, while only a partial decrease in miR-210 was observed in exosomes derived from hypoxic cells treated with the Akt inhibitor (Figure 4.5C). Next, we assessed the effect of Hypoxic<sup>EXO</sup> derived from MK-2206 treated cells on sphere formation (Figure 4.5D). Exosomes derived from hypoxic EWS cells treated with MK-2206 significantly increased the number of spheres formed compared to normoxic control cells and exosomes, however, they failed to form as many spheres as the control Hypoxic<sup>EXO</sup>. Together, these findings suggest that the Akt signaling in hypoxic cells play a significant role in the Hypoxic<sup>EXO</sup> mediated effects on sphere formation.

To study if miR-210 is required for sphere formation in EWS cells, we knocked down miR-210 using inhibitors and overexpressed miR-210 using mimics (Figure 4.6A, C) (310). Inhibition of miR-210 in hypoxic spheres resulted in a significant decrease in

sphere formation in both EWS cell lines, however, while the number of spheres formed in hypoxic SK-ES-1 knockdown cells was similar to normoxic spheres, hypoxic A673 knockdown cells had an elevated sphere formation compared to their normoxic spheres. The overexpression of miR-210 in normoxic EWS cells promoted a 9-fold and 2-fold increase in spheres formed in A673 and SK-ES-1 cells, respectively. Normoxic spheres transfected with miR-210 inhibitors or combined mimics with inhibitors demonstrated no significant change in sphere formation in either EWS cell line (310).

To evaluate the role of miR-210 in Hypoxic<sup>EXO</sup> mediated sphere formation, we treated normoxic EWS cells with Hypoxic<sup>EXO</sup> alone and in the presence of cells transfected with miR-210 inhibitors (Figure 4.6C) (310). The effects of Hypoxic<sup>EXO</sup> on sphere formation were significantly impaired in both A673 and SK-ES-1 cells treated with the miR-210 inhibitor. Together, these results indicated that miR-210 in hypoxic spheres and Hypoxic<sup>EXO</sup> plays a causal role in increasing stemness in EWS cells (310).

To identify a functional mechanism underlying the effects of miR-210 on sphere formation, we analyzed a miR-210 target gene, the proapoptotic member CASP8AP2. In hypoxic EWS spheres, expression of CASP8AP2 was significantly decreased compared to normoxic spheres and inhibition of miR-210 in hypoxic spheres restored CASP8AP2 expression when compared to normoxic spheres (Figure 4.6B) (310). Overexpression of miR-210 decreased CASP8AP2 in normoxic spheres when compared to normoxic controls (Figure 4.6D) (310). Importantly, normoxic spheres treated with Hypoxic<sup>EXO</sup> decreased CASP8AP2 levels, while miR-210 reversed the exosome mediated downregulation of CASP8AP2 (Figure 4.6D) (310).

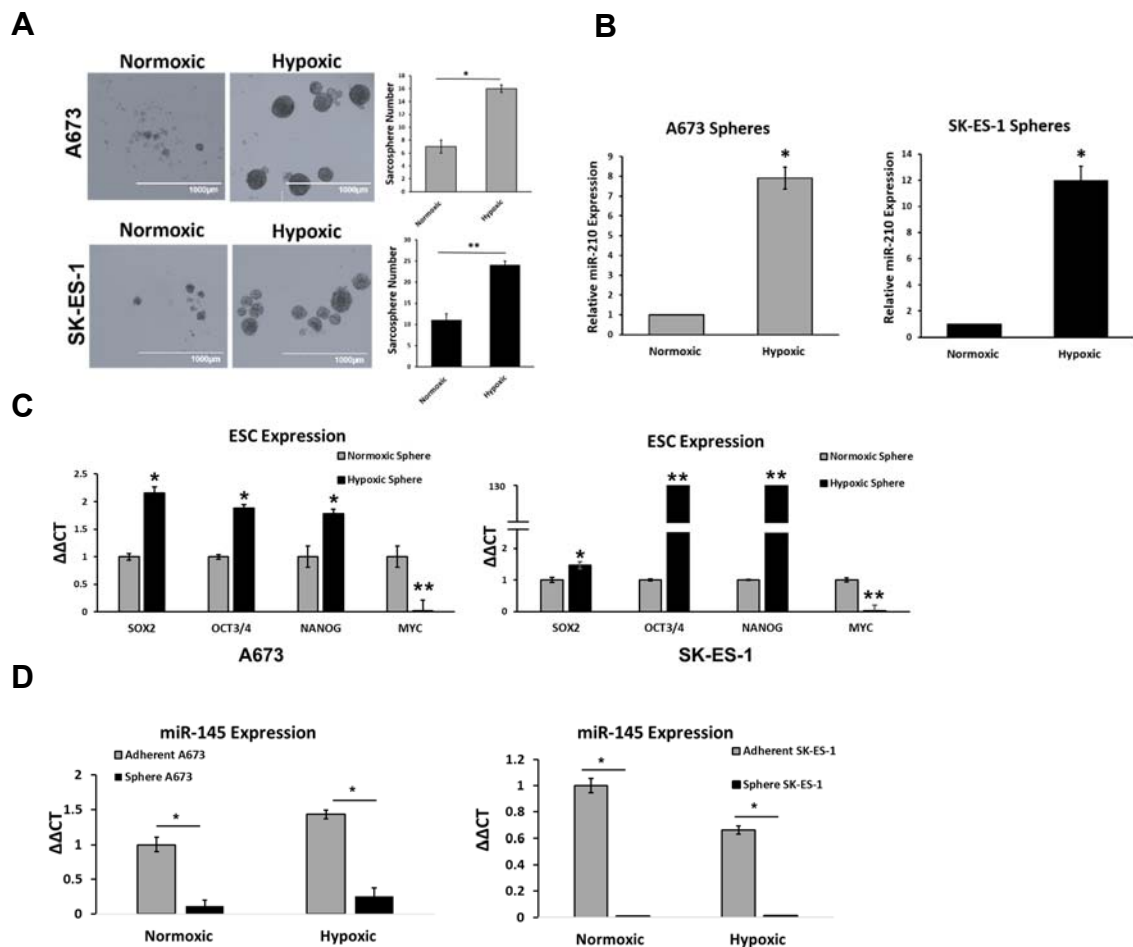
To demonstrate a direct effect of CASP8AP2 expression on sphere formation, we knocked down CASP8AP2 using siRNAs (Figure 4.7A) (310). CASP8AP2 knockdown led to significant increases in sphere formation in normoxic cells but had little effect on

hypoxic spheres when compared to hypoxic controls (Figure 4.7B) (310). To further investigate the functional role of CASP8AP2 in the survival of EWS spheres, we assessed apoptosis using Annexin V/PI staining and flow cytometry (Figure 4.7C) (310). Inhibition of CASP8AP2 in normoxic spheres significantly reduced apoptosis compared to normoxic controls in both cell lines. Interestingly, SK-ES-1 hypoxic control and CASP8AP2 knockdown spheres had similar reductions in apoptosis as the normoxic CASP8AP2 knockdowns, whereas, A673 hypoxic controls demonstrated a further decrease in apoptosis compared to normoxic CASP8AP2 knockdowns. Moreover, CASP8AP2 knockdown further decreased apoptosis in hypoxic spheres compared to the hypoxic control group. Our findings suggest that Hypoxic<sup>EXO</sup> mediated delivery of miR-210 to normoxic EWS spheres targets CASP8AP2 and promotes survival and stemness in EWS cells (310).

### Figure 4.1: Hypoxia increases sphere formation, miR-210 and ESC genes in EWS cells.

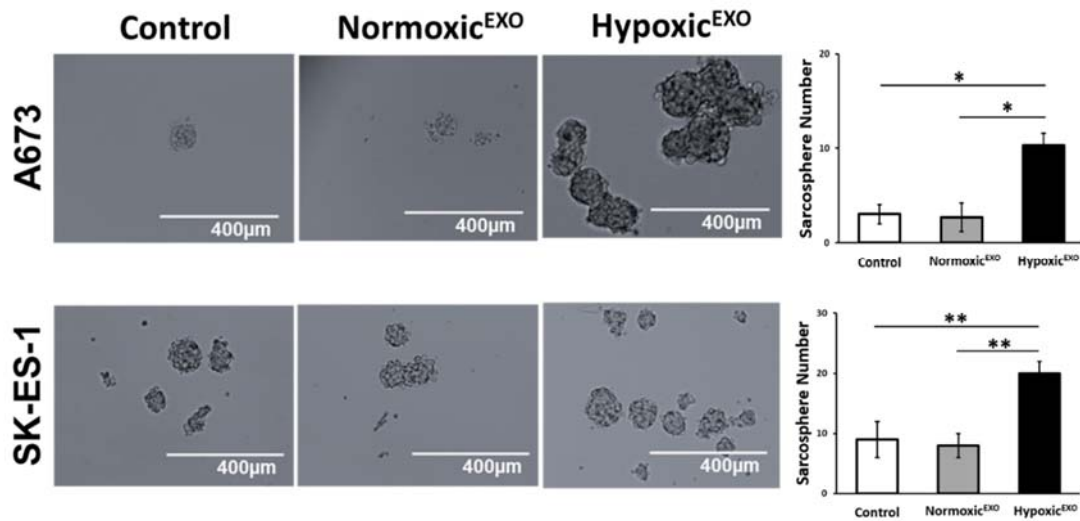
(A) Sphere assay of A673 and SK-ES-1 cells grown under normoxic and hypoxic conditions. Quantification of spheres was performed (magnification, X4) (mean+ SEM, n=3, \*,  $P \leq 0.02$ , \*\*,  $P < 0.008$ ). (B) Analysis of miR-210 expression levels in normoxic and hypoxic A673 and SK-ES-1 spheres using qRT-PCR (Mean + SEM, n=3, \*,  $P \leq 0.5$ ).

RNU6B was used as a control to normalize miRNA expression. (C) Differential expression of ESC genes *SOX2*, *OCT4*, *NANOG* and *MYC* in normoxic and hypoxic SK-ES-1 spheres assessed by qRT-PCR. *GAPDH* was used as the endogenous control (Mean  $\pm$  SEM, n=3 \*,  $P \leq 0.05$ , \*\*,  $P \leq 0.005$ ). (D) EWS epigenetic stemness marker miR-145 was measured by qRT-PCR in A673 and SK-ES-1 cells grown as adherent cells and spheres under normoxic and hypoxic conditions.

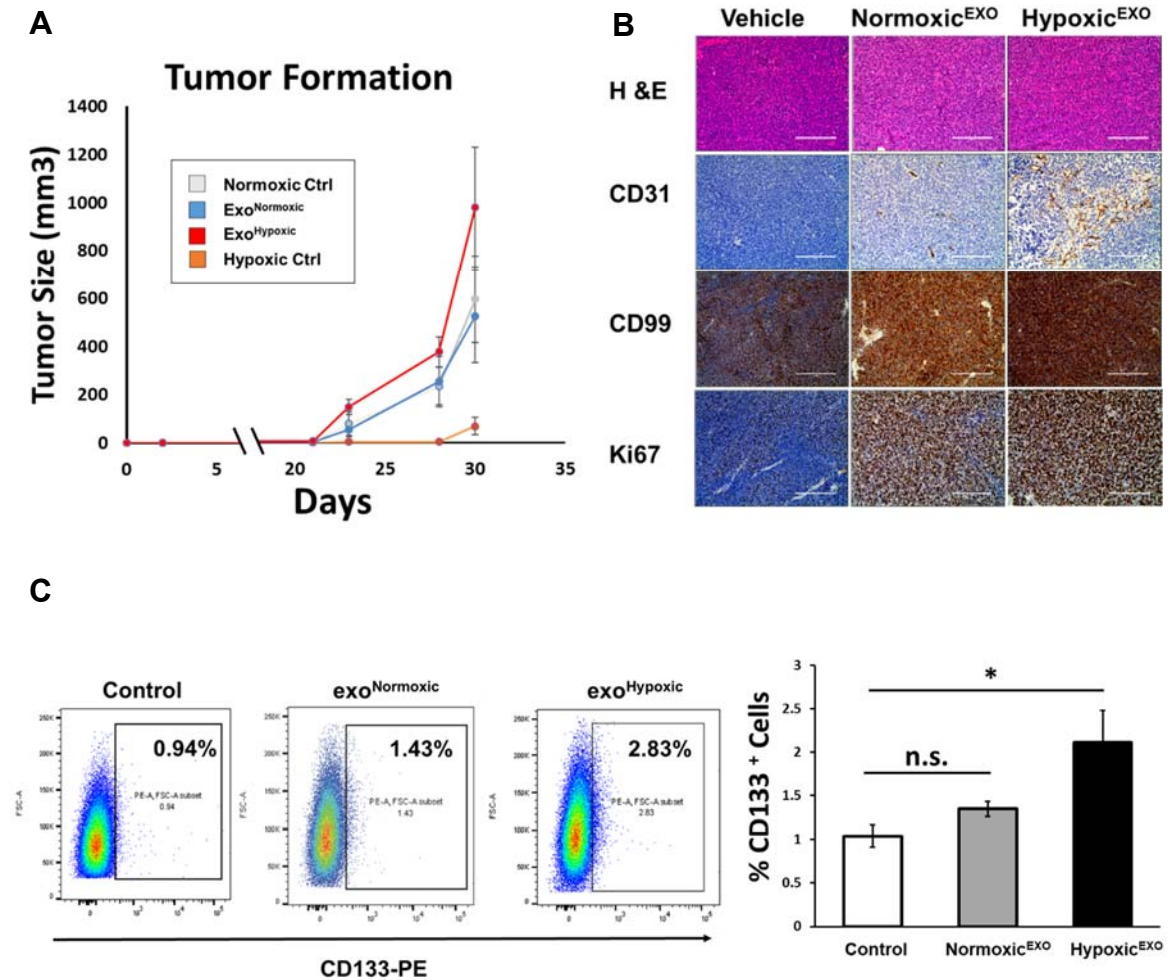


**Figure 4.2: Hypoxic<sup>EXO</sup> enhance sphere formation in EWS cells.** A673 and SK-ES-1

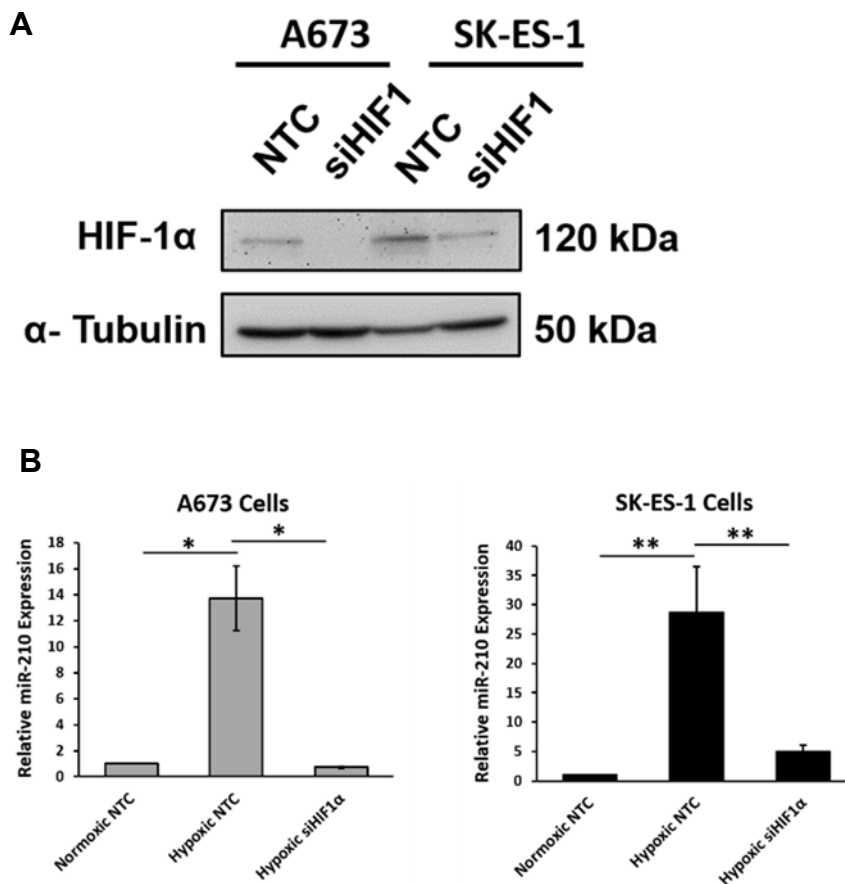
EWS cells were cultured in normoxic conditions with 20  $\mu\text{g/ml}$  of their respective normoxic and hypoxic exosomes in a sphere assay. Quantification of spheres was performed (magnification, X10) (Mean $\pm$  SEM, n=3, \*,  $P\leq 0.0008$ , \*\*,  $P\leq 0.003$ ).



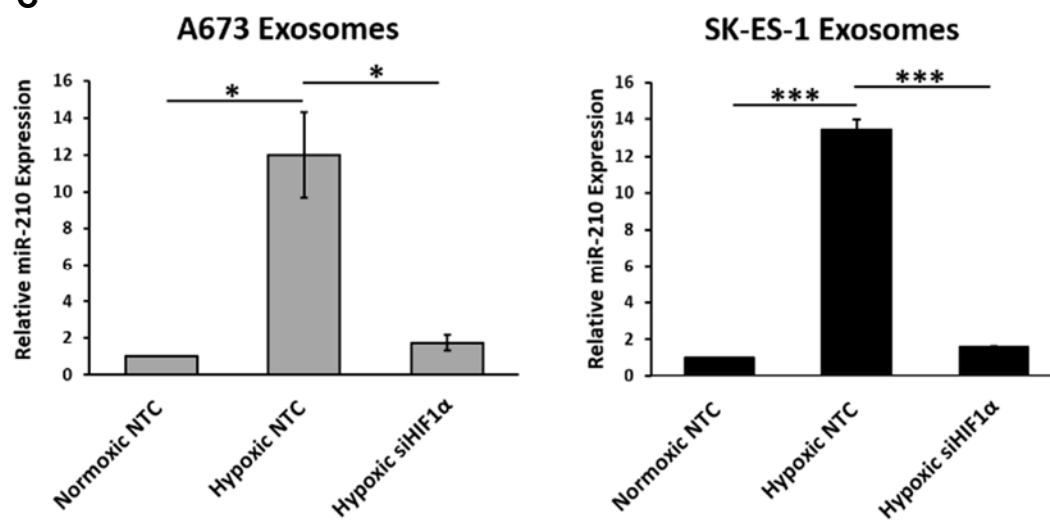
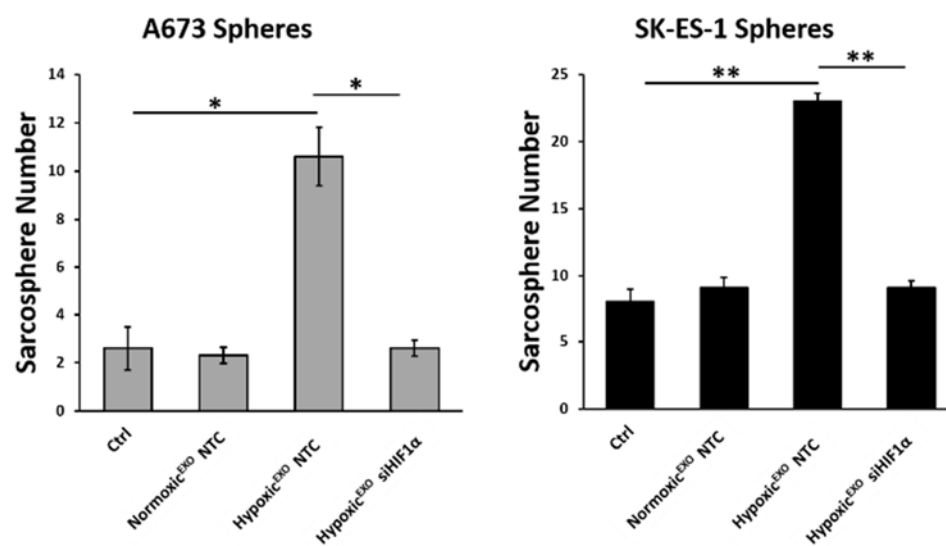
**Figure 4.3: Hypoxic<sup>EXO</sup> increases stemness in EWS tumors.** (A) Tumor growth curve of SK-ES-1 xenograft mice. (B) Representative IHC analysis for CD31, CD99 and Ki67 in SK-ES-1 mice injected bi-weekly with normoxic and hypoxic SK-ES-1 exosomes. (C) (Left) Representative FACS analysis for CD133 disaggregated xenograft tumors. (Right) Quantitative CD133 FACS analysis.



**Figure 4.4: HIF-1 $\alpha$  Regulates Hypoxic<sup>EXO</sup> miR-210 and mediates exosomal induced sphere formation.** (A) Western blot of HIF-1 $\alpha$  in hypoxic A673 and SK-ES- cells transfected with Non-Targeting control (NTC) and HIF-1 $\alpha$ -siRNA.  $\alpha$ -Tubulin was used as the internal loading control. (B) Analysis of miR-210 expression levels in A673 and SK-ES-1 cells transfected with NTC and HIF-1 $\alpha$ -siRNA, and (C) their respective exosomes using qRT-PCR (Mean  $\pm$  SEM, n=3, \*,  $P \leq 0.02$ , \*\*,  $P \leq 0.05$ , \*\*\*,  $P \leq 0.0002$ ). RNU6B and miR-16 was used as a control to normalize miRNA expression in cells and exosomes, respectively. (D) Assessment of sphere formation in A673 and SK-ES-1 EWS cells cultured in normoxic conditions with 20  $\mu$ g/ml normoxic and hypoxic exosomes derived from their respective cells transfected with NTC and HIF-1 $\alpha$ -siRNA. Quantification of spheres was performed (Mean $\pm$  SEM, n=3, \*,  $P \leq 0.0004$ , \*\*,  $P \leq 0.0001$ ).

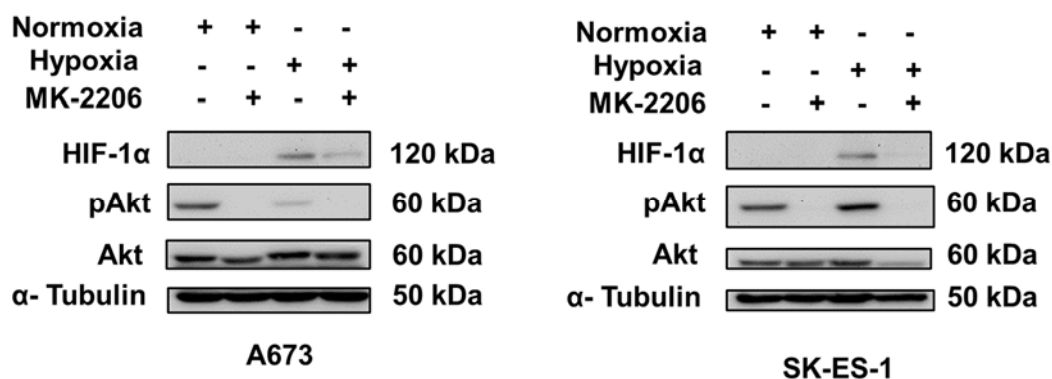




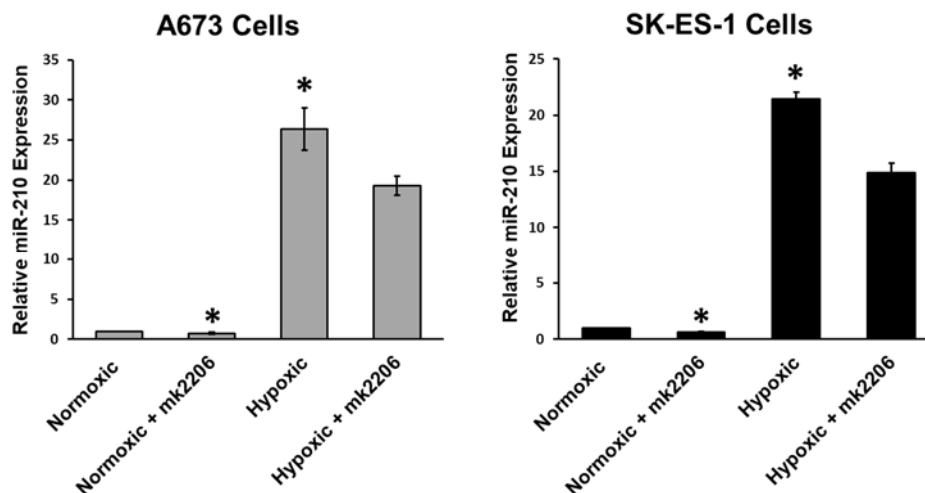
**C****D**

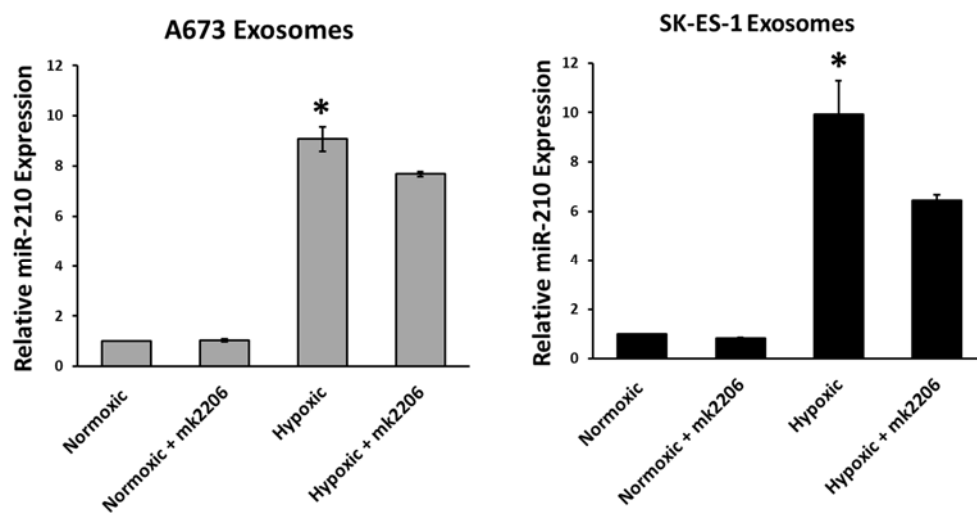
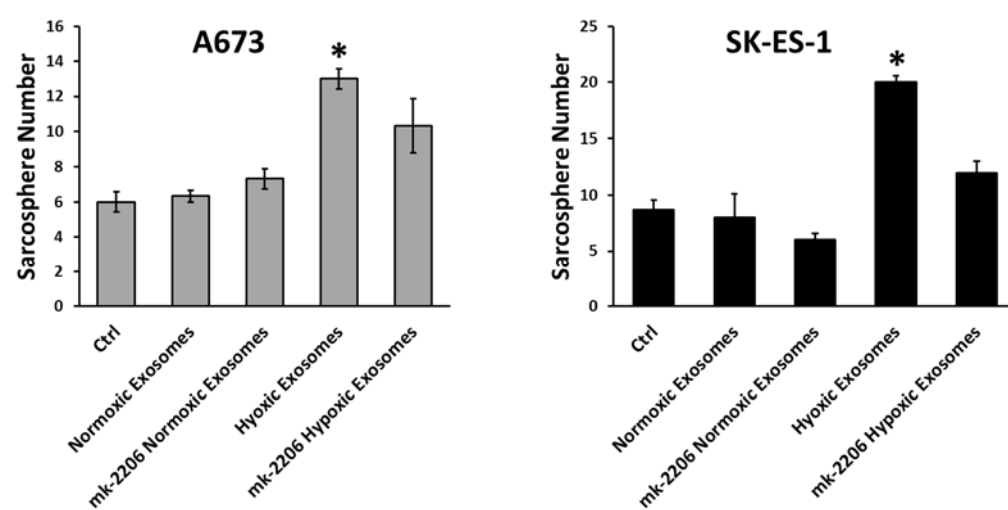
**Figure 4.5: Akt regulates miR-210 in HIF-1 $\alpha$  dependent and independent ways and mediates Hypoxic<sup>EXO</sup>-induced sphere formation.** (A) Western blot of HIF-1 $\alpha$ , pAKT and Akt in hypoxic A673 and SK-ES- cells treated with MK-2206.  $\alpha$ -Tubulin was used as the internal loading control. (B) Analysis of miR-210 expression levels in A673 and SK-ES-1 cells treated with MK-2206, and (C) their respective exosomes using qRT-PCR (Mean  $\pm$  SEM, n=3, \*,  $P \leq 0.05$ ). RNU6B and miR-16 was used as a control to normalize miRNA expression in cells and exosomes, respectively. (D) Assessment of sphere formation in A673 and SK-ES-1 EWS cells cultured in normoxic conditions with 20  $\mu$ g/ml normoxic and hypoxic exosomes derived from their respective cells treated with DMSO or MK-2206. Quantification of spheres was performed (Mean $\pm$  SEM, n=3, \*,  $P \leq 0.05$ ).

**A**



**B**

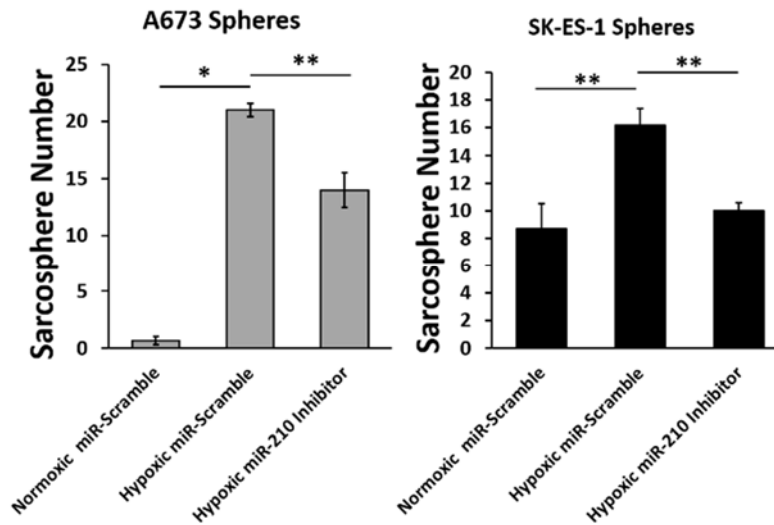


**C****D**

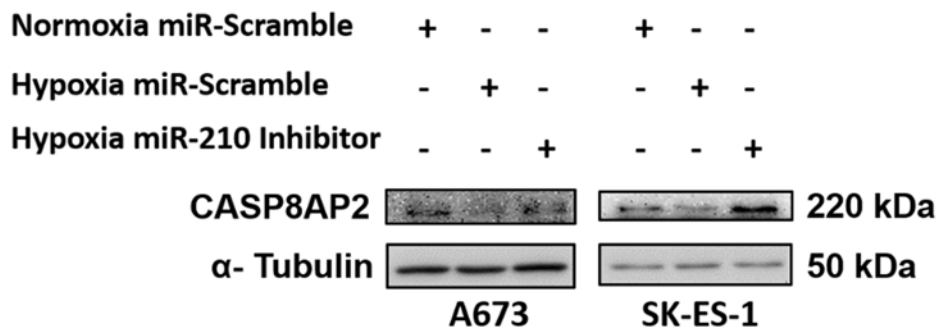
**Figure 4.6: miR-210 regulates sphere formation by targeting CASP8AP2. (A)**

Sphere assay quantifying A673 and SK-ES-1 cells transfected with either miR-scramble or miR-210 inhibitors under normoxic and hypoxic conditions. (Mean + SEM, n=3, \*,  $P \leq 0.0001$ , \*\*,  $P \leq 0.005$ ). (B) Western blot of CASP8AP2 in A673 and SK-ES-1 Spheres transfected with either miR-scramble or miR-210 inhibitors under normoxic and hypoxic conditions. (C) Sphere assay quantifying A673 and SK-ES-1 cells transfected with miR-scramble, miR-210 mimics, miR-210 inhibitors or 20  $\mu\text{g/ml}$  hypoxic exosomes. (Mean + SEM, n=3, \*,  $P \leq 0.002$ , \*\*,  $P \leq 0.0001$ ). (D) Western blot of CASP8AP2 in A673 and SK-ES-1 spheres transfected with miR-scramble, miR-210 mimics, miR-210 inhibitors or 20  $\mu\text{g/ml}$  hypoxic exosomes.

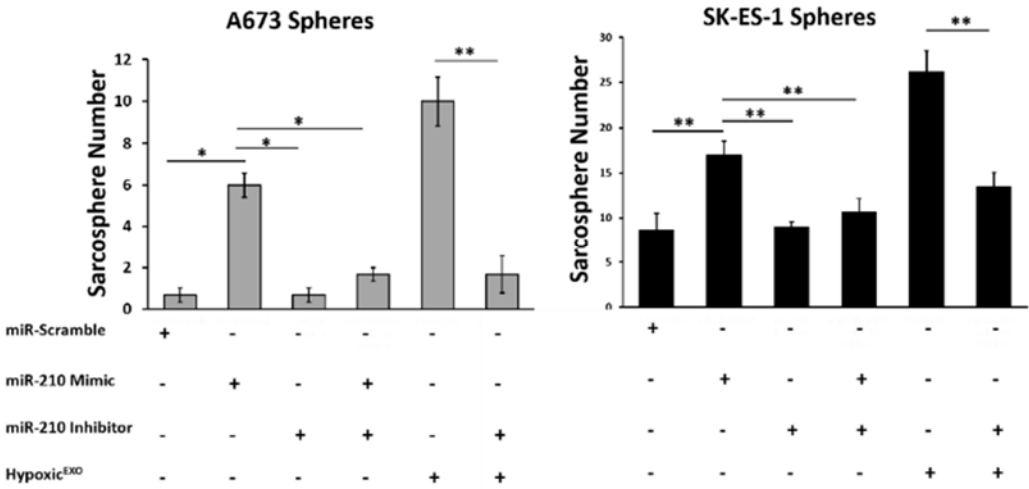
**A**



**B**



C



D

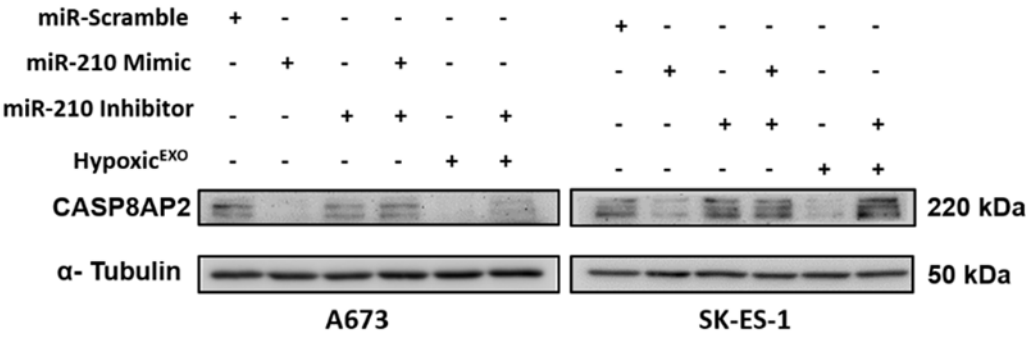
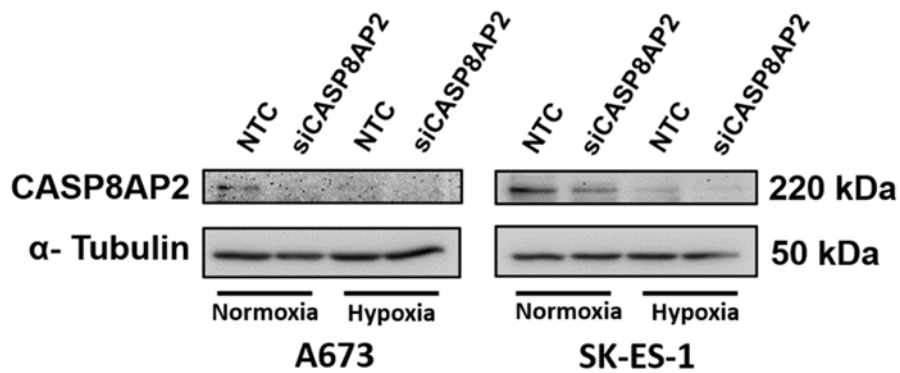
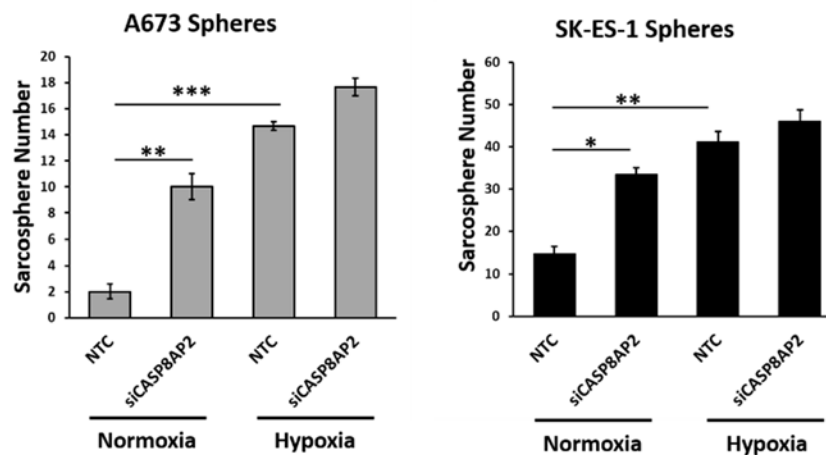


**Figure 4.7: CASP8AP2 knockdown promotes sphere formation by enhancing survival.** (A) A673 and SK-ES-1 spheres transfected with Non-Targeting control (NTC) or CASP8AP2-siRNA.  $\alpha$ -Tubulin was used as the internal loading control. (B) Sphere assay quantifying A673 and SK-ES-1 cells transfected with either NTC or CASP8AP2-siRNA under normoxic and hypoxic conditions. (Mean + SEM, n=3, \*,  $P \leq 0.002$ , \*\*,  $P \leq 0.0002$ , \*\*\*,  $P \leq 0.0001$ ). (C) Assessment of apoptosis by Annexin V-FITC/PI staining. (Left) Representative plots and (Right) Quantification of Annexin V-FITC stained A673 and SK-ES-1 spheres transfected with NTC or CASP8AP2-siRNA under normoxic and hypoxic conditions. (Mean + SEM, n=3, \*,  $P \leq 0.0008$ , \*\*,  $P \leq 0.0001$ ).

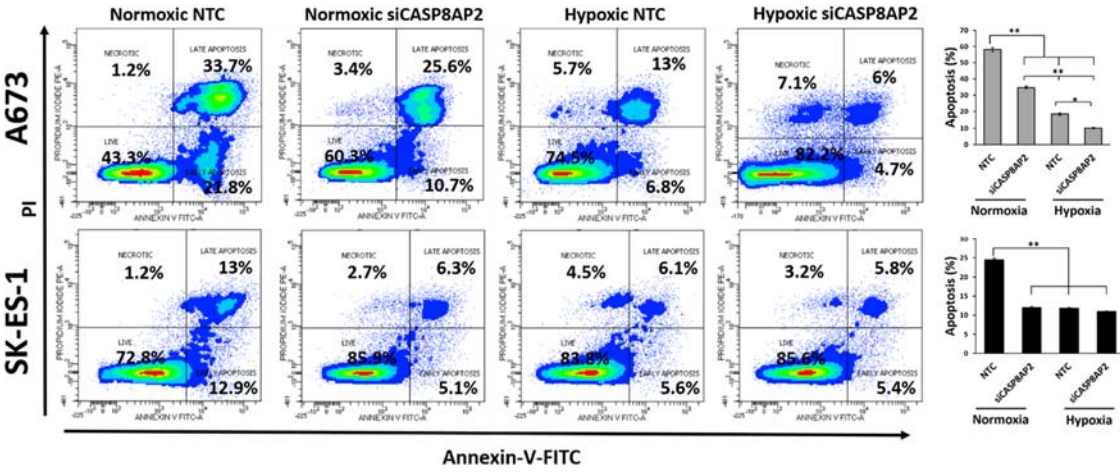
**A**



**B**



C



## Discussion

The hypoxic TME is considered a crucial driver of tumor development and therapy resistance. Aggressive tumors often consist of hypoxic regions capable of creating an environment that supports stem-like cancer cells (120, 294). In EWS, hypoxia and enrichment of stem-like cells is associated with poor patient outcomes (112, 296). Mounting evidence suggests that the hypoxic niche may be able to exert its effects beyond the local microenvironment by signaling to nearby normoxic tumor cells (233). Exosomes have been described as critical mediators of cell-cell communication within the TME and may provide an explanation for how hypoxia contributes to tumors with an aggressive phenotype. Our findings indicate that exosomes secreted under hypoxic conditions significantly increase sphere formation in normoxic EWS cells. Moreover, we show that Akt and HIF-1 $\alpha$  regulates the Hypoxic<sup>EXO</sup> mediated effect on sphere formation by enriching miR-210 within the hypoxic derived exosomes. We demonstrate that the delivery of miR-210 to recipient cells enhances stemness in EWS cells by silencing a potential target, the proapoptotic member CASP8AP2, that is critical to the survival of stem-like cells (310).

Recently, a growing body of evidence has shown that exosomes function as a bridge between neighboring cancer cells by delivering an RNA rich cargo (233, 236, 297). In hypoxic tumors, exosomes have been suggested to contribute to the aggressive phenotype by mediating the cross-talk between tumor cells in hypoxic regions and target cells in normoxic regions (233, 234). However, the association between hypoxia and exosomes in EWS has yet to be explored.

Increasing efforts are being made in elucidating the mechanism's underlying exosomal miRNAs silencing of target mRNAs in recipient cells, prompting our investigation into the miRNA profile in EWS exosomes. Recent studies in breast cancer



revealed exosomal miRNA promoted tumorigenesis in a Dicer-dependent manner and moreover, Dicer was demonstrated to facilitate miRNA processing from pre-miRNA to mature miRNA in exosomes resulting in stable miRNA capable of exerting long lasting pro-tumorigenic effects in recipient cells (264). In our study, we initially demonstrated that Hypoxic<sup>EXO</sup> carrying hypoxia regulated miRNAs enhanced tumor formation and increased the EWS stem cell-like CD133<sup>+</sup> subpopulation. Several studies have identified mechanisms describing the effects of Hypoxic<sup>EXO</sup> miRNA cargo in angiogenesis, metastasis, proliferation, migration and invasion (232, 233), but it is currently unknown how Hypoxic<sup>EXO</sup> delivery of miRNA influences stemness in recipient cells. A previous study indicated exosomes derived from hypoxic prostate cancer cells can enhance sphere formation in normoxic cells (234), however, the underlying molecular mechanism remains unclear. Since HIF-1 $\alpha$  is a primary regulator of the hypoxic response, an early study reported enrichment of miR-21 in exosomes derived from hypoxic oral squamous cell carcinoma cells was directly regulated by stable HIF-1 $\alpha$  (233). In EWS and multiple other studies, Akt signaling has been shown to stabilize and amplify the HIF-1 $\alpha$  mediated response to hypoxia (195, 226). In our study, we demonstrate that the effects of Hypoxic<sup>EXO</sup> on sphere formation in normoxic EWS cells is regulated by Akt and HIF-1 $\alpha$  remodeling of the Hypoxic<sup>EXO</sup> miRNA cargo and directly enriching for miR-210 (310). This is supported by our observations showing Hypoxic<sup>EXO</sup> derived from HIF-1 $\alpha$  knockdown and MK-2206 treated cells failed to increase sphere formation compared to normoxic control spheres and spheres co-cultured with Normoxic<sup>EXO</sup>. Interestingly, our findings suggest that packaging of miR-210 into hypoxic exosomes is primarily regulated by the stabilization HIF-1 $\alpha$  by Akt, moreover, our studies indicate that Akt enriches exosomal miR-210 by amplifying HIF-1 $\alpha$  activity. Given that miR-210 was highly expressed in both our hypoxic cells and exosomes, we are the first to show that increased miR-210 levels in Hypoxic<sup>EXO</sup> are dependent on HIF-1 $\alpha$  stabilization (310).

Together, this evidence compelled us to investigate the role of cellular and exosomal miR-210 in promoting stemness in EWS cells (310).

It is well established that a myriad of miRNAs are capable of targeting overlapping mRNA in cells, especially in recipient cells that have internalized cancer derived exosomes (244, 264, 278). Our observed effects of Hypoxic<sup>EXO</sup> miRNA content on normoxic spheres might not be the result of a single miRNA, however, our findings indicate that miR-210, is at least one miRNA capable of mediating sphere formation in hypoxic spheres and in spheres co-cultured with Hypoxic<sup>EXO</sup> (310). Previously, knockdown of miR-210 in hypoxic glioma stem cells was demonstrated to decrease sphere formation and the overall stem cell phenotype (223). In osteosarcoma stem cells, miR-210 overexpression and knockdown studies revealed that miR-210 can promote stemness and even reprogram differentiated osteosarcoma cells into Stro-1<sup>+</sup>/CD117<sup>+</sup> stem cells (221). Our study also demonstrated that inhibition of miR-210 could reduce sphere formation in hypoxic spheres (310). Moreover, when we overexpressed miR-210 in normoxic EWS spheres, it resulted in increased sphere formation consistent with previous studies demonstrating a miR-210 mediated effect on cellular reprogramming (221). Importantly, we are the first to show in EWS that hypoxia increases sphere formation and in part, sphere formation is regulated by miR-210 expression (310). In breast cancer, hypoxic derived exosomal miR-210 promoted angiogenesis and proliferation in xenograft tumors (228). Delivery of Hypoxic<sup>EXO</sup> to normoxic cells in our study indicated that exosomal miR-210 can promote sphere formation. Furthermore, we show that miR-210 can enhance stemness by targeting CASP8AP2 (310).

This is the first study to describe a mechanism where the miRNA cargo in Hypoxic<sup>EXO</sup> target a gene involved in regulating the survival of stem-like cells. In hypoxic bone marrow derived mesenchymal stem cells (BM-MSC), miR-210 targeted and

silenced CASP8AP2, resulting in an antiapoptotic affect that bolstered the survival of the BM-MSCs (222). CASP8AP2 is a proapoptotic member that participates in fas-induced and tumor necrosis factor- $\alpha$ - mediated apoptosis signaling (224). Since EWS cells are thought to derive from transformed BM-MSCs, we chose to investigate if EWS cells can adopt this prosurvival pathway to preserve its stem-like population. Consistent with previous findings, knockdown of miR-210 in our hypoxic spheres resulted in increased CASPA8AP2 expression, while overexpression of miR-210 in normoxic spheres inhibited CASP8AP2 levels (222, 225). Hypoxic<sup>EXO</sup> delivering miR-210 demonstrated a similar decrease in CASP8AP2 expression in normoxic spheres. Our data suggest that sphere formation is negatively regulated by CASP8AP2 activity. This is supported in our CASP8AP2 knockdown spheres demonstrating significant increases in sphere formation in the normoxic group and slight increases in the hypoxic group. Furthermore, knockdown of CASP8AP2 significantly decreased apoptosis in normoxic spheres. In our hypoxic spheres, CASP8AP2 correlated with a significant decrease in apoptosis, suggesting that hypoxia induces prosurvival mechanisms that are crucial for sphere formation. Supportive of our findings, previous EWS studies showed that resistance to apoptosis in hypoxic cells was dependent on HIF-1 $\alpha$  (144, 226). Together, these studies indicate that CASP8AP2 silencing by miR-210 prevents apoptosis, promoting sphere formation in hypoxic EWS cells and in normoxic cells pretreated with Hypoxic<sup>EXO</sup> (310).

This study describes a mechanism whereby EWS cells under hypoxic conditions release exosomes that enhance stemness in EWS cells. We identified a hypoxia regulated miRNA significantly expressed in hypoxic cells and Hypoxic<sup>EXO</sup> and characterized a potential target that facilitates an apoptotic pathway critical to sphere formation. Ongoing studies are investigating the role of HIF-1 $\alpha$  on regulating EWS stemness and together, our future aim is to investigate how HIF-1 $\alpha$  selectively

modulates the packaging of miRNAs into Hypoxic<sup>EXO</sup>, and validate additional miRNAs that promote aggressive hypoxic phenotypes (310).

## Chapter V

# Exosomes Secreted under Hypoxia Activate Akt signaling in Ewing's Sarcoma Spheres and Cancer-Associated Fibroblasts

### Introduction

Significant importance has been placed on the role of the tumor microenvironment (TME) in promoting tumor formation and how the interaction between cancer cells and the TME can lead to relapse, metastasis and ultimately therapy resistance (231). Targeting the TME in patients with aggressive malignancies is an emerging area and remains an opportunity to develop new therapies. EWS tumors display a diverse TME where 85% of patients are diagnosed with malignancies primarily localized within bone, but in 15% of patients, EWS arises within extra-osseous soft tissues. Moreover, aggressive tumors develop metastatic lesions in the lungs and at distant bony sites (298). This TME consists of tumor cells, osteoblasts, osteoclasts, myeloid cells, endothelial cells, mesenchymal cells and cancer-associated fibroblasts (CAFs) within normoxic and hypoxic regions. Acellular components of the TME consists of extracellular matrix, various soluble factors and extracellular vesicles that support the tumor niche (231).

Uptake of exosomes derived from cancer cells induces epigenetic changes in target cells that play a significant role in tumor growth, progression, metastasis, drug resistance, angiogenesis and induction of pre-metastatic niches (244). These protumorigenic effects are mediated not only through cross-talk between cancer cells, but between cancer cells and their surrounding stroma (230). More recently, Ramteke et al reported that exosomes secreted from hypoxic prostate cancer cells transformed

fibroblasts into CAFs and enhanced stemness in naïve prostate cancer cells (234), however, the effect that hypoxic exosomes had on inducing stem-like cells remains unclear in this study due to lack of rigor in characterizing the stem cell phenotype.

CAFs have been observed to promote tumor formation and metastasis within the TME and support the pre-metastatic niche (279). Recent evidence suggests exosomes can reprogram fibroblasts into CAFs (236). In EWS, the role of exosomes in reprogramming cancer cells into stem-like and transforming fibroblasts is unknown. Furthermore, it is unclear in any cancer model whether a hypoxic TME can modulate exosomes capable of inducing stem cell formation consistent with an established molecular CSC phenotype in their respective cancer field, and whether reprogramming of fibroblasts into CAFs can lead to a transformed tumorigenic phenotype.

In this study, we hypothesized that EWS cells under hypoxic conditions release exosomes that activate Akt in EWS spheres and transform fibroblasts that demonstrate an elevated tumorigenic CAF phenotype. Our observations strongly suggest that the Akt signaling pathway is a likely contributor to these effects and therefore, may underly an important mechanism that could explain the aggressiveness and poor outcomes associated with hypoxic tumors. Our findings indicate that Hypoxic<sup>EXO</sup> mediated delivery of multiple miRNA with overlapping and redundant targets that could be responsible for activating Akt in EWS spheres and transformed CAFs.

## Results

To test whether hypoxic exosomes promote a stem-like phenotype in EWS cells outside of a hypoxic environment, we co-cultured EWS Normoxic<sup>EXO</sup> and Hypoxic<sup>EXO</sup> with normoxic cells in a sphere-forming assay. As previously shown, EWS cells cultured under normal oxygen tension levels demonstrated enhanced sphere formation after

adding Hypoxic<sup>EXO</sup> (Figure 4.2). We further assessed the effect of EWS Hypoxic<sup>EXO</sup> on the stem-like phenotype in EWS cells by measuring the expression of ESC genes (Figure 5.2B). Hypoxic<sup>EXO</sup> increased Sox2, Oct4 and Nanog protein expression compared to normoxic control cells, however, no significant effect was observed on Myc expression. Interestingly, Normoxic<sup>EXO</sup> demonstrated a similar effect when compared to normoxic controls, however, Hypoxic<sup>EXO</sup> had a more significant effect on Sox2 and Nanog, but no significant difference was observed in Oct4 and Myc expression between exosome groups. Based on our network analysis indicating that the miRNA cargo in Hypoxic<sup>EXO</sup> target mRNAs involved in regulating Akt signaling (Figure 3.7B), we investigated the status of activated Akt in EWS cells treated with Normoxic<sup>EXO</sup> and Hypoxic<sup>EXO</sup>. Consistent with the interactome predictions (Figure 3.7B), Hypoxic<sup>EXO</sup> significantly increased phosphorylated Akt levels in EWS spheres compared to both normoxic spheres and spheres cultured with Normoxic<sup>EXO</sup> (Figure 5.2A). Akt signaling was elevated the most in hypoxic control spheres (Figure 5.1) which was expected since activated Akt is enhanced under hypoxic conditions and in TICs (195, 299, 300).

To evaluate whether Hypoxic<sup>EXO</sup> activate Akt signaling *in vivo*, we injected NSG mice with SK-ES-1 cells and proceeded to inject the mice intratumorally with Normoxic<sup>EXO</sup> and Hypoxic<sup>EXO</sup> for a period of 6 weeks. Tumors were subjected to mechanical and enzymatic disaggregation. Hypoxic<sup>EXO</sup> treated tumors displayed significantly elevated phosphorylated Akt levels (Figure 5.3) similar to the *in vitro* observations. Together, these findings suggest Hypoxic<sup>EXO</sup> delivery of enriched miRNAs targeting the Akt signaling pathway introduces a potential underlying mechanism responsible for the effects of Hypoxic<sup>EXO</sup> on normoxic EWS cells.

To examine whether EWS-derived Hypoxic<sup>EXO</sup> enhance reprogramming of fibroblasts into CAFs, NIH3T3 fibroblasts were co-cultured with Normoxic<sup>EXO</sup> and

Hypoxic<sup>EXO</sup> in a soft agar assay to assess anchorage-independent growth. The ability of cells to form colonies in a soft agar assay indicates transformation and potentially tumorigenic capabilities (301). Hypoxic<sup>EXO</sup> derived from both A673 cells significantly enhanced colony formation 1.68 fold while SK-ES-1 Hypoxic<sup>EXO</sup> increased colony formation 1.62 fold compared to their respective Normoxic<sup>EXO</sup> (Figure 5.4A). Expression of the CAF marker alpha smooth muscle actin ( $\alpha$ -SMA) (234) was assessed in NIH3T3 cells co-cultured with SK-ES-1 exosomes over a timecourse. Hypoxic<sup>EXO</sup> increased expression of  $\alpha$ -SMA 1.5 fold compared to Normoxic<sup>EXO</sup> (Figure 5.4B). Normoxic<sup>EXO</sup> induce colony formation and slight expression of  $\alpha$ -SMA in NIH3T3 cells as well, indicating a transformation effect. Together, these data suggests that Hypoxic<sup>EXO</sup> enhance fibroblast reprogramming into CAF cells.

To address the tumorigenic effects of EWS-derived exosomes on NIH3T3 fibroblasts, we conditioned NIH3T3 cells with SK-ES-1 Normoxic<sup>EXO</sup> and Hypoxic<sup>EXO</sup> for 72 hrs and mixed the exosomes with NIH3T3 cells prior to injecting NSG mice. We observed increased tumor formation in NIH3T3 tumors treated with Hypoxic<sup>EXO</sup> compared to Normoxic<sup>EXO</sup> and control treated mice (Figure 5.5A). All mice injected with NIH3T3 cells conditioned with Hypoxic<sup>EXO</sup> formed tumors while mice injected with NIH3T3 control cells or NIH3T3 mixed with Normoxic<sup>EXO</sup> formed 4/5 tumors. The control group formed tumors indicating the intrinsic tumorigenic potential of the cell line. As predicted by our interactome analysis (Figure 3.7B), activated Akt was significantly increased in tumors preconditioned with Hypoxic<sup>EXO</sup> compared to untreated and Normoxic<sup>EXO</sup> treated groups (Figure 5.5B). H&E staining in tumors demonstrated a spindle shape cell morphology in all groups (Figure 5.5C). Tumors pretreated with Hypoxic<sup>EXO</sup> demonstrated a similar increase in  $\alpha$ -SMA consistent with the *in vitro* co-



culture studies. This suggests EWS Hypoxic<sup>EXO</sup> enhance tumorigenicity in NIH3T3 cells with activated Akt signaling.

**Figure 5.1: Hypoxia activates Akt in EWS spheres.** Protein expression of IGF1R signaling pathway. IGF1R, p-Akt, Akt, p-mTORC1, mTORC1, p-ERK and ERK were assessed by western blot in A673 and SK-ES-1 normoxic and hypoxic spheres.  $\alpha$ -Tubulin was used as a loading control in western blots.

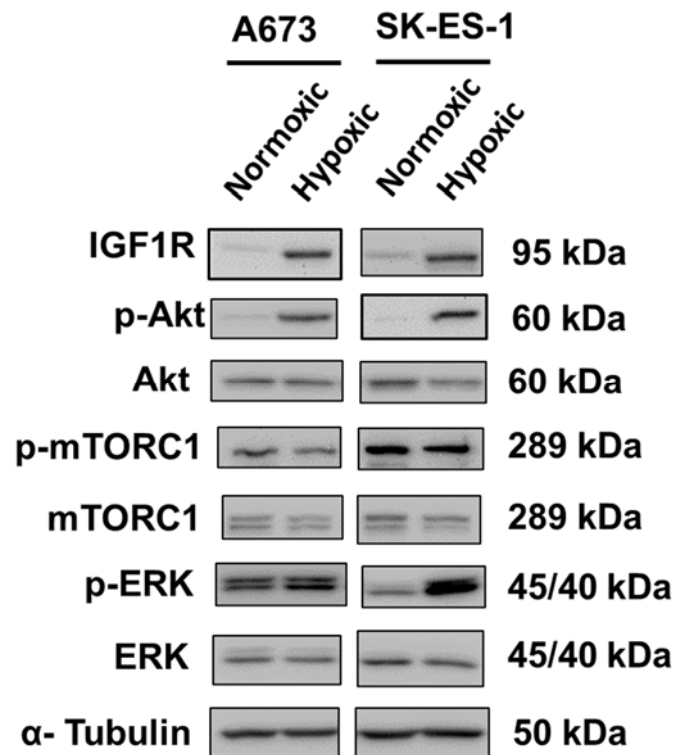
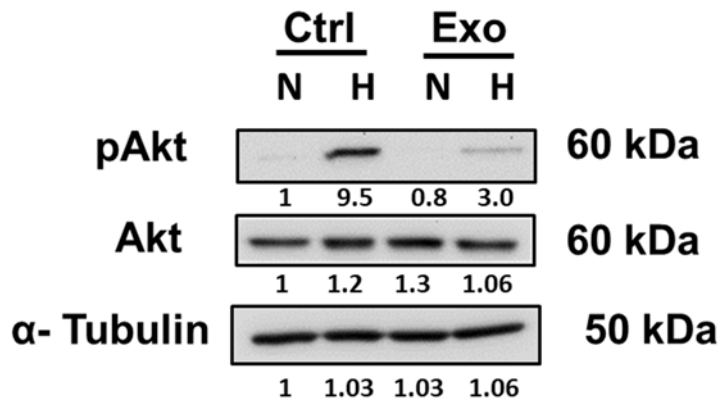


**Figure 5.2: Hypoxic<sup>EXO</sup> increase Akt and ESC gene expression in EWS spheres. (A)**

Akt and p-Akt was assessed by immunoblot in normoxic SK-ES-1 spheres co-cultured with 20 µg/ml SK-ES-1 Normoxic<sup>EXO</sup> and Hypoxic<sup>EXO</sup>. SK-ES-1 normoxic and hypoxic spheres were used as controls.  $\alpha$ -Tubulin was used as a loading control in western blots.

(B) Protein expression of embryonic stem cell genes and EWS markers Myc, Oct 3/4, Nanog and Sox2 were assessed by western blot in SK-ES-1 normoxic and hypoxic control spheres and normoxic spheres co-cultured with Normoxic<sup>EXO</sup> and Hypoxic<sup>EXO</sup>.

**A**



**B**

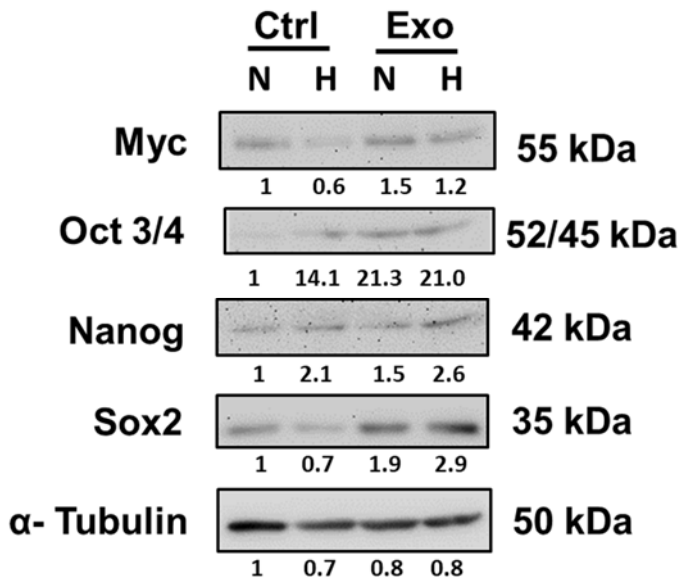


**Figure 5.3: Hypoxic<sup>EXO</sup> increase Akt in EWS tumors.** Immunoblot assessing Akt and p-Akt in SK-ES-1 tumors.  $\alpha$ -Tubulin was used as a loading control in western blots.

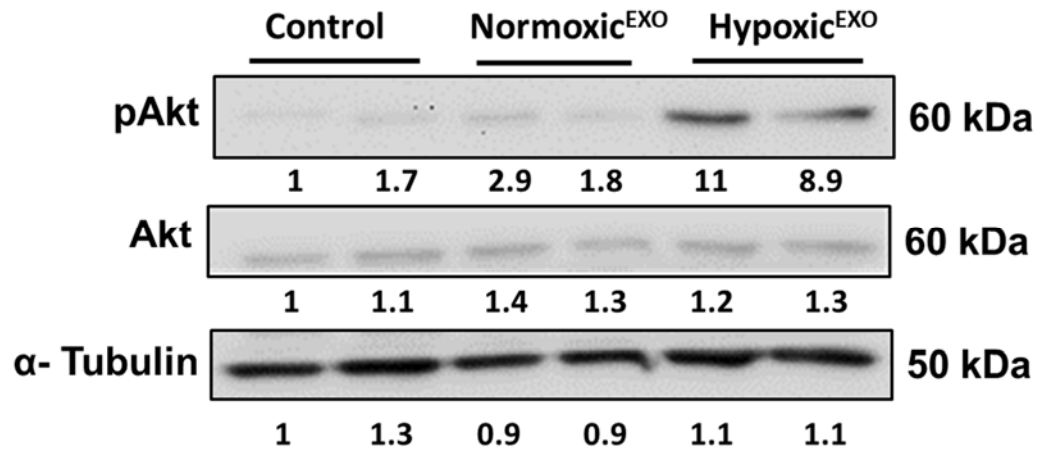


**Figure 5.4: Hypoxic<sup>EXO</sup> enhances reprogramming in NIH3T3 cells.** (A) Anchorage independent growth in NIH3T3 cells co-cultured with increasing amounts (0, 5, 10, 20  $\mu\text{g/ml}$ ) of normoxic and hypoxic SK-ES-1 and A673 exosomes in a soft agar assay. Quantification of spheres was performed (magnification, X20) (mean $\pm$  SEM, n=3, \*,  $p\leq 0.05$ , \*\*,  $p\leq 0.001$ , \*\*\*,  $p\leq 0.0001$ ). (B) Western blot of CAF marker,  $\alpha$ -SMA, was assessed in NIH3T3 cells treated with 20  $\mu\text{g}$  normoxic or hypoxic SK-ES-1 exosomes (time points: 24 and 48 hrs).  $\alpha$ -tubulin was used as the internal loading control for normalization.

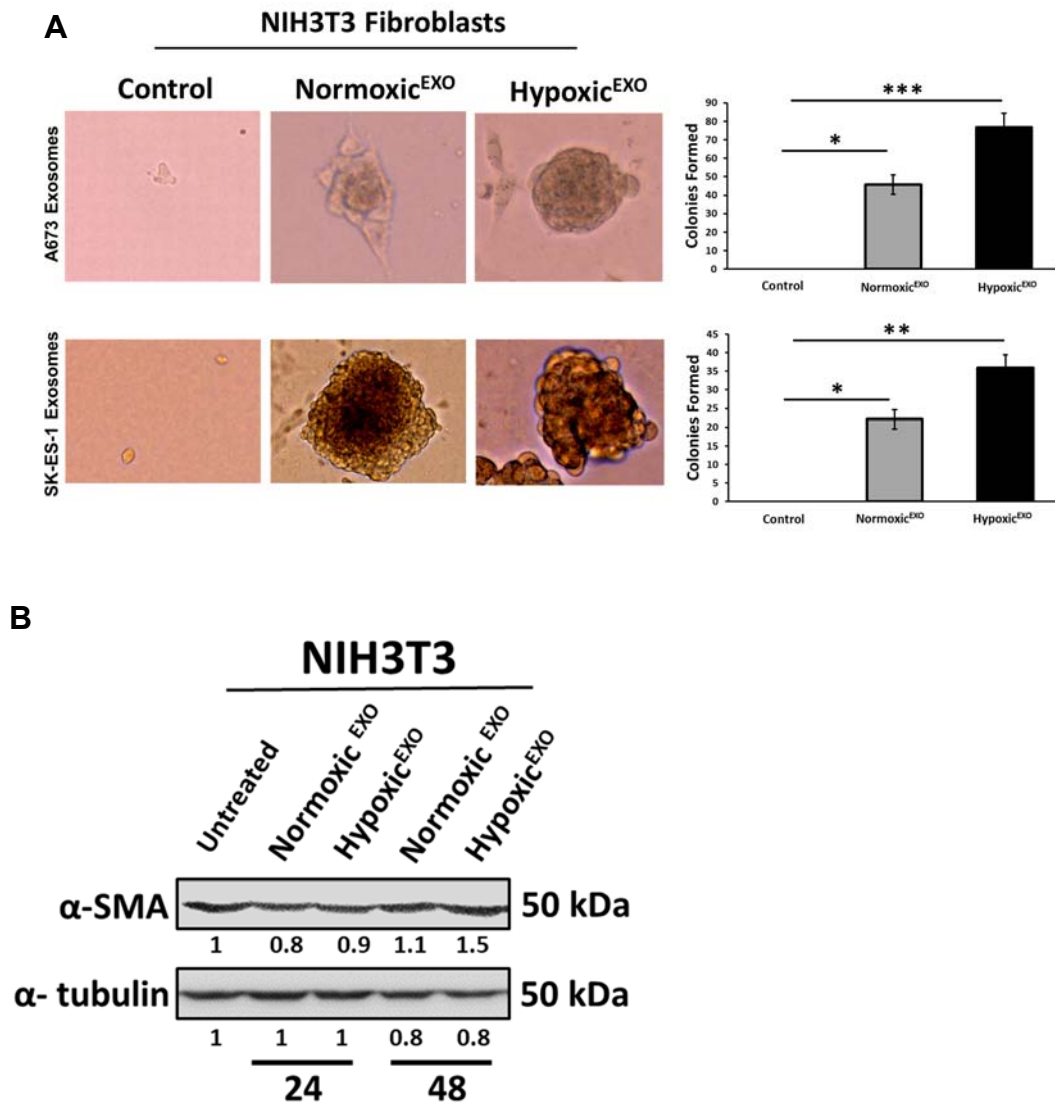
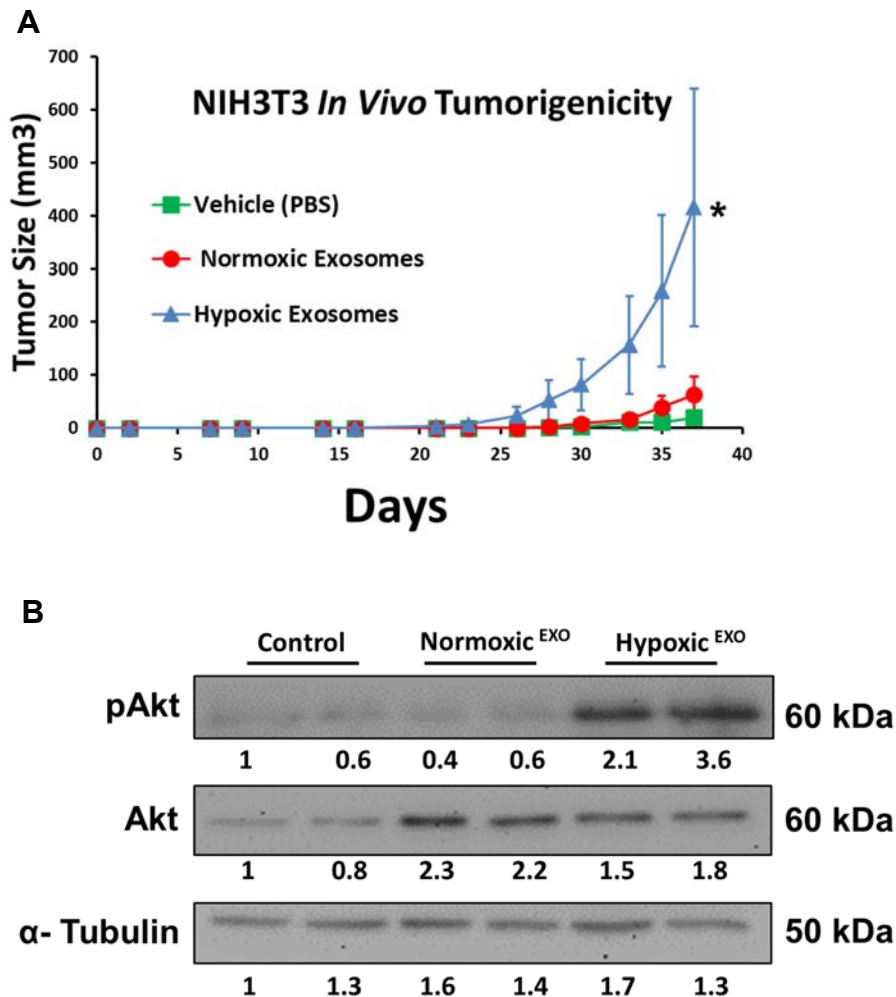
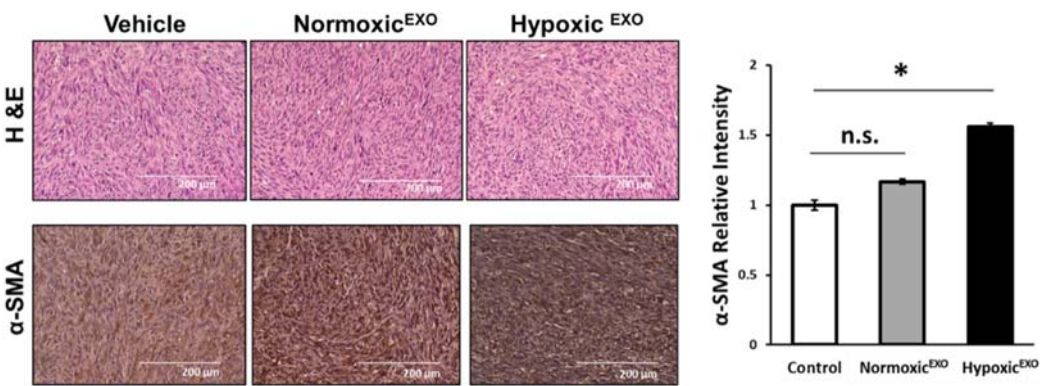


**Figure 5.5: Hypoxic<sup>EXO</sup> enhance NIH3T3 tumorigenicity.** (A) NIH3T3 cells were co-cultured with PBS, SK-ES-1 Normoxic<sup>EXO</sup> and Hypoxic<sup>EXO</sup> as described in Materials and Methods. NIH3T3 cells were harvested after 72 hrs and mixed with either PBS or 20  $\mu$ g SK-ES-1 Normoxic<sup>EXO</sup> and Hypoxic<sup>EXO</sup> and injected into NSG mice. (mean $\pm$  SEM, \*,  $p\leq 0.05$ ). Tumorigenicity and tumor growth assessed every day until tumors reached 1 cm<sup>3</sup>. (B) Western blot pAkt and Akt expression in formed NIH3T3 tumors,  $\alpha$ -tubulin was used as the internal loading control for normalization. (C) Representative H&E (*Top*) and  $\alpha$ -SMA stained (*Bottom*) NIH3T3 tumors treated with PBS (Vehicle) Normoxic<sup>EXO</sup> and Hypoxic<sup>EXO</sup>. Relative staining intensity was quantified using ImageJ (mean $\pm$  SEM, \*,  $p\leq 0.000001$ ).



C



## Discussion

The hypoxic TME is widely considered as a crucial driver in tumorigenesis and therapy resistance. Aggressive tumors often consist of hypoxic regions capable of creating an environment that supports stem cell-like TICs (120, 294). In EWS, hypoxia and enrichment of TICs is associated with poor patient outcomes (112, 296). Mounting evidence suggests that the hypoxic niche may be able to exert its effects beyond the local microenvironment by signaling to nearby normoxic tumor cells and the surrounding stroma (233). Exosomes have been described as critical mediators of cell-cell communication within the TME and may provide an explanation for how hypoxia contributes to tumors with an aggressive phenotype (233). Our findings indicate that hypoxia and exosomes secreted under these conditions may be one of the underlying mechanisms responsible for inducing TIC-like formation in EWS cells and reprogramming fibroblasts into CAFs with enhanced tumorigenicity.

Regions within tumors experiencing long-lasting hypoxia result in necrosis and are linked to poor patient survival. A clinical study in EWS reported primary tumors with necrotic regions that correlated with the worst overall survival in patients who had an increased chance for metastasis (296). In prostate cancer, stabilization and activation of the HIFs under chronic hypoxia has been shown to increase sphere formation and induce expression of ESC genes (120). In primary EWS tumors, the isolated TIC subpopulation displayed increased ESC expression and the ability to grow as spheres with resistance to doxorubicin (14, 112), however, it has been unclear how hypoxia impacts stemness in EWS. In this present study, prolonged hypoxia enhanced sphere formation in EWS cells and upregulated the ESC genes *SOX2*, *OCT4* and *NANOG*. These results are the first in EWS describing the role of hypoxia in promoting a TIC-like phenotype consistent with EWS TICs.



It is well established that the internalization of cancer derived exosomes into recipient cells introduces a miRNA capable of interacting with the same mRNA in the host cell that elicit similar oncogenic effects (244, 264, 278). Network analysis of our miRNA cargo revealed enrichment of eight miRNAs (miR-19b-3p, miR-92a-3p, miR-25, miR-181a-5p, miR-27a-3p, miR-29b-39 and miR-30c-5p) in our Hypoxic<sup>EXO</sup> that all converge on the Akt signaling pathway. In addition, differential expression of the exosomal miRNA revealed elevated levels of the hypoxia regulated miRNA, miR-10b, in Hypoxic<sup>EXO</sup>. Previous studies indicate that these miRNAs activate Akt by directly silencing gene expression of proteins involved in negatively regulating the Akt pathway (302-309), however, only miR-19b-3p has been shown to affect Akt signaling via exosome mediated transfer to target cells. These findings suggest a broader and more intricate regulatory network which may underly the effects observed in EWS TICs and CAFs treated with EWS Hypoxic<sup>EXO</sup>.

Functionally, the delivery of Hypoxic<sup>EXO</sup> miRNA have been demonstrated to enhance migration and invasion in normoxic cancer cells (233), however, the capability of Hypoxic<sup>EXO</sup> miRNA to regulate TIC formation is unknown. Our *in vitro* findings revealed Hypoxic<sup>EXO</sup> significantly enhanced sphere formation and ESC expression of Sox2, Oct4 and Nanog compared to the normoxic control. Interestingly, Normoxic<sup>EXO</sup> displayed a similar result but to a lesser extent than the Hypoxic<sup>EXO</sup>. Moreover, no difference was observed in Oct4 expression between exosome treated spheres. Exosomes derived from hypoxic prostate cancer cells demonstrated a similar Hypoxic<sup>EXO</sup> mediated effect on sphere formation (234), but did not further characterize an effect on stemness by measuring ESC markers in the exosome treated spheres. Consistent with our miRNA network analysis prediction, we showed that spheres treated with Hypoxic<sup>EXO</sup> had significant elevation of phosphorylated Akt indicating activation of the Akt signaling

pathway. Similar effects were observed in our EWS spheres grown under hypoxia suggesting Akt signaling as an underlying mechanism in EWS sphere formation. *In vivo*, SK-ES-1 tumors treated with Hypoxic<sup>EXO</sup> displayed a significant increase in the transmembrane protein CD133 (Figure 4.3C), which has been previously reported as a TIC marker in EWS tumors. Consistent with our sphere co-culture studies, tumors treated with Hypoxic<sup>EXO</sup> displayed similar activation in Akt signaling. The role of Akt underlying the cancer stem cell phenotype is supported by studies in hypoxic glioma cells demonstrating increased sphere formation, expansion of CD133<sup>+</sup> glioma cancer stem cells and elevated Akt signaling (195). Furthermore, abrogation of Akt in glioma CD133<sup>+</sup> cancer stem cells decreased tumor-initiation in a xenograft mouse model (227). Here we are the first to report that Hypoxic<sup>EXO</sup> enhance the TIC-like population in EWS and together, our data suggests that the Hypoxic<sup>EXO</sup> miRNA cargo may underly the mechanism activating Akt signaling in EWS TICs.

Cancer-associated fibroblasts participate in the TME by supporting cancer cell invasion, proliferation and metastasis (279) CAFs overexpress  $\alpha$ -SMA compared to normal fibroblasts and detection of  $\alpha$ -SMA is generally used as a reliable CAF marker (279). The mechanism describing how normal fibroblasts are reprogrammed into CAFs is still unclear. However, mounting evidence suggests the CAFs arise from exosomes secreted from cancer cells in the local TME (234) and currently, no studies in EWS have reported an exosome mediated induction of the CAF phenotype. Exosomes secreted from hypoxic prostate cancer cells induced expression of  $\alpha$ -SMA in prostate fibroblasts, suggesting that hypoxia enhances CAF reprogramming via an exosome mediated process (234). Recently, breast cancer derived exosomes delivering miR-9 to human breast fibroblasts was demonstrated to enhance the switch to CAFs (236). Another study in breast cancer revealed the miRNA cargo in breast cancer derived exosomes

transformed endothelial cells with tumorigenic capabilities (264). Based on the evidence in these studies, we questioned whether exosomes could promote a CAF phenotype in fibroblasts and moreover, could these transformed CAFs exhibit the ability to form tumors in a xenograft model. In our *in vitro* studies, we observed enhanced anchorage-independent growth and increased expression of the CAF marker  $\alpha$ -SMA in NIH3T3 fibroblasts treated with Hypoxic<sup>EXO</sup> compared to Normoxic<sup>EXO</sup> treated cells. Similar to our findings, a previous report demonstrated exosomes derived from colorectal cancer cells induced  $\alpha$ -SMA expression and anchorage-independent growth in recipient fibroblasts (280). *In vivo*, we observed increased tumorigenicity in mice injected with fibroblasts pretreated with Hypoxic<sup>EXO</sup>, where control fibroblasts and Normoxic<sup>EXO</sup> pretreated fibroblasts displayed significantly limited tumorigenic capabilities with 4/5 mice forming tumors. Similar to our findings, an early EWS study reported that control NIH3T3 fibroblasts were unable to form colonies *in vitro*, but possessed limited tumor forming abilities in mice (18). Recently, gastric cancer derived exosomes were shown to mediate CAF induction by increasing Akt signaling (281) and in several other reports, activated Akt signaling was observed to underly development and progression of malignant fibrosarcoma (282, 283). In our tumors preconditioned with Hypoxic<sup>EXO</sup>, they demonstrated significantly elevated levels of  $\alpha$ -SMA and phosphorylated Akt reflecting a fibrosarcoma phenotype. These findings are further supported by our Hypoxic<sup>EXO</sup> miRNA network analysis predicting activating Akt signaling as a primary target in recipient cells. Here we report for the first time an exosome mediated effect on CAF induction with tumorigenic capabilities.

In conclusion, EWS cells under these hypoxic conditions release exosomes that enhance the TIC-like phenotype in EWS cells and transform fibroblasts that demonstrate an elevated tumorigenic CAF phenotype. Ongoing studies are investigating the role of

hypoxia on selectively modulating the packaging of miRNAs into Hypoxic<sup>EXO</sup>, and validate the miRNAs involved in Akt activation leading to an aggressive hypoxic phenotype.

## Chapter VI

### General Discussion

#### Overview and Impact of Study

Currently, areas of exosome research are exploring the heterogeneity in size and content of cancer exosomes. This knowledge is helping us better understand tumor progression and the effects of therapies on cancer cells. Liquid biopsy techniques that isolate patient serum exosomes and analyze exosomal DNA, RNA and protein are now aiding in diagnosis, prognosis and the detection of minimal residual disease following patient therapies. The findings presented in this dissertation contribute to the greater body of knowledge in the exosome field and provides a new mechanism underlying the functional effects of hypoxic exosomes on cells composing the TME. Moreover, this work introduces an exosomal RNA profile that can be utilized to detect aggressive hypoxic tumors in patients (244).

Given the existing challenges involved with current exosome isolation methods, we first had to determine an optimal isolation approach that can reliably yield vesicles consistent with exosomes and are suitable for functional studies. Our observations led us to conclude that the standard exosome isolation method followed by microfiltration yielded the highest quality of exosomes appropriate for downstream analysis and functional studies. Further characterization of our normoxic and hypoxic exosomes isolated using the standard approach revealed an RNA and protein profile that could be utilized as biomarkers with diagnostic and prognostic potential. Importantly, the hypoxic EWS exosomes demonstrated significantly elevated levels of EWS-FLI1 mRNA and increased protein expression of EZH2, EWS-FLI1 and CD99. These findings can aid in

both detection of EWS and potentially predict outcomes associated with hypoxic tumors. Moreover, we are the first to report a molecular profile in hypoxic EWS exosomes.

When we performed RNA-seq analysis on our exosomes, we observed differentially expressed mRNA and miRNA content between our normoxic and hypoxic exosomes. Interestingly, the miRNA in the Hypoxic<sup>EXO</sup> demonstrated a similar profile compared to their parental hypoxic cells, suggesting Hypoxic<sup>EXO</sup> may reflect the parental tumor and could be used for prognostic purposes. Surprisingly, the mRNA expression patterns in the Hypoxic<sup>EXO</sup> failed to reflect their parental cells. Bioinformatical analysis of our cellular and exosomal miRNA revealed miR-210 as the most significant and most differentially expressed miRNA. Consistent with previous studies (228), this finding suggests exosomal miR-210 as a prognostic indicator of hypoxic tumors. This is the first report showing miR-210 in EWS exosomes.

IPA network analysis revealed both hypoxic exosomal mRNA and miRNA networks that converge on the Akt signaling pathway. Prior to this discovery, we had observed increased Akt signaling in hypoxic spheres, suggesting a regulatory role for Akt activation in mediating stemness in EWS. However, our preliminary data (not shown) using Akt inhibitors failed to decrease Akt phosphorylation and sphere formation in hypoxic EWS spheres but was able to significantly inhibit Akt signaling and sphere formation under normoxia. This finding indicated that hypoxic EWS spheres demonstrate therapy resistance which prevented us from further analysis of Akt activity in hypoxic spheres. We proceeded to test whether hypoxic exosomes affected Akt signaling in EWS spheres and developing tumors. Both *in vitro* and *in vivo* exosome treatment studies, Hypoxic<sup>EXO</sup> significantly increased sphere and tumor formation as well as Akt signaling. Moreover, both spheres and tumors treated with Hypoxic<sup>EXO</sup> demonstrated increased expression of ESC markers. This is the first evidence showing a Hypoxic<sup>EXO</sup>

mediated effect on stemness. In addition to the effect of Hypoxic<sup>EXO</sup> on EWS cells, our findings showed Hypoxic<sup>EXO</sup> could enhance CAF formation in NIH3T3 cells by increasing anchorage independent growth and  $\alpha$ -SMA expression. Furthermore, in NSG mice injected with NIH3T3 cells and EWS exosomes, Hypoxic<sup>EXO</sup> stimulated Akt signaling and increased tumor formation. These observations are the first to describe an exosomal mediated effect on driving tumorigenesis in CAFs.

Based on the miRNA-seq analysis revealing miR-210 as the top miRNA expressed in hypoxic EWS cells and their derived exosomes, we proceeded to investigate miR-210 levels in hypoxic spheres. Not surprisingly, miR-210 was significantly increased in hypoxic spheres and given hypoxia has been shown in our study to increase sphere formation, miR-210 expression could be used as a prognostic biomarker for hypoxic tumor cells with increased stemness. Further examination of the hypoxic EWS spheres revealed elevated ESC gene expression and decreased miR-145 levels. This is the first finding in EWS demonstrating a stem-like phenotype associated with hypoxia and hypoxically regulated miRNA. Moreover, the hypoxia mediated effect on EWS spheres demonstrated a similar phenotype as primary EWS CSCs. Given that hypoxic exosomes have been shown to propagate a phenotype outside their hypoxic niche, we wondered if hypoxic exosomal miR-210 could underly the Hypoxic<sup>EXO</sup> mediated effects on sphere formation.

Initially, we observed normoxic EWS spheres co-cultured with Hypoxic<sup>EXO</sup> increased sphere formation and expression of ESC genes. *In vivo*, Hypoxic<sup>EXO</sup> increased tumor growth in NSG mice and enhanced expression of the EWS CSC marker CD133. Immunohistochemistry staining revealed increased angiogenesis and proliferation, indicated by CD31 and Ki67 respectively. These observations are the first to describe a Hypoxic<sup>EXO</sup> mediated effect on stemness *in vivo*. In a previous study in breast cancer,

hypoxic exosomes enriched with miR-210 resulted in significant increases in tumor proliferation and angiogenesis using a xenograft mouse model. Together, this evidence prompted us to further investigate the underlying exosomal miR-210 effects on stemness in EWS and would be the first study to describe an exosomal mediated mechanism responsible for enhancing stemness in cancer cells.

In an attempt to describe a comprehensive mechanism underlying how Hypoxic<sup>EXO</sup> facilitate the cross-talk between normoxic and hypoxic cells, and extend the hypoxic stem-like phenotype beyond the hypoxic niche, we knocked down the hypoxia master regulator, HIF-1 $\alpha$ , in hypoxic EWS cells and measured the knockdown effect on exosomal miR-210 expression on sphere formation. This approach revealed a HIF-1 $\alpha$  mediated effect on exosomal miR-210 packaging and moreover, exosomes derived from HIF-1 $\alpha$  knockdown cells failed to enhance sphere formation. Furthermore, we were able to shown that exosomal miR-210 regulates EWS sphere formation by targeting the proapoptotic member CASP8AP2. Together, this is the first report communicating an axis whereby HIF-1 $\alpha$  regulates exosomal miRNA packaging and as a result, drives a stem-like phenotype in EWS cells by interfering with the apoptotic machinery. These findings introduce a new survival mechanism in EWS responsible for promoting stemness.

### **Limitations of Study and Future Work**

The precise physiological functions of exosomes in cancer remain unclear. However, in this study and others, the role of exosomes in facilitating intercellular cross-talk between cancer cells and cells that compose the TME are beginning to elucidate an emerging mechanism for cell-to-cell communication (244). Currently, exosome functional studies are limited mainly by *in vitro* experiments utilizing exosomes concentrations considered to be rough approximations of physiological levels, but possibly may not be



relevant *in vivo*. The exosome concentrations used in our work were determined by using an exosome dose response in a sphere assay and the rationale for this approach remains the standard in the field (289), however, this may not be physiological as previously mentioned. This potential pitfall could be addressed by exploring the role of exosomes in animal models where exosome secretion can be manipulated to assess the physiological role of exosomes. In addition, an *in vitro* solution implementing a trans-well assay could provide a more physiological model for intercellular signaling, but limits downstream applications.

One of the biggest pitfalls often reported in exosome research is the comparison of the molecular profiles (RNA or protein) between exosomes and their parental cells. These comparisons can be useful when trying to determine the selective packaging of exosomal cargo, however, at best, this approach can be helpful as a fishing experiment when trying to find novel molecules or determine if the exosomes represent a similar profile that represents the cell of origin. The mistake commonly made is when either the RNA or protein content differential expression is compared. This comparison can't be made since there is no mechanism to properly normalize the content. Currently, either total RNA or protein is used for-omic wide analysis. Comparisons using PCR commonly use standard house keeping genes such as GAPDH or  $\beta$ -actin. An alternative approach could try to normalize expression based on a standardized approach that takes cell number and exosome secretion into account, however, making direct comparisons utilizing this approach still might not solve this issue because you would still be comparing two different biological entities.

A fundamental limitation of this study concerns the exosome isolation approach. This pitfall is still the most significant challenge facing the exosome field in general. Essentially, due to the overlap in size and exosome lipid bilayer, isolation approaches

based on size exclusion or buoyant density fail to isolate pure exosome populations. Complicating the issue, density gradients assessing protein and RNA content in different density layers are reporting tremendous overlap (289). Future approaches have been suggested to identify exosome specific cargo and generate affinity-based isolation methods. Currently, a panel commissioned by the Journal of Extracellular vesicles proposed harvesting exosomes using a discontinuous density gradient and running downstream assays in parallel using vesicles from the different density layers (289). As you can imagine, this approach would be incredibly tedious, but may be necessary to better understand the molecular content and role of exosomes.

During the characterization of our normoxic and hypoxic exosomes, we identified a diverse RNA and protein profile that may contribute to the functional differences observed between normoxic and hypoxic exosomes. Analysis of our Hypoxic<sup>EXO</sup> content revealed elevated levels of EWS-FLI1 RNA and significantly increased EWS-FLI1, EZH2 and CD99 protein expression. Future studies will implement knockdown approaches to determine the role of this RNA and protein profile on Hypoxic<sup>EXO</sup> mediated sphere formation and other oncogenic processes. Future work will explore and elucidate the role of other hypoxically regulated miRNAs. Furthermore, the RNAs identified targeting the Akt signaling axis will be examined closely to determine if a single RNA or more likely, an intricate network of RNAs influence Akt activity. Clinically, more studies are needed to match patient serum exosome content with their parental tumor in order to enhance detection and development of better therapies for aggressive tumors.

Our findings showing Hypoxic<sup>EXO</sup> increase sphere and tumor formation in EWS cells has promising implications towards better understanding CSC biology within a hypoxic TME. Importantly, an *in vivo* limiting dilution assay is needed to determine an exosomal effect on generating CSCs or mediating dedifferentiation of non-tumor forming

EWS cells into tumor-initiating cells. This approach combined with FACS analysis will help identify cells susceptible to cellular reprogramming. A likely pitfall is that hypoxia and Hypoxic<sup>EXO</sup> are mediating a stem-like phenotype and given these cell lines are immortalized, will never truly reflect the CSC phenotype observed in primary cells. Alternatively, isolating patient serum and co-culturing patient derived exosomes with cells harvested from their parental tumor is needed to confirm the physiological importance of our study.

The use of siRNAs and miRNA mimics and inhibitors in our work limits the impact of our findings due to their transient effects. Future work implementing lentiviral mediated overexpression, knockdown or knockout methods will provide stable genetic manipulation. Stable overexpression or knockdown of HIF-1 $\alpha$ , miR-210 and CASP8AP2 is needed in the future to determine the role of these molecules in sphere formation. Importantly, stable transduction is needed in sphere assays because of the long incubation times and the effects of transient transduction are difficult to determine. In addition, stable knockdown of HIF-1 $\alpha$  will help determine the hypoxia dependent and independent effects of Akt on miR-210 expression and the downstream effects on survival mechanisms in hypoxic cells.

Lastly, our observations showing Hypoxic<sup>EXO</sup> can reprogram NIH3T3 cells and increase tumorigenicity presents a new role for exosomes within the TME. Our findings demonstrating Hypoxic<sup>EXO</sup> increase Akt signaling in transformed CAFs and Akt activation may underly the observed tumorigenic effects. Future work will identify and confirm miRNA involved in activating the Akt signaling axis. In addition, given Hypoxic<sup>EXO</sup> are carrying elevated levels of EWS-FLI1 transcript and protein, future studies with FLAG tag EWS-FLI1 and look for stable expression within the NIH3T3 cells exposed to Hypoxic<sup>EXO</sup>.

## **Analysis of Pitfalls in EWS Hypoxia Studies**

Early in my research, I encountered many pitfalls when I began conducting my hypoxia experiments. Current studies investigating the role of hypoxia in EWS contain tremendous contradictions with work done by hypoxia experts in other fields. Here, I wanted to highlight and critique these pitfalls in EWS hypoxia research and provide the logical rationale that led to my approach to studying hypoxia in EWS.

Hypoxia research investigating the temporal expression of the HIFs have encountered conflicting and often paradoxical results that can largely be attributed to previously mentioned variables such as cell type, severity of hypoxic conditions and duration, culture conditions and proper control of both HIF-1 $\alpha$  and HIF-2 $\alpha$  during interpretation of results. An additional challenge to hypoxia research lies in the technical challenges of harvesting cells once they have been removed from their hypoxic environment. HIFs undergo proteasomal degradation within minutes and must be processed quickly on ice followed by snap freezing in liquid nitrogen to preserve the intact HIF protein. In addition, the use of polyclonal antibodies will detect the intact 120 kDa HIF proteins as well as the degraded 90 kDa forms which are present under normoxia. Special attention must be paid to the different molecular weights when using polyclonal antibodies against the HIFs, however, commercial monoclonal antibodies only detect the 120 kDa form. One must always be skeptical of studies reporting HIF expression under normoxic conditions, however, loss of function mutations in HIF regulatory proteins or upregulation of miRNAs targeting HIF regulators in context dependent models would provide the obvious caveat to this problem. The use of hypoxia mimetics introduces another confounding variable that is mainly used as a control or as a replacement for hypoxia reducing the technical challenges associated with hypoxic cells. A common mimetic used is CoCl<sub>2</sub>, this mimetic stabilizes the HIFs by inhibiting

PHD enzymatic hydroxylation of the HIF proline residues through replacement of Fe with Co resulting in stable HIF expression (143). This approach has largely been deemed acceptable by the field when employed as a positive control for HIF analysis, and certain considerations should be taken into account when using this techniques since HIF regulation is finely tuned under hypoxia and the mimetics might produce results not seen in a hypoxic environment.

In EWS hypoxia research, observations of the temporal expression of HIF-1 $\alpha$  and HIF-2 $\alpha$  have been limited where many studies focus primarily on HIF-1 $\alpha$  without accounting for HIF-2 $\alpha$ . In addition, all of these studies have implemented the various approaches previously mentioned leading to conflicting outcomes between studies. The first study in EWS investigated the effects of hypoxia on apoptosis, here they observed that hypoxic EWS cells cultured under severe hypoxia (<0.1% O<sub>2</sub>) were resistant to apoptosis. HIF-1 $\alpha$  expression was observed at 6 hrs and steadily increased over a 72 hr period (144). This observation has been supported in other studies conducting experiments under severe hypoxia (140), however, under moderate (1% O<sub>2</sub>) hypoxia, HIF-1 $\alpha$  normally stabilizes at 6 hrs and decreases to a lower basal expression level. Severe hypoxia resembles necrotic regions in tumors and interestingly, is associated with the worst overall outcome in EWS patients (142). This study revealed HIF-1 $\alpha$  siRNA knockdown resulted in apoptosis by downregulating the known HIF-1 $\alpha$  target GLUT1 (144). HIF-2 $\alpha$  also targets GLUT1 under prolonged moderate hypoxia. In this study, severe hypoxia stabilized HIF-1 $\alpha$  at high levels over days which probably complicated interpretations of HIF-1 $\alpha$  function in EWS at the time. The hypoxia mimetic CoCl<sub>2</sub> was used in a limited capacity as a positive control in this study (144).

The seminal EWS hypoxia study was conducted by Aryee et al in 2010, here they were the first to report the expression of HIF-1 $\alpha$  in primary EWS tumors and the

effect of hypoxia on EWS-FLI1 expression (143). In addition, they demonstrated that hypoxia increases invasion and anchorage independent growth in EWS cell lines. Significantly, they demonstrated that shHIF-1 $\alpha$  knockdown resulted in decreased EWS-FLI1 expression, however, these experiments were conducted under normoxic conditions with CoCl<sub>2</sub>. They showed that EWS-FLI1 protein expression increased upon HIF-1 $\alpha$  stabilization, yet was unchanged at the mRNA level suggesting posttranscription modulation of EWS-FLI1. In some of their western blots, HIF-1 $\alpha$  expression continued to elevate for a duration of days under moderate (1% O<sub>2</sub>) hypoxia while in other cell lines, HIF-1 $\alpha$  remained stable over the same period. Both of these findings are not consistent with the temporal expression of HIF-1 $\alpha$  reported in other studies, including our own observations. A potential explanation may lie in inconsistent oxygen tension levels, timely processing of the cells or in the use of the polyclonal HIF-1 $\alpha$  antibody reported in their methods sections (143).

Later that same year, Knowles et al. reported HIF-1 $\alpha$  and HIF-2 $\alpha$  expression in EWS patient tumors along with HIF co-localization but did not discuss any association with patient outcomes (145). Their findings demonstrating HIF-1 $\alpha$  regulation of GLUT1 were similar to Aryee et al., however, Knowles et al. conducted their experiments under 0.1% O<sub>2</sub> while Aryee et al. performed all of their studies at 1% O<sub>2</sub>. In addition, Knowles et al. cultured their cells under hypoxia for 24 hr. where Aryee et al. used multiple time points. Interestingly, knockdown of HIF1 $\alpha$  in the Knowles study revealed decreased levels of GLUT1 and VEGFA but no difference was observed in the shHIF-2 $\alpha$  EWS cells. Both HIFs have been demonstrated to target these genes but under temporally different periods of hypoxic exposure. HIF-2 $\alpha$  is generally stabilized and active at 48 hrs which this study failed to explore. However, they performed all of their studies under 0.1% O<sub>2</sub>

which results in the time dependent accumulation of stable HIF-1 $\alpha$  which would explain the stronger effect of HIF-1 $\alpha$  (145).

The only EWS study that has reported a HIF-1 $\alpha$  temporal expression pattern consistent with the hypoxia field and our own findings was conducted by Tilan et al in 2013 (147). This group demonstrated HIF-1 $\alpha$  maximal expression at 6 hrs followed by decreased stable expression in the subsequent time points. Interestingly, the oxygen levels in this study were 0.1% which conflicts with the observations reported by the Knowles and Kilic labs. Future work is needed to clarify these inconsistencies in HIF expression in hypoxic EWS cells. Additionally, the main focus of the study investigated the effects of hypoxia on stemness in EWS cells. Here, they reported that hypoxia increased the Aldh<sup>+</sup> cells expressing OCT4 suggesting enrichment of a CSC subpopulation, however, this study did not perform any sphere assays which measure *in vitro* stemness (147).

## Chapter VII

### Bibliography

1. Ewing J. Classics in oncology. Diffuse endothelioma of bone. James Ewing. Proceedings of the New York Pathological Society, 1921. *CA Cancer J Clin.* 1972;22(2):95-8.
2. Triche TJ. Morphologic tumor markers. *Semin Oncol.* 1987;14(2):139-72.
3. Grier HE. The Ewing family of tumors. Ewing's sarcoma and primitive neuroectodermal tumors. *Pediatr Clin North Am.* 1997;44(4):991-1004.
4. Paulussen M, Frohlich B, Jurgens H. Ewing tumour: incidence, prognosis and treatment options. *Paediatr Drugs.* 2001;3(12):899-913.
5. Fraumeni JF, Jr., Glass AG. Rarity of Ewing's sarcoma among U.S. Negro children. *Lancet.* 1970;1(7642):366-7.
6. Cotterill SJ, Ahrens S, Paulussen M, Jurgens HF, Voute PA, Gadner H, Craft AW. Prognostic factors in Ewing's tumor of bone: analysis of 975 patients from the European Intergroup Cooperative Ewing's Sarcoma Study Group. *J Clin Oncol.* 2000;18(17):3108-14.
7. Potratz J, Jurgens H, Craft A, Dirksen U. Ewing sarcoma: biology-based therapeutic perspectives. *Pediatr Hematol Oncol.* 2012;29(1):12-27.
8. Riggi N, Stamenkovic I. The Biology of Ewing sarcoma. *Cancer Lett.* 2007;254(1):1-10.
9. Kovar H, Dworzak M, Strehl S, Schnell E, Ambros IM, Ambros PF, Gadner H. Overexpression of the pseudoautosomal gene MIC2 in Ewing's sarcoma and peripheral primitive neuroectodermal tumor. *Oncogene.* 1990;5(7):1067-70.
10. Perlman EJ, Dickman PS, Askin FB, Grier HE, Miser JS, Link MP. Ewing's sarcoma--routine diagnostic utilization of MIC2 analysis: a Pediatric Oncology Group/Children's Cancer Group Intergroup Study. *Hum Pathol.* 1994;25(3):304-7.
11. Delattre O, Zucman J, Plougastel B, Desmaze C, Melot T, Peter M, Kovar H, Joubert I, de Jong P, Rouleau G, et al. Gene fusion with an ETS DNA-binding domain caused by chromosome translocation in human tumours. *Nature.* 1992;359(6391):162-5.
12. Delattre O, Zucman J, Melot T, Garau XS, Zucker JM, Lenoir GM, Ambros PF, Sheer D, Turc-Carel C, Triche TJ, et al. The Ewing family of tumors--a subgroup of small-round-cell tumors defined by specific chimeric transcripts. *N Engl J Med.* 1994;331(5):294-9.
13. Cavazzana AO, Miser JS, Jefferson J, Triche TJ. Experimental evidence for a neural origin of Ewing's sarcoma of bone. *Am J Pathol.* 1987;127(3):507-18.
14. Suva ML, Riggi N, Stehle JC, Baumer K, Tercier S, Joseph JM, Suva D, Clement V, Provero P, Cironi L, Osterheld MC, Guillou L, Stamenkovic I. Identification of cancer stem cells in Ewing's sarcoma. *Cancer Res.* 2009;69(5):1776-81.
15. Riggi N, Cironi L, Provero P, Suva ML, Kaloulis K, Garcia-Echeverria C, Hoffmann F, Trumpp A, Stamenkovic I. Development of Ewing's sarcoma from primary bone marrow-derived mesenchymal progenitor cells. *Cancer Res.* 2005;65(24):11459-68.



16. May WA, Lessnick SL, Braun BS, Klemsz M, Lewis BC, Lunsford LB, Hromas R, Denny CT. The Ewing's sarcoma EWS/FLI-1 fusion gene encodes a more potent transcriptional activator and is a more powerful transforming gene than FLI-1. *Mol Cell Biol.* 1993;13(12):7393-8.
17. Lessnick SL, Braun BS, Denny CT, May WA. Multiple domains mediate transformation by the Ewing's sarcoma EWS/FLI-1 fusion gene. *Oncogene.* 1995;10(3):423-31.
18. Thompson AD, Teitell MA, Arvand A, Denny CT. Divergent Ewing's sarcoma EWS/ETS fusions confer a common tumorigenic phenotype on NIH3T3 cells. *Oncogene.* 1999;18(40):5506-13.
19. Ohno T, Rao VN, Reddy ES. EWS/Fli-1 chimeric protein is a transcriptional activator. *Cancer Res.* 1993;53(24):5859-63.
20. Bailly RA, Bosselut R, Zucman J, Cormier F, Delattre O, Roussel M, Thomas G, Ghysdael J. DNA-binding and transcriptional activation properties of the EWS-FLI-1 fusion protein resulting from the t(11;22) translocation in Ewing sarcoma. *Mol Cell Biol.* 1994;14(5):3230-41.
21. Aryee DN, Sommergruber W, Muehlbacher K, Dockhorn-Dworniczak B, Zoubek A, Kovar H. Variability in gene expression patterns of Ewing tumor cell lines differing in EWS-FLI1 fusion type. *Lab Invest.* 2000;80(12):1833-44.
22. de Alava E, Lozano MD, Patino A, Sierrasesumaga L, Pardo-Mindan FJ. Ewing family tumors: potential prognostic value of reverse-transcriptase polymerase chain reaction detection of minimal residual disease in peripheral blood samples. *Diagn Mol Pathol.* 1998;7(3):152-7.
23. Jaishankar S, Zhang J, Roussel MF, Baker SJ. Transforming activity of EWS/FLI is not strictly dependent upon DNA-binding activity. *Oncogene.* 1999;18(40):5592-7.
24. Sorensen PH, Lessnick SL, Lopez-Terrada D, Liu XF, Triche TJ, Denny CT. A second Ewing's sarcoma translocation, t(21;22), fuses the EWS gene to another ETS-family transcription factor, ERG. *Nat Genet.* 1994;6(2):146-51.
25. Jeon IS, Davis JN, Braun BS, Sublett JE, Roussel MF, Denny CT, Shapiro DN. A variant Ewing's sarcoma translocation (7;22) fuses the EWS gene to the ETS gene ETV1. *Oncogene.* 1995;10(6):1229-34.
26. Kaneko Y, Yoshida K, Handa M, Toyoda Y, Nishihira H, Tanaka Y, Sasaki Y, Ishida S, Higashino F, Fujinaga K. Fusion of an ETS-family gene, EIAF, to EWS by t(17;22)(q12;q12) chromosome translocation in an undifferentiated sarcoma of infancy. *Genes Chromosomes Cancer.* 1996;15(2):115-21.
27. Peter M, Couturier J, Pacquement H, Michon J, Thomas G, Magdelenat H, Delattre O. A new member of the ETS family fused to EWS in Ewing tumors. *Oncogene.* 1997;14(10):1159-64.
28. Rossow KL, Janknecht R. The Ewing's sarcoma gene product functions as a transcriptional activator. *Cancer Res.* 2001;61(6):2690-5.
29. Aman P, Panagopoulos I, Lassen C, Fioretos T, Mencinger M, Toresson H, Hoglund M, Forster A, Rabbitts TH, Ron D, Mandahl N, Mitelman F. Expression patterns of the human sarcoma-associated genes FUS and EWS and the genomic structure of FUS. *Genomics.* 1996;37(1):1-8.

30. Crozat A, Aman P, Mandahl N, Ron D. Fusion of CHOP to a novel RNA-binding protein in human myxoid liposarcoma. *Nature*. 1993;363(6430):640-4.
31. Deloulme JC, Prichard L, Delattre O, Storm DR. The prooncogene EWS binds calmodulin and is phosphorylated by protein kinase C through an IQ domain. *J Biol Chem*. 1997;272(43):27369-77.
32. Perrotti D, Bonatti S, Trotta R, Martinez R, Skorski T, Salomoni P, Grassilli E, Lozzo RV, Cooper DR, Calabretta B. TLS/FUS, a pro-oncogene involved in multiple chromosomal translocations, is a novel regulator of BCR/ABL-mediated leukemogenesis. *EMBO J*. 1998;17(15):4442-55.
33. Brou C, Chaudhary S, Davidson I, Lutz Y, Wu J, Egly JM, Tora L, Chambon P. Distinct TFIIID complexes mediate the effect of different transcriptional activators. *EMBO J*. 1993;12(2):489-99.
34. Petermann R, Mossier BM, Aryee DN, Khazak V, Golemis EA, Kovar H. Oncogenic EWS-Fli1 interacts with hSRPB7, a subunit of human RNA polymerase II. *Oncogene*. 1998;17(5):603-10.
35. Calvio C, Neubauer G, Mann M, Lamond AI. Identification of hnRNP P2 as TLS/FUS using electrospray mass spectrometry. *RNA*. 1995;1(7):724-33.
36. Chansky HA, Hu M, Hickstein DD, Yang L. Oncogenic TLS/ERG and EWS/Fli-1 fusion proteins inhibit RNA splicing mediated by YB-1 protein. *Cancer Res*. 2001;61(9):3586-90.
37. Tamir A, Howard J, Higgins RR, Li YJ, Berger L, Zacksenhaus E, Reis M, Ben-David Y. Fli-1, an Ets-related transcription factor, regulates erythropoietin-induced erythroid proliferation and differentiation: evidence for direct transcriptional repression of the Rb gene during differentiation. *Mol Cell Biol*. 1999;19(6):4452-64.
38. Rao VN, Ohno T, Prasad DD, Bhattacharya G, Reddy ES. Analysis of the DNA-binding and transcriptional activation functions of human Fli-1 protein. *Oncogene*. 1993;8(8):2167-73.
39. Graves BJ, Petersen JM. Specificity within the ets family of transcription factors. *Adv Cancer Res*. 1998;75:1-55.
40. Meyer D, Wolff CM, Stiegler P, Senan F, Befort N, Befort JJ, Remy P. Xl-fli, the *Xenopus* homologue of the fli-1 gene, is expressed during embryogenesis in a restricted pattern evocative of neural crest cell distribution. *Mech Dev*. 1993;44(2-3):109-21.
41. Mager AM, Grapin-Botton A, Ladjali K, Meyer D, Wolff CM, Stiegler P, Bonnin MA, Remy P. The avian fli gene is specifically expressed during embryogenesis in a subset of neural crest cells giving rise to mesenchyme. *Int J Dev Biol*. 1998;42(4):561-72.
42. Brown LA, Rodaway AR, Schilling TF, Jowett T, Ingham PW, Patient RK, Sharrocks AD. Insights into early vasculogenesis revealed by expression of the ETS-domain transcription factor Fli-1 in wild-type and mutant zebrafish embryos. *Mech Dev*. 2000;90(2):237-52.
43. Maroulakou IG, Bowe DB. Expression and function of Ets transcription factors in mammalian development: a regulatory network. *Oncogene*. 2000;19(55):6432-42.
44. Hart A, Melet F, Grossfeld P, Chien K, Jones C, Tunnacliffe A, Favier R, Bernstein A. Fli-1 is required for murine vascular and megakaryocytic development and is hemizygously deleted in patients with thrombocytopenia. *Immunity*. 2000;13(2):167-77.

45. Spyropoulos DD, Pharr PN, Lavenburg KR, Jackers P, Papas TS, Ogawa M, Watson DK. Hemorrhage, impaired hematopoiesis, and lethality in mouse embryos carrying a targeted disruption of the Fli1 transcription factor. *Mol Cell Biol.* 2000;20(15):5643-52.
46. Zhang L, Eddy A, Teng YT, Fritzler M, Kluppel M, Melet F, Bernstein A. An immunological renal disease in transgenic mice that overexpress Fli-1, a member of the ets family of transcription factor genes. *Mol Cell Biol.* 1995;15(12):6961-70.
47. Pereira R, Quang CT, Lesault I, Dolznig H, Beug H, Ghysdael J. FLI-1 inhibits differentiation and induces proliferation of primary erythroblasts. *Oncogene.* 1999;18(8):1597-608.
48. Janknecht R. EWS-ETS oncoproteins: the linchpins of Ewing tumors. *Gene.* 2005;363:1-14.
49. Riggi N, Knoechel B, Gillespie SM, Rheinbay E, Boulay G, Suva ML, Rossetti NE, Boonseng WE, Oksuz O, Cook EB, Formey A, Patel A, Gymrek M, et al. EWS-FLI1 utilizes divergent chromatin remodeling mechanisms to directly activate or repress enhancer elements in Ewing sarcoma. *Cancer Cell.* 2014;26(5):668-81.
50. Kim S, Denny CT, Wisdom R. Cooperative DNA binding with AP-1 proteins is required for transformation by EWS-Ets fusion proteins. *Mol Cell Biol.* 2006;26(7):2467-78.
51. Ramakrishnan R, Fujimura Y, Zou JP, Liu F, Lee L, Rao VN, Reddy ES. Role of protein-protein interactions in the antiapoptotic function of EWS-Fli-1. *Oncogene.* 2004;23(42):7087-94.
52. Spahn L, Petermann R, Siligan C, Schmid JA, Aryee DN, Kovar H. Interaction of the EWS NH2 terminus with BARD1 links the Ewing's sarcoma gene to a common tumor suppressor pathway. *Cancer Res.* 2002;62(16):4583-7.
53. Toretsky JA, Erkizan V, Levenson A, Abaan OD, Parvin JD, Cripe TP, Rice AM, Lee SB, Uren A. Oncoprotein EWS-FLI1 activity is enhanced by RNA helicase A. *Cancer Res.* 2006;66(11):5574-81.
54. Mendiola M, Carrillo J, Garcia E, Lalli E, Hernandez T, de Alava E, Tirode F, Delattre O, Garcia-Miguel P, Lopez-Barea F, Pestana A, Alonso J. The orphan nuclear receptor DAX1 is up-regulated by the EWS/FLI1 oncoprotein and is highly expressed in Ewing tumors. *Int J Cancer.* 2006;118(6):1381-9.
55. Bertolotti A, Lutz Y, Heard DJ, Chambon P, Tora L. hTAF(II)68, a novel RNA/ssDNA-binding protein with homology to the pro-oncoproteins TLS/FUS and EWS is associated with both TFIID and RNA polymerase II. *EMBO J.* 1996;15(18):5022-31.
56. Hahm KB. Repression of the gene encoding the TGF-beta type II receptor is a major target of the EWS-FLI1 oncoprotein. *Nat Genet.* 1999;23(4):481.
57. Prieur A, Tirode F, Cohen P, Delattre O. EWS/FLI-1 silencing and gene profiling of Ewing cells reveal downstream oncogenic pathways and a crucial role for repression of insulin-like growth factor binding protein 3. *Mol Cell Biol.* 2004;24(16):7275-83.
58. Nishimori H, Sasaki Y, Yoshida K, Irifune H, Zembutsu H, Tanaka T, Aoyama T, Hosaka T, Kawaguchi S, Wada T, Hata J, Toguchida J, Nakamura Y, et al. The Id2 gene is a novel target of transcriptional activation by EWS-ETS fusion proteins in Ewing family tumors. *Oncogene.* 2002;21(54):8302-9.

59. Fukuma M, Okita H, Hata J, Umezawa A. Upregulation of Id2, an oncogenic helix-loop-helix protein, is mediated by the chimeric EWS/ets protein in Ewing sarcoma. *Oncogene*. 2003;22(1):1-9.
60. Abaan OD, Levenson A, Khan O, Furth PA, Uren A, Toretsky JA. PTPL1 is a direct transcriptional target of EWS-FLI1 and modulates Ewing's Sarcoma tumorigenesis. *Oncogene*. 2005;24(16):2715-22.
61. Nozawa S, Ohno T, Banno Y, Dohjima T, Wakahara K, Fan DG, Shimizu K. Inhibition of platelet-derived growth factor-induced cell growth signaling by a short interfering RNA for EWS-Flt1 via down-regulation of phospholipase D2 in Ewing sarcoma cells. *J Biol Chem*. 2005;280(30):27544-51.
62. Knoop LL, Baker SJ. The splicing factor U1C represses EWS/FLI-mediated transactivation. *J Biol Chem*. 2000;275(32):24865-71.
63. Uren A, Tcherkasskaya O, Toretsky JA. Recombinant EWS-FLI1 oncoprotein activates transcription. *Biochemistry*. 2004;43(42):13579-89.
64. Yang L, Chansky HA, Hickstein DD. EWS.Fli-1 fusion protein interacts with hyperphosphorylated RNA polymerase II and interferes with serine-arginine protein-mediated RNA splicing. *J Biol Chem*. 2000;275(48):37612-8.
65. Ghildiyal M, Xu J, Seitz H, Weng Z, Zamore PD. Sorting of Drosophila small silencing RNAs partitions microRNA\* strands into the RNA interference pathway. *RNA*. 2010;16(1):43-56.
66. Marcinkowska M, Szymanski M, Krzyzosiak WJ, Kozlowski P. Copy number variation of microRNA genes in the human genome. *BMC Genomics*. 2011;12:183.
67. Xiao F, Qiu H, Zhou L, Shen X, Yang L, Ding K. WSS25 inhibits Dicer, downregulating microRNA-210, which targets Ephrin-A3, to suppress human microvascular endothelial cell (HMEC-1) tube formation. *Glycobiology*. 2013;23(5):524-35.
68. Rottiers V, Naar AM. MicroRNAs in metabolism and metabolic disorders. *Nat Rev Mol Cell Biol*. 2012;13(4):239-50.
69. Kim NH, Kim HS, Li XY, Lee I, Choi HS, Kang SE, Cha SY, Ryu JK, Yoon D, Fearon ER, Rowe RG, Lee S, Maher CA, et al. A p53/miRNA-34 axis regulates Snail1-dependent cancer cell epithelial-mesenchymal transition. *J Cell Biol*. 2011;195(3):417-33.
70. Perri R, Nares S, Zhang S, Barros SP, Offenbacher S. MicroRNA modulation in obesity and periodontitis. *J Dent Res*. 2012;91(1):33-8.
71. Tuddenham L, Wheeler G, Ntounia-Fousara S, Waters J, Hajihosseini MK, Clark I, Dalmay T. The cartilage specific microRNA-140 targets histone deacetylase 4 in mouse cells. *FEBS Lett*. 2006;580(17):4214-7.
72. Wilfred BR, Wang WX, Nelson PT. Energizing miRNA research: a review of the role of miRNAs in lipid metabolism, with a prediction that miR-103/107 regulates human metabolic pathways. *Mol Genet Metab*. 2007;91(3):209-17.
73. Sotiropoulou G, Pampalakis G, Lianidou E, Mourelatos Z. Emerging roles of microRNAs as molecular switches in the integrated circuit of the cancer cell. *RNA*. 2009;15(8):1443-61.
74. Visone R, Croce CM. MiRNAs and cancer. *Am J Pathol*. 2009;174(4):1131-8.

75. Davis BN, Hata A. Regulation of MicroRNA Biogenesis: A miRiad of mechanisms. *Cell Commun Signal*. 2009;7:18.
76. Fan M, Krutilina R, Sun J, Sethuraman A, Yang CH, Wu ZH, Yue J, Pfeffer LM. Comprehensive analysis of microRNA (miRNA) targets in breast cancer cells. *J Biol Chem*. 2013;288(38):27480-93.
77. Fernandez-Hernando C, Baldan A. MicroRNAs and Cardiovascular Disease. *Curr Genet Med Rep*. 2013;1(1):30-8.
78. Paroo Z, Liu Q, Wang X. Biochemical mechanisms of the RNA-induced silencing complex. *Cell Res*. 2007;17(3):187-94.
79. McKinsey EL, Parrish JK, Irwin AE, Niemeyer BF, Kern HB, Birks DK, Jedlicka P. A novel oncogenic mechanism in Ewing sarcoma involving IGF pathway targeting by EWS/FLI1-regulated microRNAs. *Oncogene*. 2011;30(49):4910-20.
80. De Vito C, Riggi N, Suva ML, Janiszewska M, Horlbeck J, Baumer K, Provero P, Stamenkovic I. Let-7a is a direct EWS-FLI-1 target implicated in Ewing's sarcoma development. *PLoS One*. 2011;6(8):e23592.
81. Ban J, Jug G, Mestdagh P, Schwentner R, Kauer M, Aryee DN, Schaefer KL, Nakatani F, Scotlandi K, Reiter M, Strunk D, Speleman F, Vandesompele J, et al. Hsa-mir-145 is the top EWS-FLI1-repressed microRNA involved in a positive feedback loop in Ewing's sarcoma. *Oncogene*. 2011;30(18):2173-80.
82. Franzetti GA, Laud-Duval K, Bellanger D, Stern MH, Sastre-Garau X, Delattre O. MiR-30a-5p connects EWS-FLI1 and CD99, two major therapeutic targets in Ewing tumor. *Oncogene*. 2013;32(33):3915-21.
83. Nakatani F, Ferracin M, Manara MC, Ventura S, Del Monaco V, Ferrari S, Alberghini M, Grilli A, Knuutila S, Schaefer KL, Mattia G, Negrini M, Picci P, et al. miR-34a predicts survival of Ewing's sarcoma patients and directly influences cell chemo-sensitivity and malignancy. *J Pathol*. 2012;226(5):796-805.
84. Karnuth B, Dedy N, Spieker T, Lawlor ER, Gattenlohner S, Ranft A, Dirksen U, Jurgens H, Brauning A. Differentially expressed miRNAs in Ewing sarcoma compared to mesenchymal stem cells: low miR-31 expression with effects on proliferation and invasion. *PLoS One*. 2014;9(3):e93067.
85. Iida K, Fukushi J, Matsumoto Y, Oda Y, Takahashi Y, Fujiwara T, Fujiwara-Okada Y, Hatano M, Nabashima A, Kamura S, Iwamoto Y. miR-125b develops chemoresistance in Ewing sarcoma/primitive neuroectodermal tumor. *Cancer Cell Int*. 2013;13(1):21.
86. Jurgens H, Bier V, Dunst J, Harms D, Jobke A, Kotz R, Kuhl J, Muller-Wehrich S, Ritter J, Salzer-Kuntschik M, et al. [The German Society of Pediatric Oncology Cooperative Ewing Sarcoma Studies CESS 81/86: report after 6 1/2 years]. *Klin Padiatr*. 1988;200(3):243-52.
87. Kung FH, Pratt CB, Vega RA, Jaffe N, Strother D, Schwenn M, Nitschke R, Homans AC, Holbrook CT, Golembe B, et al. Ifosfamide/etoposide combination in the treatment of recurrent malignant solid tumors of childhood. A Pediatric Oncology Group Phase II study. *Cancer*. 1993;71(5):1898-903.
88. May WA, Gishizky ML, Lessnick SL, Lunsford LB, Lewis BC, Delattre O, Zucman J, Thomas G, Denny CT. Ewing sarcoma 11;22 translocation produces a chimeric transcription factor that requires the DNA-binding domain encoded by FLI1 for transformation. *Proc Natl Acad Sci U S A*. 1993;90(12):5752-6.

89. Toretzky JA, Gorlick R. IGF-1R targeted treatment of sarcoma. *Lancet Oncol.* 2010;11(2):105-6.
90. Tanaka K, Iwakuma T, Harimaya K, Sato H, Iwamoto Y. EWS-Flt1 antisense oligodeoxynucleotide inhibits proliferation of human Ewing's sarcoma and primitive neuroectodermal tumor cells. *J Clin Invest.* 1997;99(2):239-47.
91. Hu-Lieskovan S, Heidel JD, Bartlett DW, Davis ME, Triche TJ. Sequence-specific knockdown of EWS-FLI1 by targeted, nonviral delivery of small interfering RNA inhibits tumor growth in a murine model of metastatic Ewing's sarcoma. *Cancer Res.* 2005;65(19):8984-92.
92. Erkizan HV, Uversky VN, Toretzky JA. Oncogenic partnerships: EWS-FLI1 protein interactions initiate key pathways of Ewing's sarcoma. *Clin Cancer Res.* 2010;16(16):4077-83.
93. Yee D, Favoni RE, Lebovic GS, Lombana F, Powell DR, Reynolds CP, Rosen N. Insulin-like growth factor I expression by tumors of neuroectodermal origin with the t(11;22) chromosomal translocation. A potential autocrine growth factor. *J Clin Invest.* 1990;86(6):1806-14.
94. Ban J, Bennani-Baiti IM, Kauer M, Schaefer KL, Poremba C, Jug G, Schwentner R, Smrzka O, Muehlbacher K, Aryee DN, Kovar H. EWS-FLI1 suppresses NOTCH-activated p53 in Ewing's sarcoma. *Cancer Res.* 2008;68(17):7100-9.
95. Li Y, Tanaka K, Fan X, Nakatani F, Li X, Nakamura T, Takasaki M, Yamamoto S, Iwamoto Y. Inhibition of the transcriptional function of p53 by EWS-Flt1 chimeric protein in Ewing Family Tumors. *Cancer Lett.* 2010;294(1):57-65.
96. Lain S, Hollick JJ, Campbell J, Staples OD, Higgins M, Aoubala M, McCarthy A, Appleyard V, Murray KE, Baker L, Thompson A, Mathers J, Holland SJ, et al. Discovery, in vivo activity, and mechanism of action of a small-molecule p53 activator. *Cancer Cell.* 2008;13(5):454-63.
97. Pishas KI, Al-Ejeh F, Zinonos I, Kumar R, Evdokiou A, Brown MP, Callen DF, Neilsen PM. Nutlin-3a is a potential therapeutic for ewing sarcoma. *Clin Cancer Res.* 2011;17(3):494-504.
98. Vignot S, Faivre S, Aguirre D, Raymond E. mTOR-targeted therapy of cancer with rapamycin derivatives. *Ann Oncol.* 2005;16(4):525-37.
99. O'Reilly KE, Rojo F, She QB, Solit D, Mills GB, Smith D, Lane H, Hofmann F, Hicklin DJ, Ludwig DL, Baselga J, Rosen N. mTOR inhibition induces upstream receptor tyrosine kinase signaling and activates Akt. *Cancer Res.* 2006;66(3):1500-8.
100. Mateo-Lozano S, Tirado OM, Notario V. Rapamycin induces the fusion-type independent downregulation of the EWS/FLI-1 proteins and inhibits Ewing's sarcoma cell proliferation. *Oncogene.* 2003;22(58):9282-7.
101. Guan H, Zhou Z, Wang H, Jia SF, Liu W, Kleinerman ES. A small interfering RNA targeting vascular endothelial growth factor inhibits Ewing's sarcoma growth in a xenograft mouse model. *Clin Cancer Res.* 2005;11(7):2662-9.
102. Ricotti E, Fagioli F, Garelli E, Linari C, Crescenzo N, Horenstein AL, Pistamiglio P, Vai S, Berger M, di Montezemolo LC, Madon E, Basso G. c-kit is expressed in soft tissue sarcoma of neuroectodermic origin and its ligand prevents apoptosis of neoplastic cells. *Blood.* 1998;91(7):2397-405.

103. Smithey BE, Pappo AS, Hill DA. C-kit expression in pediatric solid tumors: a comparative immunohistochemical study. *Am J Surg Pathol*. 2002;26(4):486-92.
104. Riggi N, Suva ML, De Vito C, Provero P, Stehle JC, Baumer K, Cironi L, Janiszewska M, Petricevic T, Suva D, Tercier S, Joseph JM, Guillou L, et al. EWS-FLI-1 modulates miRNA145 and SOX2 expression to initiate mesenchymal stem cell reprogramming toward Ewing sarcoma cancer stem cells. *Genes Dev*. 2010;24(9):916-32.
105. Sohn HW, Choi EY, Kim SH, Lee IS, Chung DH, Sung UA, Hwang DH, Cho SS, Jun BH, Jang JJ, Chi JG, Park SH. Engagement of CD99 induces apoptosis through a calcineurin-independent pathway in Ewing's sarcoma cells. *Am J Pathol*. 1998;153(6):1937-45.
106. Scotlandi K, Baldini N, Cerisano V, Manara MC, Benini S, Serra M, Lollini PL, Nanni P, Nicoletti G, Bernard G, Bernard A, Picci P. CD99 engagement: an effective therapeutic strategy for Ewing tumors. *Cancer Res*. 2000;60(18):5134-42.
107. McKian KP, Haluska P. Cixutumumab. *Expert Opin Investig Drugs*. 2009;18(7):1025-33.
108. Scartozzi M, Bianconi M, Maccaroni E, Giampieri R, Berardi R, Cascinu S. Dalotuzumab, a recombinant humanized mAb targeted against IGFR1 for the treatment of cancer. *Curr Opin Mol Ther*. 2010;12(3):361-71.
109. Torres-Ruiz R, Martinez-Lage M, Martin MC, Garcia A, Bueno C, Castano J, Ramirez JC, Menendez P, Cigudosa JC, Rodriguez-Perales S. Efficient Recreation of t(11;22) EWSR1-FLI1(+) in Human Stem Cells Using CRISPR/Cas9. *Stem Cell Reports*. 2017;8(5):1408-20.
110. Deneen B, Denny CT. Loss of p16 pathways stabilizes EWS/FLI1 expression and complements EWS/FLI1 mediated transformation. *Oncogene*. 2001;20(46):6731-41.
111. Riggi N, Suva ML, Suva D, Cironi L, Provero P, Tercier S, Joseph JM, Stehle JC, Baumer K, Kindler V, Stamenkovic I. EWS-FLI-1 expression triggers a Ewing's sarcoma initiation program in primary human mesenchymal stem cells. *Cancer Res*. 2008;68(7):2176-85.
112. Cornaz-Buros S, Riggi N, DeVito C, Sarre A, Letovanec I, Provero P, Stamenkovic I. Targeting cancer stem-like cells as an approach to defeating cellular heterogeneity in Ewing sarcoma. *Cancer Res*. 2014;74(22):6610-22.
113. Miller IV, Raposo G, Welsch U, Prazeres da Costa O, Thiel U, Lebar M, Maurer M, Bender HU, von Luetichau I, Richter GH, Burdach S, Grunewald TG. First identification of Ewing's sarcoma-derived extracellular vesicles and exploration of their biological and potential diagnostic implications. *Biol Cell*. 2013;105(7):289-303.
114. De Feo A, Sciandra M, Ferracin M, Felicetti F, Astolfi A, Pignochino Y, Picci P, Care A, Scotlandi K. Exosomes from CD99-deprived Ewing sarcoma cells reverse tumor malignancy by inhibiting cell migration and promoting neural differentiation. *Cell Death Dis*. 2019;10(7):471.
115. Ventura S, Aryee DN, Felicetti F, De Feo A, Mancarella C, Manara MC, Picci P, Colombo MP, Kovar H, Care A, Scotlandi K. CD99 regulates neural differentiation of Ewing sarcoma cells through miR-34a-Notch-mediated control of NF-kappaB signaling. *Oncogene*. 2016;35(30):3944-54.
116. Richter GH, Plehm S, Fasan A, Rossler S, Unland R, Bennani-Baiti IM, Hotfilder M, Lowel D, von Luetichau I, Mossbrugger I, Quintanilla-Martinez L, Kovar H, Staeger MS, et al. EZH2 is a mediator of EWS/FLI1 driven tumor growth and metastasis blocking

- endothelial and neuro-ectodermal differentiation. *Proc Natl Acad Sci U S A*. 2009;106(13):5324-9.
117. Bao S, Wu Q, McLendon RE, Hao Y, Shi Q, Hjelmeland AB, Dewhirst MW, Bigner DD, Rich JN. Glioma stem cells promote radioresistance by preferential activation of the DNA damage response. *Nature*. 2006;444(7120):756-60.
  118. Diehn M, Cho RW, Lobo NA, Kalisky T, Dorie MJ, Kulp AN, Qian D, Lam JS, Ailles LE, Wong M, Joshua B, Kaplan MJ, Wapnir I, et al. Association of reactive oxygen species levels and radioresistance in cancer stem cells. *Nature*. 2009;458(7239):780-3.
  119. Clarke MF, Dick JE, Dirks PB, Eaves CJ, Jamieson CH, Jones DL, Visvader J, Weissman IL, Wahl GM. Cancer stem cells--perspectives on current status and future directions: AACR Workshop on cancer stem cells. *Cancer Res*. 2006;66(19):9339-44.
  120. Bae KM, Dai Y, Vieweg J, Siemann DW. Hypoxia regulates SOX2 expression to promote prostate cancer cell invasion and sphere formation. *Am J Cancer Res*. 2016;6(5):1078-88.
  121. Kreso A, Dick JE. Evolution of the cancer stem cell model. *Cell Stem Cell*. 2014;14(3):275-91.
  122. Jaenisch R, Young R. Stem cells, the molecular circuitry of pluripotency and nuclear reprogramming. *Cell*. 2008;132(4):567-82.
  123. Baylin SB, Jones PA. A decade of exploring the cancer epigenome - biological and translational implications. *Nat Rev Cancer*. 2011;11(10):726-34.
  124. Iorio MV, Croce CM. MicroRNA dysregulation in cancer: diagnostics, monitoring and therapeutics. A comprehensive review. *EMBO Mol Med*. 2012;4(3):143-59.
  125. Covello KL, Kehler J, Yu H, Gordan JD, Arsham AM, Hu CJ, Labosky PA, Simon MC, Keith B. HIF-2alpha regulates Oct-4: effects of hypoxia on stem cell function, embryonic development, and tumor growth. *Genes Dev*. 2006;20(5):557-70.
  126. Lapidot T, Sirard C, Vormoor J, Murdoch B, Hoang T, Caceres-Cortes J, Minden M, Paterson B, Caligiuri MA, Dick JE. A cell initiating human acute myeloid leukaemia after transplantation into SCID mice. *Nature*. 1994;367(6464):645-8.
  127. Al-Hajj M, Wicha MS, Benito-Hernandez A, Morrison SJ, Clarke MF. Prospective identification of tumorigenic breast cancer cells. *Proc Natl Acad Sci U S A*. 2003;100(7):3983-8.
  128. Gerlinger M, Rowan AJ, Horswell S, Math M, Larkin J, Endesfelder D, Gronroos E, Martinez P, Matthews N, Stewart A, Tarpey P, Varela I, Phillimore B, et al. Intratumor heterogeneity and branched evolution revealed by multiregion sequencing. *N Engl J Med*. 2012;366(10):883-92.
  129. Lawson DA, Bhakta NR, Kessenbrock K, Prummel KD, Yu Y, Takai K, Zhou A, Eyob H, Balakrishnan S, Wang CY, Yaswen P, Goga A, Werb Z. Single-cell analysis reveals a stem-cell program in human metastatic breast cancer cells. *Nature*. 2015;526(7571):131-5.
  130. Trucco M, Loeb D. Sarcoma stem cells: do we know what we are looking for? *Sarcoma*. 2012;2012:291705.
  131. Awad O, Yustein JT, Shah P, Gul N, Katuri V, O'Neill A, Kong Y, Brown ML, Toretsky JA, Loeb DM. High ALDH activity identifies chemotherapy-resistant Ewing's sarcoma stem cells that retain sensitivity to EWS-FLI1 inhibition. *PLoS One*. 2010;5(11):e13943.



132. Armstrong L, Stojkovic M, Dimmick I, Ahmad S, Stojkovic P, Hole N, Lako M. Phenotypic characterization of murine primitive hematopoietic progenitor cells isolated on basis of aldehyde dehydrogenase activity. *Stem Cells*. 2004;22(7):1142-51.
133. Cai J, Cheng A, Luo Y, Lu C, Mattson MP, Rao MS, Furukawa K. Membrane properties of rat embryonic multipotent neural stem cells. *J Neurochem*. 2004;88(1):212-26.
134. Crabb DW, Matsumoto M, Chang D, You M. Overview of the role of alcohol dehydrogenase and aldehyde dehydrogenase and their variants in the genesis of alcohol-related pathology. *Proc Nutr Soc*. 2004;63(1):49-63.
135. Iwasaki H, Suda T. Cancer stem cells and their niche. *Cancer Sci*. 2009;100(7):1166-72.
136. Basak GW, Srivastava AS, Malhotra R, Carrier E. Multiple myeloma bone marrow niche. *Curr Pharm Biotechnol*. 2009;10(3):345-6.
137. Gaspar N, Hawkins DS, Dirksen U, Lewis IJ, Ferrari S, Le Deley MC, Kovar H, Grimer R, Whelan J, Claude L, Delattre O, Paulussen M, Picci P, et al. Ewing Sarcoma: Current Management and Future Approaches Through Collaboration. *J Clin Oncol*. 2015;33(27):3036-46.
138. Heddlestone JM, Li Z, Lathia JD, Bao S, Hjelmeland AB, Rich JN. Hypoxia inducible factors in cancer stem cells. *Br J Cancer*. 2010;102(5):789-95.
139. Holmquist-Mengelbier L, Fredlund E, Lofstedt T, Noguera R, Navarro S, Nilsson H, Pietras A, Vallon-Christersson J, Borg A, Gradin K, Poellinger L, Pahlman S. Recruitment of HIF-1alpha and HIF-2alpha to common target genes is differentially regulated in neuroblastoma: HIF-2alpha promotes an aggressive phenotype. *Cancer Cell*. 2006;10(5):413-23.
140. Soni S, Padwad YS. HIF-1 in cancer therapy: two decade long story of a transcription factor. *Acta Oncol*. 2017;56(4):503-15.
141. Semenza GL. The hypoxic tumor microenvironment: A driving force for breast cancer progression. *Biochim Biophys Acta*. 2016;1863(3):382-91.
142. Dunst J, Ahrens S, Paulussen M, Burdach S, Jurgens H. Prognostic impact of tumor perfusion in MR-imaging studies in Ewing tumors. *Strahlenther Onkol*. 2001;177(3):153-9.
143. Aryee DN, Niedan S, Kauer M, Schwentner R, Bennani-Baiti IM, Ban J, Muehlbacher K, Kreppel M, Walker RL, Meltzer P, Poremba C, Kofler R, Kovar H. Hypoxia modulates EWS-FLI1 transcriptional signature and enhances the malignant properties of Ewing's sarcoma cells in vitro. *Cancer Res*. 2010;70(10):4015-23.
144. Kilic M, Kasperczyk H, Fulda S, Debatin KM. Role of hypoxia inducible factor-1 alpha in modulation of apoptosis resistance. *Oncogene*. 2007;26(14):2027-38.
145. Knowles HJ, Schaefer KL, Dirksen U, Athanasou NA. Hypoxia and hypoglycaemia in Ewing's sarcoma and osteosarcoma: regulation and phenotypic effects of Hypoxia-Inducible Factor. *BMC Cancer*. 2010;10:372.
146. Hameiri-Grossman M, Porat-Klein A, Yaniv I, Ash S, Cohen IJ, Kodman Y, Haklai R, Elad-Sfadia G, Kloog Y, Chepurko E, Feinmesser M, Issakov J, Sher O, et al. The association between let-7, RAS and HIF-1alpha in Ewing Sarcoma tumor growth. *Oncotarget*. 2015;6(32):33834-48.
147. Tilan JU, Lu C, Galli S, Izycka-Swieszewska E, Earnest JP, Shabbir A, Everhart LM, Wang S, Martin S, Horton M, Mahajan A, Christian D, O'Neill A, et al. Hypoxia shifts

- activity of neuropeptide Y in Ewing sarcoma from growth-inhibitory to growth-promoting effects. *Oncotarget*. 2013;4(12):2487-501.
148. Semenza GL, Wang GL. A nuclear factor induced by hypoxia via de novo protein synthesis binds to the human erythropoietin gene enhancer at a site required for transcriptional activation. *Mol Cell Biol*. 1992;12(12):5447-54.
  149. Wang GL, Jiang BH, Rue EA, Semenza GL. Hypoxia-inducible factor 1 is a basic-helix-loop-helix-PAS heterodimer regulated by cellular O<sub>2</sub> tension. *Proc Natl Acad Sci U S A*. 1995;92(12):5510-4.
  150. Gu YZ, Moran SM, Hogenesch JB, Wartman L, Bradfield CA. Molecular characterization and chromosomal localization of a third alpha-class hypoxia inducible factor subunit, HIF3alpha. *Gene Expr*. 1998;7(3):205-13.
  151. Ema M, Taya S, Yokotani N, Sogawa K, Matsuda Y, Fujii-Kuriyama Y. A novel bHLH-PAS factor with close sequence similarity to hypoxia-inducible factor 1alpha regulates the VEGF expression and is potentially involved in lung and vascular development. *Proc Natl Acad Sci U S A*. 1997;94(9):4273-8.
  152. Iyer NV, Leung SW, Semenza GL. The human hypoxia-inducible factor 1alpha gene: HIF1A structure and evolutionary conservation. *Genomics*. 1998;52(2):159-65.
  153. Huang LE, Gu J, Schau M, Bunn HF. Regulation of hypoxia-inducible factor 1alpha is mediated by an O<sub>2</sub>-dependent degradation domain via the ubiquitin-proteasome pathway. *Proc Natl Acad Sci U S A*. 1998;95(14):7987-92.
  154. O'Rourke JF, Tian YM, Ratcliffe PJ, Pugh CW. Oxygen-regulated and transactivating domains in endothelial PAS protein 1: comparison with hypoxia-inducible factor-1alpha. *J Biol Chem*. 1999;274(4):2060-71.
  155. Ivan M, Kondo K, Yang H, Kim W, Valiando J, Ohh M, Salic A, Asara JM, Lane WS, Kaelin WG, Jr. HIFalpha targeted for VHL-mediated destruction by proline hydroxylation: implications for O<sub>2</sub> sensing. *Science*. 2001;292(5516):464-8.
  156. Majmundar AJ, Wong WJ, Simon MC. Hypoxia-inducible factors and the response to hypoxic stress. *Mol Cell*. 2010;40(2):294-309.
  157. Greer SN, Metcalf JL, Wang Y, Ohh M. The updated biology of hypoxia-inducible factor. *EMBO J*. 2012;31(11):2448-60.
  158. Tian H, McKnight SL, Russell DW. Endothelial PAS domain protein 1 (EPAS1), a transcription factor selectively expressed in endothelial cells. *Genes Dev*. 1997;11(1):72-82.
  159. Jiang BH, Rue E, Wang GL, Roe R, Semenza GL. Dimerization, DNA binding, and transactivation properties of hypoxia-inducible factor 1. *J Biol Chem*. 1996;271(30):17771-8.
  160. Jiang BH, Zheng JZ, Leung SW, Roe R, Semenza GL. Transactivation and inhibitory domains of hypoxia-inducible factor 1alpha. Modulation of transcriptional activity by oxygen tension. *J Biol Chem*. 1997;272(31):19253-60.
  161. Lendahl U, Lee KL, Yang H, Poellinger L. Generating specificity and diversity in the transcriptional response to hypoxia. *Nat Rev Genet*. 2009;10(12):821-32.
  162. Dengler VL, Galbraith M, Espinosa JM. Transcriptional regulation by hypoxia inducible factors. *Crit Rev Biochem Mol Biol*. 2014;49(1):1-15.

163. Maynard MA, Qi H, Chung J, Lee EH, Kondo Y, Hara S, Conaway RC, Conaway JW, Ohh M. Multiple splice variants of the human HIF-3 alpha locus are targets of the von Hippel-Lindau E3 ubiquitin ligase complex. *J Biol Chem*. 2003;278(13):11032-40.
164. Pasanen A, Heikkila M, Rautavuoma K, Hirsila M, Kivirikko KI, Myllyharju J. Hypoxia-inducible factor (HIF)-3alpha is subject to extensive alternative splicing in human tissues and cancer cells and is regulated by HIF-1 but not HIF-2. *Int J Biochem Cell Biol*. 2010;42(7):1189-200.
165. Ema M, Hirota K, Mimura J, Abe H, Yodoi J, Sogawa K, Poellinger L, Fujii-Kuriyama Y. Molecular mechanisms of transcription activation by HLF and HIF1alpha in response to hypoxia: their stabilization and redox signal-induced interaction with CBP/p300. *EMBO J*. 1999;18(7):1905-14.
166. Dayan F, Roux D, Brahimi-Horn MC, Pouyssegur J, Mazure NM. The oxygen sensor factor-inhibiting hypoxia-inducible factor-1 controls expression of distinct genes through the bifunctional transcriptional character of hypoxia-inducible factor-1alpha. *Cancer Res*. 2006;66(7):3688-98.
167. Hu CJ, Sataur A, Wang L, Chen H, Simon MC. The N-terminal transactivation domain confers target gene specificity of hypoxia-inducible factors HIF-1alpha and HIF-2alpha. *Mol Biol Cell*. 2007;18(11):4528-42.
168. Berra E, Benizri E, Ginouves A, Volmat V, Roux D, Pouyssegur J. HIF prolyl-hydroxylase 2 is the key oxygen sensor setting low steady-state levels of HIF-1alpha in normoxia. *EMBO J*. 2003;22(16):4082-90.
169. Appelhoff RJ, Tian YM, Raval RR, Turley H, Harris AL, Pugh CW, Ratcliffe PJ, Gleadle JM. Differential function of the prolyl hydroxylases PHD1, PHD2, and PHD3 in the regulation of hypoxia-inducible factor. *J Biol Chem*. 2004;279(37):38458-65.
170. Ohh M, Park CW, Ivan M, Hoffman MA, Kim TY, Huang LE, Pavletich N, Chau V, Kaelin WG. Ubiquitination of hypoxia-inducible factor requires direct binding to the beta-domain of the von Hippel-Lindau protein. *Nat Cell Biol*. 2000;2(7):423-7.
171. Foxler DE, Bridge KS, James V, Webb TM, Mee M, Wong SC, Feng Y, Constantin-Teodosiu D, Petursdottir TE, Bjornsson J, Ingvarsson S, Ratcliffe PJ, Longmore GD, et al. The LIMD1 protein bridges an association between the prolyl hydroxylases and VHL to repress HIF-1 activity. *Nat Cell Biol*. 2012;14(2):201-8.
172. Jaakkola P, Mole DR, Tian YM, Wilson MI, Gielbert J, Gaskell SJ, von Kriegsheim A, Hebestreit HF, Mukherji M, Schofield CJ, Maxwell PH, Pugh CW, Ratcliffe PJ. Targeting of HIF-alpha to the von Hippel-Lindau ubiquitylation complex by O2-regulated prolyl hydroxylation. *Science*. 2001;292(5516):468-72.
173. Masson N, Willam C, Maxwell PH, Pugh CW, Ratcliffe PJ. Independent function of two destruction domains in hypoxia-inducible factor-alpha chains activated by prolyl hydroxylation. *EMBO J*. 2001;20(18):5197-206.
174. Mahon PC, Hirota K, Semenza GL. FIH-1: a novel protein that interacts with HIF-1alpha and VHL to mediate repression of HIF-1 transcriptional activity. *Genes Dev*. 2001;15(20):2675-86.
175. Lando D, Peet DJ, Gorman JJ, Whelan DA, Whitelaw ML, Bruick RK. FIH-1 is an asparaginyl hydroxylase enzyme that regulates the transcriptional activity of hypoxia-inducible factor. *Genes Dev*. 2002;16(12):1466-71.

176. Dames SA, Martinez-Yamout M, De Guzman RN, Dyson HJ, Wright PE. Structural basis for Hif-1 alpha /CBP recognition in the cellular hypoxic response. *Proc Natl Acad Sci U S A*. 2002;99(8):5271-6.
177. Liu YV, Baek JH, Zhang H, Diez R, Cole RN, Semenza GL. RACK1 competes with HSP90 for binding to HIF-1alpha and is required for O(2)-independent and HSP90 inhibitor-induced degradation of HIF-1alpha. *Mol Cell*. 2007;25(2):207-17.
178. Koh MY, Darnay BG, Powis G. Hypoxia-associated factor, a novel E3-ubiquitin ligase, binds and ubiquitinates hypoxia-inducible factor 1alpha, leading to its oxygen-independent degradation. *Mol Cell Biol*. 2008;28(23):7081-95.
179. Luo W, Zhong J, Chang R, Hu H, Pandey A, Semenza GL. Hsp70 and CHIP selectively mediate ubiquitination and degradation of hypoxia-inducible factor (HIF)-1alpha but not HIF-2alpha. *J Biol Chem*. 2010;285(6):3651-63.
180. Schodel J, Oikonomopoulos S, Ragoussis J, Pugh CW, Ratcliffe PJ, Mole DR. High-resolution genome-wide mapping of HIF-binding sites by ChIP-seq. *Blood*. 2011;117(23):e207-17.
181. Mole DR, Blancher C, Copley RR, Pollard PJ, Gleadle JM, Ragoussis J, Ratcliffe PJ. Genome-wide association of hypoxia-inducible factor (HIF)-1alpha and HIF-2alpha DNA binding with expression profiling of hypoxia-inducible transcripts. *J Biol Chem*. 2009;284(25):16767-75.
182. Villar D, Ortiz-Barahona A, Gomez-Maldonado L, Pescador N, Sanchez-Cabo F, Hackl H, Rodriguez BA, Trajanoski Z, Dopazo A, Huang TH, Yan PS, Del Peso L. Cooperativity of stress-responsive transcription factors in core hypoxia-inducible factor binding regions. *PLoS One*. 2012;7(9):e45708.
183. Semenza GL. Hypoxia-inducible factors: mediators of cancer progression and targets for cancer therapy. *Trends Pharmacol Sci*. 2012;33(4):207-14.
184. Pawlus MR, Hu CJ. Enhanceosomes as integrators of hypoxia inducible factor (HIF) and other transcription factors in the hypoxic transcriptional response. *Cell Signal*. 2013;25(9):1895-903.
185. Wenger RH, Stiehl DP, Camenisch G. Integration of oxygen signaling at the consensus HRE. *Sci STKE*. 2005;2005(306):re12.
186. Chi JT, Wang Z, Nuyten DS, Rodriguez EH, Schaner ME, Salim A, Wang Y, Kristensen GB, Helland A, Borresen-Dale AL, Giaccia A, Longaker MT, Hastie T, et al. Gene expression programs in response to hypoxia: cell type specificity and prognostic significance in human cancers. *PLoS Med*. 2006;3(3):e47.
187. Koh MY, Lemos R, Jr., Liu X, Powis G. The hypoxia-associated factor switches cells from HIF-1alpha- to HIF-2alpha-dependent signaling promoting stem cell characteristics, aggressive tumor growth and invasion. *Cancer Res*. 2011;71(11):4015-27.
188. Baumann M, Krause M, Hill R. Exploring the role of cancer stem cells in radioresistance. *Nat Rev Cancer*. 2008;8(7):545-54.
189. Eyler CE, Rich JN. Survival of the fittest: cancer stem cells in therapeutic resistance and angiogenesis. *J Clin Oncol*. 2008;26(17):2839-45.
190. Vaupel P, Mayer A. Hypoxia in cancer: significance and impact on clinical outcome. *Cancer Metastasis Rev*. 2007;26(2):225-39.

191. Yoshida Y, Takahashi K, Okita K, Ichisaka T, Yamanaka S. Hypoxia enhances the generation of induced pluripotent stem cells. *Cell Stem Cell*. 2009;5(3):237-41.
192. Mukherjee T, Kim WS, Mandal L, Banerjee U. Interaction between Notch and Hif-alpha in development and survival of Drosophila blood cells. *Science*. 2011;332(6034):1210-3.
193. Hu CJ, Wang LY, Chodosh LA, Keith B, Simon MC. Differential roles of hypoxia-inducible factor 1alpha (HIF-1alpha) and HIF-2alpha in hypoxic gene regulation. *Mol Cell Biol*. 2003;23(24):9361-74.
194. Li Z, Bao S, Wu Q, Wang H, Eyler C, Sathornsumetee S, Shi Q, Cao Y, Lathia J, McLendon RE, Hjelmeland AB, Rich JN. Hypoxia-inducible factors regulate tumorigenic capacity of glioma stem cells. *Cancer Cell*. 2009;15(6):501-13.
195. Soeda A, Park M, Lee D, Mintz A, Androutsellis-Theotokis A, McKay RD, Engh J, Iwama T, Kunisada T, Kassam AB, Pollack IF, Park DM. Hypoxia promotes expansion of the CD133-positive glioma stem cells through activation of HIF-1alpha. *Oncogene*. 2009;28(45):3949-59.
196. Shen G, Li X, Jia YF, Piazza GA, Xi Y. Hypoxia-regulated microRNAs in human cancer. *Acta Pharmacol Sin*. 2013;34(3):336-41.
197. Huang X, Ding L, Bennewith KL, Tong RT, Welford SM, Ang KK, Story M, Le QT, Giaccia AJ. Hypoxia-inducible mir-210 regulates normoxic gene expression involved in tumor initiation. *Mol Cell*. 2009;35(6):856-67.
198. Bruning U, Cerone L, Neufeld Z, Fitzpatrick SF, Cheong A, Scholz CC, Simpson DA, Leonard MO, Tambuwala MM, Cummins EP, Taylor CT. MicroRNA-155 promotes resolution of hypoxia-inducible factor 1alpha activity during prolonged hypoxia. *Mol Cell Biol*. 2011;31(19):4087-96.
199. Crosby ME, Kulshreshtha R, Ivan M, Glazer PM. MicroRNA regulation of DNA repair gene expression in hypoxic stress. *Cancer Res*. 2009;69(3):1221-9.
200. Polytarchou C, Iliopoulos D, Hatzia Apostolou M, Kottakis F, Maroulakou I, Struhl K, Tsichlis PN. Akt2 regulates all Akt isoforms and promotes resistance to hypoxia through induction of miR-21 upon oxygen deprivation. *Cancer Res*. 2011;71(13):4720-31.
201. Haque I, Banerjee S, Mehta S, De A, Majumder M, Mayo MS, Kambhampati S, Campbell DR, Banerjee SK. Cysteine-rich 61-connective tissue growth factor-nephroblastoma-overexpressed 5 (CCN5)/Wnt-1-induced signaling protein-2 (WISP-2) regulates microRNA-10b via hypoxia-inducible factor-1alpha-TWIST signaling networks in human breast cancer cells. *J Biol Chem*. 2011;286(50):43475-85.
202. Wu C, So J, Davis-Dusenbery BN, Qi HH, Bloch DB, Shi Y, Lagna G, Hata A. Hypoxia potentiates microRNA-mediated gene silencing through posttranslational modification of Argonaute2. *Mol Cell Biol*. 2011;31(23):4760-74.
203. Hofbauer KH, Gess B, Lohaus C, Meyer HE, Katschinski D, Kurtz A. Oxygen tension regulates the expression of a group of procollagen hydroxylases. *Eur J Biochem*. 2003;270(22):4515-22.
204. Devlin C, Greco S, Martelli F, Ivan M. miR-210: More than a silent player in hypoxia. *IUBMB Life*. 2011;63(2):94-100.
205. Huang X, Le QT, Giaccia AJ. MiR-210--micromanager of the hypoxia pathway. *Trends Mol Med*. 2010;16(5):230-7.

206. Zhang Z, Sun H, Dai H, Walsh RM, Imakura M, Schelter J, Burchard J, Dai X, Chang AN, Diaz RL, Marszalek JR, Bartz SR, Carleton M, et al. MicroRNA miR-210 modulates cellular response to hypoxia through the MYC antagonist MNT. *Cell Cycle*. 2009;8(17):2756-68.
207. Bartel DP. MicroRNAs: genomics, biogenesis, mechanism, and function. *Cell*. 2004;116(2):281-97.
208. Zhang Y, Fei M, Xue G, Zhou Q, Jia Y, Li L, Xin H, Sun S. Elevated levels of hypoxia-inducible microRNA-210 in pre-eclampsia: new insights into molecular mechanisms for the disease. *J Cell Mol Med*. 2012;16(2):249-59.
209. Mutharasan RK, Nagpal V, Ichikawa Y, Ardehali H. microRNA-210 is upregulated in hypoxic cardiomyocytes through Akt- and p53-dependent pathways and exerts cytoprotective effects. *Am J Physiol Heart Circ Physiol*. 2011;301(4):H1519-30.
210. Chan YC, Banerjee J, Choi SY, Sen CK. miR-210: the master hypoxamir. *Microcirculation*. 2012;19(3):215-23.
211. Kelly TJ, Souza AL, Clish CB, Puigserver P. A hypoxia-induced positive feedback loop promotes hypoxia-inducible factor 1 $\alpha$  stability through miR-210 suppression of glycerol-3-phosphate dehydrogenase 1-like. *Mol Cell Biol*. 2011;31(13):2696-706.
212. Tsuchiya S, Fujiwara T, Sato F, Shimada Y, Tanaka E, Sakai Y, Shimizu K, Tsujimoto G. MicroRNA-210 regulates cancer cell proliferation through targeting fibroblast growth factor receptor-like 1 (FGFRL1). *J Biol Chem*. 2011;286(1):420-8.
213. Biswas S, Roy S, Banerjee J, Hussain SR, Khanna S, Meenakshisundaram G, Kuppusamy P, Friedman A, Sen CK. Hypoxia inducible microRNA 210 attenuates keratinocyte proliferation and impairs closure in a murine model of ischemic wounds. *Proc Natl Acad Sci U S A*. 2010;107(15):6976-81.
214. Hanahan D, Weinberg RA. The hallmarks of cancer. *Cell*. 2000;100(1):57-70.
215. Chan SY, Zhang YY, Hemann C, Mahoney CE, Zweier JL, Loscalzo J. MicroRNA-210 controls mitochondrial metabolism during hypoxia by repressing the iron-sulfur cluster assembly proteins ISCU1/2. *Cell Metab*. 2009;10(4):273-84.
216. Chen Z, Li Y, Zhang H, Huang P, Luthra R. Hypoxia-regulated microRNA-210 modulates mitochondrial function and decreases ISCU and COX10 expression. *Oncogene*. 2010;29(30):4362-8.
217. Puissegur MP, Mazure NM, Bertero T, Pradelli L, Grosso S, Robbe-Sermesant K, Maurin T, Lebrigand K, Cardinaud B, Hofman V, Fourre S, Magnone V, Ricci JE, et al. miR-210 is overexpressed in late stages of lung cancer and mediates mitochondrial alterations associated with modulation of HIF-1 activity. *Cell Death Differ*. 2011;18(3):465-78.
218. Fasanaro P, D'Alessandra Y, Di Stefano V, Melchionna R, Romani S, Pompilio G, Capogrossi MC, Martelli F. MicroRNA-210 modulates endothelial cell response to hypoxia and inhibits the receptor tyrosine kinase ligand Ephrin-A3. *J Biol Chem*. 2008;283(23):15878-83.
219. Fasanaro P, Greco S, Lorenzi M, Pescatori M, Brioschi M, Kulshreshtha R, Banfi C, Stubbs A, Calin GA, Ivan M, Capogrossi MC, Martelli F. An integrated approach for experimental target identification of hypoxia-induced miR-210. *J Biol Chem*. 2009;284(50):35134-43.

220. Liu F, Lou YL, Wu J, Ruan QF, Xie A, Guo F, Cui SP, Deng ZF, Wang Y. Upregulation of microRNA-210 regulates renal angiogenesis mediated by activation of VEGF signaling pathway under ischemia/perfusion injury in vivo and in vitro. *Kidney Blood Press Res.* 2012;35(3):182-91.
221. Zhang H, Mai Q, Chen J. MicroRNA-210 is increased and it is required for dedifferentiation of osteosarcoma cell line. *Cell Biol Int.* 2017;41(3):267-75.
222. Kim HW, Haider HK, Jiang S, Ashraf M. Ischemic preconditioning augments survival of stem cells via miR-210 expression by targeting caspase-8-associated protein 2. *J Biol Chem.* 2009;284(48):33161-8.
223. Yang W, Wei J, Guo T, Shen Y, Liu F. Knockdown of miR-210 decreases hypoxic glioma stem cells stemness and radioresistance. *Exp Cell Res.* 2014;326(1):22-35.
224. Imai Y, Kimura T, Murakami A, Yajima N, Sakamaki K, Yonehara S. The CED-4-homologous protein FLASH is involved in Fas-mediated activation of caspase-8 during apoptosis. *Nature.* 1999;398(6730):777-85.
225. Li T, Song X, Zhang J, Zhao L, Shi Y, Li Z, Liu J, Liu N, Yan Y, Xiao Y, Tian X, Sun W, Guan Y, et al. Protection of Human Umbilical Vein Endothelial Cells against Oxidative Stress by MicroRNA-210. *Oxid Med Cell Longev.* 2017;2017:3565613.
226. Kilic-Eren M, Boylu T, Tabor V. Targeting PI3K/Akt represses Hypoxia inducible factor-1alpha activation and sensitizes Rhabdomyosarcoma and Ewing's sarcoma cells for apoptosis. *Cancer Cell Int.* 2013;13:36.
227. Wei Y, Jiang Y, Zou F, Liu Y, Wang S, Xu N, Xu W, Cui C, Xing Y, Liu Y, Cao B, Liu C, Wu G, et al. Activation of PI3K/Akt pathway by CD133-p85 interaction promotes tumorigenic capacity of glioma stem cells. *Proc Natl Acad Sci U S A.* 2013;110(17):6829-34.
228. Jung KO, Youn H, Lee CH, Kang KW, Chung JK. Visualization of exosome-mediated miR-210 transfer from hypoxic tumor cells. *Oncotarget.* 2017;8(6):9899-910.
229. Paget S. The distribution of secondary growths in cancer of the breast. 1889. *Cancer Metastasis Rev.* 1989;8(2):98-101.
230. Meng W, Hao Y, He C, Li L, Zhu G. Exosome-orchestrated hypoxic tumor microenvironment. *Mol Cancer.* 2019;18(1):57.
231. Redini F, Heymann D. Bone Tumor Environment as a Potential Therapeutic Target in Ewing Sarcoma. *Front Oncol.* 2015;5:279.
232. Hsu YL, Hung JY, Chang WA, Lin YS, Pan YC, Tsai PH, Wu CY, Kuo PL. Hypoxic lung cancer-secreted exosomal miR-23a increased angiogenesis and vascular permeability by targeting prolyl hydroxylase and tight junction protein ZO-1. *Oncogene.* 2017;36(34):4929-42.
233. Li L, Li C, Wang S, Wang Z, Jiang J, Wang W, Li X, Chen J, Liu K, Li C, Zhu G. Exosomes Derived from Hypoxic Oral Squamous Cell Carcinoma Cells Deliver miR-21 to Normoxic Cells to Elicit a Prometastatic Phenotype. *Cancer Res.* 2016;76(7):1770-80.
234. Ramteke A, Ting H, Agarwal C, Mateen S, Somasagara R, Hussain A, Graner M, Frederick B, Agarwal R, Deep G. Exosomes secreted under hypoxia enhance invasiveness and stemness of prostate cancer cells by targeting adherens junction molecules. *Mol Carcinog.* 2015;54(7):554-65.

235. Kuzet SE, Gaggioli C. Fibroblast activation in cancer: when seed fertilizes soil. *Cell Tissue Res.* 2016;365(3):607-19.
236. Baroni S, Romero-Cordoba S, Plantamura I, Dugo M, D'Ippolito E, Cataldo A, Cosentino G, Angeloni V, Rossini A, Daidone MG, Iorio MV. Exosome-mediated delivery of miR-9 induces cancer-associated fibroblast-like properties in human breast fibroblasts. *Cell Death Dis.* 2016;7(7):e2312.
237. Lugini L, Valtieri M, Federici C, Cecchetti S, Meschini S, Condello M, Signore M, Fais S. Exosomes from human colorectal cancer induce a tumor-like behavior in colonic mesenchymal stromal cells. *Oncotarget.* 2016;7(31):50086-98.
238. Harding C, Heuser J, Stahl P. Endocytosis and intracellular processing of transferrin and colloidal gold-transferrin in rat reticulocytes: demonstration of a pathway for receptor shedding. *Eur J Cell Biol.* 1984;35(2):256-63.
239. Raposo G, Stoorvogel W. Extracellular vesicles: exosomes, microvesicles, and friends. *J Cell Biol.* 2013;200(4):373-83.
240. Kowal J, Arras G, Colombo M, Jouve M, Morath JP, Primdal-Bengtson B, Dingli F, Loew D, Tkach M, Thery C. Proteomic comparison defines novel markers to characterize heterogeneous populations of extracellular vesicle subtypes. *Proc Natl Acad Sci U S A.* 2016;113(8):E968-77.
241. Kahlert C, Melo SA, Protopopov A, Tang J, Seth S, Koch M, Zhang J, Weitz J, Chin L, Futreal A, Kalluri R. Identification of double-stranded genomic DNA spanning all chromosomes with mutated KRAS and p53 DNA in the serum exosomes of patients with pancreatic cancer. *J Biol Chem.* 2014;289(7):3869-75.
242. Valadi H, Ekstrom K, Bossios A, Sjostrand M, Lee JJ, Lotvall JO. Exosome-mediated transfer of mRNAs and microRNAs is a novel mechanism of genetic exchange between cells. *Nat Cell Biol.* 2007;9(6):654-9.
243. Yin J, Yan X, Yao X, Zhang Y, Shan Y, Mao N, Yang Y, Pan L. Secretion of annexin A3 from ovarian cancer cells and its association with platinum resistance in ovarian cancer patients. *J Cell Mol Med.* 2012;16(2):337-48.
244. Kalluri R. The biology and function of exosomes in cancer. *J Clin Invest.* 2016;126(4):1208-15.
245. Melo SA, Luecke LB, Kahlert C, Fernandez AF, Gammon ST, Kaye J, LeBleu VS, Mittendorf EA, Weitz J, Rahbari N, Reissfelder C, Pilarsky C, Fraga MF, et al. Glypican-1 identifies cancer exosomes and detects early pancreatic cancer. *Nature.* 2015;523(7559):177-82.
246. Caradec J, Kharmate G, Hosseini-Beheshti E, Adomat H, Gleave M, Guns E. Reproducibility and efficiency of serum-derived exosome extraction methods. *Clin Biochem.* 2014;47(13-14):1286-92.
247. Raiborg C, Stenmark H. The ESCRT machinery in endosomal sorting of ubiquitylated membrane proteins. *Nature.* 2009;458(7237):445-52.
248. Hurley JH, Hanson PI. Membrane budding and scission by the ESCRT machinery: it's all in the neck. *Nat Rev Mol Cell Biol.* 2010;11(8):556-66.
249. Trajkovic K, Hsu C, Chiantia S, Rajendran L, Wenzel D, Wieland F, Schwille P, Brugger B, Simons M. Ceramide triggers budding of exosome vesicles into multivesicular endosomes. *Science.* 2008;319(5867):1244-7.



250. Colombo M, Raposo G, Thery C. Biogenesis, secretion, and intercellular interactions of exosomes and other extracellular vesicles. *Annu Rev Cell Dev Biol.* 2014;30:255-89.
251. Wubbolts R, Leckie RS, Veenhuizen PT, Schwarzmann G, Mobius W, Hoernschemeyer J, Slot JW, Geuze HJ, Stoorvogel W. Proteomic and biochemical analyses of human B cell-derived exosomes. Potential implications for their function and multivesicular body formation. *J Biol Chem.* 2003;278(13):10963-72.
252. Laulagnier K, Motta C, Hamdi S, Roy S, Fauvelle F, Pageaux JF, Kobayashi T, Salles JP, Perret B, Bonnerot C, Record M. Mast cell- and dendritic cell-derived exosomes display a specific lipid composition and an unusual membrane organization. *Biochem J.* 2004;380(Pt 1):161-71.
253. Subra C, Laulagnier K, Perret B, Record M. Exosome lipidomics unravels lipid sorting at the level of multivesicular bodies. *Biochimie.* 2007;89(2):205-12.
254. Brouwers JF, Aalberts M, Jansen JW, van Niel G, Wauben MH, Stout TA, Helms JB, Stoorvogel W. Distinct lipid compositions of two types of human prostasomes. *Proteomics.* 2013;13(10-11):1660-6.
255. Simons M, Raposo G. Exosomes--vesicular carriers for intercellular communication. *Curr Opin Cell Biol.* 2009;21(4):575-81.
256. Zoller M. Tetraspanins: push and pull in suppressing and promoting metastasis. *Nat Rev Cancer.* 2009;9(1):40-55.
257. Thery C, Zitvogel L, Amigorena S. Exosomes: composition, biogenesis and function. *Nat Rev Immunol.* 2002;2(8):569-79.
258. Zhang X, Yuan X, Shi H, Wu L, Qian H, Xu W. Exosomes in cancer: small particle, big player. *J Hematol Oncol.* 2015;8:83.
259. Mincheva-Nilsson L, Baranov V. Cancer exosomes and NKG2D receptor-ligand interactions: impairing NKG2D-mediated cytotoxicity and anti-tumour immune surveillance. *Semin Cancer Biol.* 2014;28:24-30.
260. Aga M, Bentz GL, Raffa S, Torrisi MR, Kondo S, Wakisaka N, Yoshizaki T, Pagano JS, Shackelford J. Exosomal HIF1alpha supports invasive potential of nasopharyngeal carcinoma-associated LMP1-positive exosomes. *Oncogene.* 2014;33(37):4613-22.
261. Ratajczak J, Miekus K, Kucia M, Zhang J, Reca R, Dvorak P, Ratajczak MZ. Embryonic stem cell-derived microvesicles reprogram hematopoietic progenitors: evidence for horizontal transfer of mRNA and protein delivery. *Leukemia.* 2006;20(5):847-56.
262. Gusachenko ON, Zenkova MA, Vlassov VV. Nucleic acids in exosomes: disease markers and intercellular communication molecules. *Biochemistry (Mosc).* 2013;78(1):1-7.
263. Huang X, Yuan T, Tschannen M, Sun Z, Jacob H, Du M, Liang M, Dittmar RL, Liu Y, Liang M, Kohli M, Thibodeau SN, Boardman L, et al. Characterization of human plasma-derived exosomal RNAs by deep sequencing. *BMC Genomics.* 2013;14:319.
264. Melo SA, Sugimoto H, O'Connell JT, Kato N, Villanueva A, Vidal A, Qiu L, Vitkin E, Perelman LT, Melo CA, Lucci A, Ivan C, Calin GA, et al. Cancer exosomes perform cell-independent microRNA biogenesis and promote tumorigenesis. *Cancer Cell.* 2014;26(5):707-21.
265. Villarroya-Beltri C, Baixauli F, Gutierrez-Vazquez C, Sanchez-Madrid F, Mittelbrunn M. Sorting it out: regulation of exosome loading. *Semin Cancer Biol.* 2014;28:3-13.

266. Bolukbasi MF, Mizrak A, Ozdener GB, Madlener S, Strobel T, Erkan EP, Fan JB, Breakefield XO, Saydam O. miR-1289 and "Zipcode"-like Sequence Enrich mRNAs in Microvesicles. *Mol Ther Nucleic Acids*. 2012;1:e10.
267. Deregibus MC, Cantaluppi V, Calogero R, Lo Iacono M, Tetta C, Biancone L, Bruno S, Bussolati B, Camussi G. Endothelial progenitor cell derived microvesicles activate an angiogenic program in endothelial cells by a horizontal transfer of mRNA. *Blood*. 2007;110(7):2440-8.
268. Waldenstrom A, Genneback N, Hellman U, Ronquist G. Cardiomyocyte microvesicles contain DNA/RNA and convey biological messages to target cells. *PLoS One*. 2012;7(4):e34653.
269. Cai H, Reinisch K, Ferro-Novick S. Coats, tethers, Rabs, and SNAREs work together to mediate the intracellular destination of a transport vesicle. *Dev Cell*. 2007;12(5):671-82.
270. Savina A, Vidal M, Colombo MI. The exosome pathway in K562 cells is regulated by Rab11. *J Cell Sci*. 2002;115(Pt 12):2505-15.
271. Ostrowski M, Carmo NB, Krumeich S, Faret J, Raposo G, Savina A, Moita CF, Schauer K, Hume AN, Freitas RP, Goud B, Benaroch P, Hacohen N, et al. Rab27a and Rab27b control different steps of the exosome secretion pathway. *Nat Cell Biol*. 2010;12(1):19-30; sup pp 1-13.
272. Hsu C, Morohashi Y, Yoshimura S, Manrique-Hoyos N, Jung S, Lauterbach MA, Bakhti M, Gronborg M, Mobius W, Rhee J, Barr FA, Simons M. Regulation of exosome secretion by Rab35 and its GTPase-activating proteins TBC1D10A-C. *J Cell Biol*. 2010;189(2):223-32.
273. Rao SK, Huynh C, Proux-Gillardeaux V, Galli T, Andrews NW. Identification of SNAREs involved in synaptotagmin VII-regulated lysosomal exocytosis. *J Biol Chem*. 2004;279(19):20471-9.
274. Fader CM, Sanchez DG, Mestre MB, Colombo MI. TI-VAMP/VAMP7 and VAMP3/cellubrevin: two v-SNARE proteins involved in specific steps of the autophagy/multivesicular body pathways. *Biochim Biophys Acta*. 2009;1793(12):1901-16.
275. Laulagnier K, Grand D, Dujardin A, Hamdi S, Vincent-Schneider H, Lankar D, Salles JP, Bonnerot C, Perret B, Record M. PLD2 is enriched on exosomes and its activity is correlated to the release of exosomes. *FEBS Lett*. 2004;572(1-3):11-4.
276. Christianson HC, Svensson KJ, van Kuppevelt TH, Li JP, Belting M. Cancer cell exosomes depend on cell-surface heparan sulfate proteoglycans for their internalization and functional activity. *Proc Natl Acad Sci U S A*. 2013;110(43):17380-5.
277. Segura E, Guerin C, Hogg N, Amigorena S, Thery C. CD8+ dendritic cells use LFA-1 to capture MHC-peptide complexes from exosomes in vivo. *J Immunol*. 2007;179(3):1489-96.
278. Figueroa J, Phillips LM, Shahar T, Hossain A, Gumin J, Kim H, Bean AJ, Calin GA, Fueyo J, Walters ET, Kalluri R, Verhaak RG, Lang FF. Exosomes from Glioma-Associated Mesenchymal Stem Cells Increase the Tumorigenicity of Glioma Stem-like Cells via Transfer of miR-1587. *Cancer Res*. 2017;77(21):5808-19.
279. Yang X, Li Y, Zou L, Zhu Z. Role of Exosomes in Crosstalk Between Cancer-Associated Fibroblasts and Cancer Cells. *Front Oncol*. 2019;9:356.

280. Rai A, Greening DW, Chen M, Xu R, Ji H, Simpson RJ. Exosomes Derived from Human Primary and Metastatic Colorectal Cancer Cells Contribute to Functional Heterogeneity of Activated Fibroblasts by Reprogramming Their Proteome. *Proteomics*. 2019;19(8):e1800148.
281. Ning X, Zhang H, Wang C, Song X. Exosomes Released by Gastric Cancer Cells Induce Transition of Pericytes Into Cancer-Associated Fibroblasts. *Med Sci Monit*. 2018;24:2350-9.
282. Zhu QS, Ren W, Korchin B, Lahat G, Dicker A, Lu Y, Mills G, Pollock RE, Lev D. Soft tissue sarcoma cells are highly sensitive to AKT blockade: a role for p53-independent up-regulation of GADD45 alpha. *Cancer Res*. 2008;68(8):2895-903.
283. Lim HJ, Wang X, Crowe P, Goldstein D, Yang JL. Targeting the PI3K/PTEN/AKT/mTOR Pathway in Treatment of Sarcoma Cell Lines. *Anticancer Res*. 2016;36(11):5765-71.
284. Villasante A, Marturano-Kruik A, Ambati SR, Liu Z, Godier-Furnemont A, Parsa H, Lee BW, Moore MA, Vunjak-Novakovic G. Recapitulating the Size and Cargo of Tumor Exosomes in a Tissue-Engineered Model. *Theranostics*. 2016;6(8):1119-30.
285. Thery C, Amigorena S, Raposo G, Clayton A. Isolation and characterization of exosomes from cell culture supernatants and biological fluids. *Curr Protoc Cell Biol*. 2006;Chapter 3:Unit 3 22.
286. Raposo G, Nijman HW, Stoorvogel W, Liejendekker R, Harding CV, Melief CJ, Geuze HJ. B lymphocytes secrete antigen-presenting vesicles. *J Exp Med*. 1996;183(3):1161-72.
287. Chaturvedi NK, McGuire TR, Coulter DW, Shukla A, McIntyre EM, Sharp JG, Joshi SS. Improved therapy for neuroblastoma using a combination approach: superior efficacy with vismodegib and topotecan. *Oncotarget*. 2016;7(12):15215-29.
288. Crescitelli R, Lasser C, Szabo TG, Kittel A, Eldh M, Dianzani I, Buzas EI, Lotvall J. Distinct RNA profiles in subpopulations of extracellular vesicles: apoptotic bodies, microvesicles and exosomes. *J Extracell Vesicles*. 2013;2.
289. Thery C, Witwer KW, Aikawa E, Alcaraz MJ, Anderson JD, Andriantsitohaina R, Antoniou A, Arab T, Archer F, Atkin-Smith GK, Ayre DC, Bach JM, Bachurski D, et al. Minimal information for studies of extracellular vesicles 2018 (MISEV2018): a position statement of the International Society for Extracellular Vesicles and update of the MISEV2014 guidelines. *J Extracell Vesicles*. 2018;7(1):1535750.
290. King HW, Michael MZ, Gleadle JM. Hypoxic enhancement of exosome release by breast cancer cells. *BMC Cancer*. 2012;12:421.
291. Reclusa P, Taverna S, Pucci M, Durendez E, Calabuig S, Manca P, Serrano MJ, Sober L, Pauwels P, Russo A, Rolfo C. Exosomes as diagnostic and predictive biomarkers in lung cancer. *J Thorac Dis*. 2017;9(Suppl 13):S1373-S82.
292. Singh R, Pochampally R, Watabe K, Lu Z, Mo YY. Exosome-mediated transfer of miR-10b promotes cell invasion in breast cancer. *Mol Cancer*. 2014;13:256.
293. Sun Z, Shi K, Yang S, Liu J, Zhou Q, Wang G, Song J, Li Z, Zhang Z, Yuan W. Effect of exosomal miRNA on cancer biology and clinical applications. *Mol Cancer*. 2018;17(1):147.
294. Rankin EB, Nam JM, Giaccia AJ. Hypoxia: Signaling the Metastatic Cascade. *Trends Cancer*. 2016;2(6):295-304.

295. Ludwig N, Yerneni SS, Razzo BM, Whiteside TL. Exosomes from HNSCC Promote Angiogenesis through Reprogramming of Endothelial Cells. *Mol Cancer Res*. 2018;16(11):1798-808.
296. Dunst J, Stadler P, Becker A, Kuhnt T, Lautenschlager C, Molls M, Haensgen G. Tumor hypoxia and systemic levels of vascular endothelial growth factor (VEGF) in head and neck cancers. *Strahlenther Onkol*. 2001;177(9):469-73.
297. Zhou X, Yan T, Huang C, Xu Z, Wang L, Jiang E, Wang H, Chen Y, Liu K, Shao Z, Shang Z. Melanoma cell-secreted exosomal miR-155-5p induce proangiogenic switch of cancer-associated fibroblasts via SOCS1/JAK2/STAT3 signaling pathway. *J Exp Clin Cancer Res*. 2018;37(1):242.
298. Potratz J, Dirksen U, Jurgens H, Craft A. Ewing sarcoma: clinical state-of-the-art. *Pediatr Hematol Oncol*. 2012;29(1):1-11.
299. Blancher C, Moore JW, Robertson N, Harris AL. Effects of ras and von Hippel-Lindau (VHL) gene mutations on hypoxia-inducible factor (HIF)-1alpha, HIF-2alpha, and vascular endothelial growth factor expression and their regulation by the phosphatidylinositol 3'-kinase/Akt signaling pathway. *Cancer Res*. 2001;61(19):7349-55.
300. Eyler CE, Foo WC, LaFiura KM, McLendon RE, Hjelmeland AB, Rich JN. Brain cancer stem cells display preferential sensitivity to Akt inhibition. *Stem Cells*. 2008;26(12):3027-36.
301. Horibata S, Vo TV, Subramanian V, Thompson PR, Coonrod SA. Utilization of the Soft Agar Colony Formation Assay to Identify Inhibitors of Tumorigenicity in Breast Cancer Cells. *J Vis Exp*. 2015(99):e52727.
302. Wang L, Yang G, Zhao D, Wang J, Bai Y, Peng Q, Wang H, Fang R, Chen G, Wang Z, Wang K, Li G, Yang Y, et al. CD103-positive CSC exosome promotes EMT of clear cell renal cell carcinoma: role of remote MiR-19b-3p. *Mol Cancer*. 2019;18(1):86.
303. Ke TW, Wei PL, Yeh KT, Chen WT, Cheng YW. MiR-92a Promotes Cell Metastasis of Colorectal Cancer Through PTEN-Mediated PI3K/AKT Pathway. *Ann Surg Oncol*. 2015;22(8):2649-55.
304. Wan W, Wan W, Long Y, Li Q, Jin X, Wan G, Zhang F, Lv Y, Zheng G, Li Z, Zhu Y. MiR-25-3p promotes malignant phenotypes of retinoblastoma by regulating PTEN/Akt pathway. *Biomed Pharmacother*. 2019;118:109111.
305. Strotbek M, Schmid S, Sanchez-Gonzalez I, Boerries M, Busch H, Olayioye MA. miR-181 elevates Akt signaling by co-targeting PHLPP2 and INPP4B phosphatases in luminal breast cancer. *Int J Cancer*. 2017;140(10):2310-20.
306. Wu J, Sun Z, Sun H, Li Y. MicroRNA27a promotes tumorigenesis via targeting AKT in triple negative breast cancer. *Mol Med Rep*. 2018;17(1):562-70.
307. Xu X, Kong X, Liu T, Zhou L, Wu J, Fu J, Wang Y, Zhu M, Yao S, Ding Y, Ding L, Li R, Zhu X, et al. Metastasis-associated protein 1, modulated by miR-30c, promotes endometrial cancer progression through AKT/mTOR/4E-BP1 pathway. *Gynecol Oncol*. 2019;154(1):207-17.
308. Wang C, Bian Z, Wei D, Zhang JG. miR-29b regulates migration of human breast cancer cells. *Mol Cell Biochem*. 2011;352(1-2):197-207.

309. Wu K, Hu Y, Yan K, Qi Y, Zhang C, Zhu D, Liu D, Zhao S. microRNA-10b confers cisplatin resistance by activating AKT/mTOR/P70S6K signaling via targeting PPARgamma in esophageal cancer. *J Cell Physiol.* 2019.
310. Kling M, Chaturvedi N, Keshewani V, Coulter D, McGuire T, Sharp J, Joshi S. Exosomes Secreted under Hypoxia Enhance Stemness in Ewing's Sarcoma through miR-210 Delivery. *Oncotarget.* 2019. Licensed under <https://creativecommons.org/licenses/by/3.0/>.